Published in Antioxidants & Redox Signaling 10, issue 7, 1235-1274, 2008
which should be used for any reference to this work

The Ferredoxin/Thioredoxin System of Oxygenic Photosynthesis[1]

PETER SCHÜRMANN[2] and BOB B. BUCHANAN[3]

[1]This review is dedicated to Professor Hans Eklund to commemorate his retirement from the Swedish University of Agricultural Sciences in Uppsala. His contributions over the entirety of his career have been fundamental to the development of the redox biology field. In addition to enriching the pages of textbooks, they will serve as a reference for researchers for years to come.

[2]Laboratoire de Biologie Moléculaire et Cellulaire, Université de Neuchâtel, Neuchâtel, Switzerland.
[3]Department of Plant and Microbial Biology, University of California, Berkeley, California.

ABSTRACT

Forty years ago, ferredoxin (Fdx) was shown to activate fructose 1,6-bisphosphatase in illuminated chloroplast preparations, thereby laying the foundation for the field now known as "redox biology." Enzyme activation was later shown to require the ubiquitous protein thioredoxin (Trx), reduced photosynthetically by Fdx via an enzyme then unknown—-ferredoxin:thioredoxin reductase (FTR). These proteins, Fdx, FTR, and Trx, constitute a regulatory ensemble, the "Fdx/Trx system." The redox biology field has since grown beyond all expectations and now embraces a spectrum of processes throughout biology. Progress has been notable with plants that possess not only the plastid Fdx/Trx system, but also the earlier known NADP/Trx system in the cytosol, endoplasmic reticulum, and mitochondria. Plants contain at least 19 types of Trx (nine in chloroplasts). In this review, we focus on the structure and mechanism of action of members of the photosynthetic Fdx/Trx system and on biochemical processes linked to Trx. We also summarize recent evidence that extends the Fdx/Trx system to amyloplasts—-heterotrophic plastids functional in the biosynthesis of starch and other cell components. The review highlights the plant as a model system to uncover principles of redox biology that apply to other organisms.

I. INTRODUCTION

PLANTS CAN FULFILL THEIR ENERGY REQUIREMENT through photosynthesis. However, light, the energy source that sustains this process, is variable, forcing plants to adjust their metabolism to changing conditions. In addition, as vascular plants live at fixed locations, they cannot move to avoid unfavorable environmental conditions, but have to cope by adapting their metabolism to different light intensities and qualities, changing temperature, water, nutrient supply, and internal carbon dioxide concentration. Evolutionary pressure has guided plants toward the development

of intricate regulatory networks well adapted to their particular lifestyles.

Early experiments with algal cells indicated that light not only provides the necessary metabolic energy, but acts as a regulatory signal, allowing the cells to switch between dark and light metabolism (26). Experiments with chloroplast extracts (stroma) later established a connection between a light-initiated redox event—the photochemical reduction of ferredoxin (Fdx)—and a change in the activity of an important regulatory enzyme of carbon assimilation, fructose 1,6-bisphosphatase (FBPase). The systematic analysis of the relation between Fdx and FBPase and other light-activated enzymes revealed the presence of a light-dependent redox regulatory system (cascade) in chloroplasts, the ferredoxin/thioredoxin (Fdx/Trx) system (an account of the historical development of the system is given in ref. 30). Photosynthetic enzymes, however, turned out not to be the only targets of redox regulation. During the past 25 years, the field of redox biology has developed dramatically and revealed a regulatory role for redox now in practically every type of living organism. The redox environment of the cell is now recognized as extremely important for controlling numerous functions of metabolism, not only in plants, but also in animals and microorganisms. In plants, redox signaling and regulation via disulfide interchange reactions have gained broad interest since they appear to be involved not only in regulation of photosynthetic enzymes and light harvesting, but also in processes occurring throughout the plants (*e.g.*, germination, transcription, translation, apoptosis, and detoxification).

This review will focus on redox-regulated events that depend on the Fdx/Trx system. We describe the participants of the system and the mechanism by which the redox signal is transferred to target proteins—both established and recently found. A number of reviews published during the past seven years have described different aspects of redox regulation in plants (9, 21, 28, 60, 74, 84, 85, 124, 163, 181, 194, 233, 235, 245, 248, 258), some more specifically focused on the Fdx/Trx system (51–53, 101, 125, 141, 180, 255–257, 286). In the present article, we give an in-depth account of the Fdx/Trx system, building on its history and including new developments in the field. We also discuss recent evidence that extends the occurrence of the Fdx/Trx system to amyloplasts—plastids of heterotrophic plant tissues that carry out many of the biosynthetic activities of chloroplasts including the synthesis of starch.

II. PROCESSES LINKED TO THE CHLOROPLAST FERREDOXIN/ THIOREDOXIN SYSTEM

Electrons transported through the photosystems during photosynthesis reduce Fdx. Reduced Fdx, in turn, interacts with the enzyme ferredoxin:thioredoxin reductase (FTR) that converts a light-activated electron signal into a thiol signal that is transmitted to one of a family of thioredoxins (Trxs) present in the plastid as isoforms. Once reduced, Trxs interact with specific disulfide sites on target proteins—enzymes participating in different metabolic pathways—to increase or decrease their activity, and with proteins linked to stress responses (Fig. 1). This light-dependent redox regulatory system, the Fdx/Trx system, is present only in oxygenic photosynthetic organisms, and when associated with chlorophyll, it links the activity of target enzymes to light, thereby regulating carbon flow and other biochemical processes. In practical terms, Trx acts as an "eye" of the chloroplast, enabling it to respond biochemically to light and dark. As described below, the system has recently been found to occur in amyloplasts—starch-storing plastids in heterotrophic plant tissues—where it appears to be linked to sugars formed in the reactions of photosynthesis and transported to heterotrophic (sink) tissues.

A. Enzyme regulation

The photosynthetic Fdx/Trx system, a regulatory mechanism linking light to the activity of associated enzymes, allows an organism to use absorbed light-energy efficiently in a spectrum of biosynthetic reactions related to the assimilation of carbon dioxide and the formation of cellular energy reserves in the form of starch or other storage products. Thus, during the day, biosynthetic enzymes are activated, whereas counterparts participating in catabolic pathways are deactivated. This is achieved by reduction of regulatory disulfide bonds that are typically present in the chloroplast (and in some cases cyanobacterial) forms of the enzymes but absent from cytoplasmic homologues. The reduction of the disulfide to the sulfhydryl form is accompanied by a structural change that modifies the catalytic capability of the enzyme. When light intensity decreases, at night, and probably also under damaging oxidizing conditions, the regulatory dithiols are oxidized by Trxs through a re-

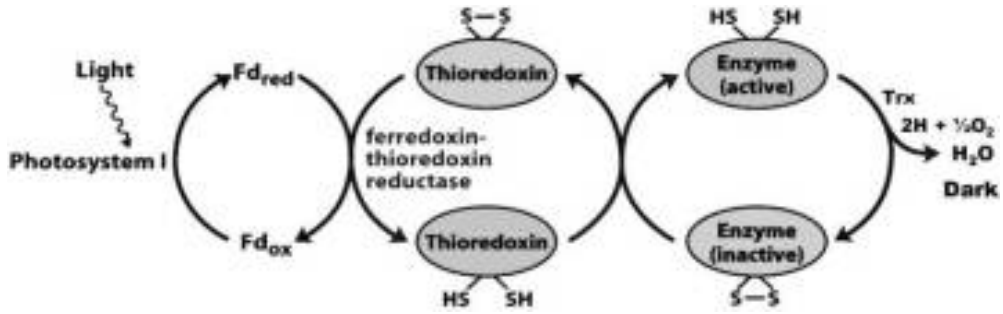

FIG. 1. The Fdx/Trx system of oxygenic photosynthetic organisms. Schematic representation of transfer of the light signal via Fdx and FTR to a target enzyme. Adapated from ref. 159a.

versal of the regulatory electron flow as suggested by experiments with intact chloroplasts (158) and with the reconstituted Fdx/Trx system (253).

B. Detoxification

Trx serves as a source of reducing equivalents not only for the regulation of enzymes in plastids, but also as a substrate for reducing methionine sulfoxide (271), thereby restoring methionines of heat shock and other proteins after sulfoxidation due to oxidative stress. Similarly, as shown in work that led to its discovery, Trx can serve as a substrate in the synthesis of deoxyribose (157). Because of their close tie to enzyme regulation, we summarize briefly below recent progress on chloroplast peroxiredoxins in relation to the Fdx/Trx system.

III. COMPONENTS OF THE CHLOROPLAST SYSTEM

A. Ferredoxin

Fdx is the first soluble stromal electron acceptor for electrons supplied by the photosynthetic electron transport chain. This carrier mediates one-electron transfer between chloroplast photosystem I and several Fdx-dependent enzymes, including Fdx:NADP reductase, nitrite reductase, sulfite reductase, glutamate synthase (GOGAT), and FTR. The plant-type Fdxs involved in oxygenic photosynthesis are small (~11 kDa) acidic proteins containing a single $[2Fe–2S]^{+1/+2}$ cluster. The cluster, which is attached to the protein by four Cys ligands, has a redox potential equivalent to that of the hydrogen electrode, $E_{m,\ pH\ 7.0} \sim -420$ mV (Table 1), clearly more negative than the redox potential of FTR for which it provides electrons (see below). The Fdxs are a well-studied protein family. The primary structures, which are known for a large number of members, show that the positions of the four Cys ligating the cluster are present in a highly conserved cluster-binding motif ($CX_4CX_2CX_{22–33}C$). Three-dimensional structures solved either by crystallography or NMR exhibit extensive similarities including the same fold (77). Fdx displays strong interaction with the associated electron acceptor proteins, forming electrostatic complexes in which it contributes negative charges and its reaction partner contributes complementary positive charges (101). Despite the generally very high amino acid sequence similarity among plant Fdxs, differences in charge distribution can influence the stability of their interactions. The complementarity of the charges may lend specificity to the interaction between Fdx and its electron acceptor proteins. However, exact complementarity is not an absolute requirement since it is often possible to reduce Fdx-dependent enzymes in heterologous systems.

The Fdx structures reveal two patches of negative surface charges on either side of the Fe–S cluster that are essential for its interaction with other proteins (101). Differential chemical modification of free and target bound Fdx indicates that the interaction with positively charged FTR involves essentially only one such negative domain and that Glu92 in spinach Fdx is one of the important residues (57). This conclusion was supported by mutagenesis experiments in which the replacement of this C-terminal glutamate residue resulted in a protein incapable of reducing FTR (129). These observations have been corroborated and extended by the recent structural studies (50, 303) discussed below. Work during the past several years has also added a new dimension to the function of Fdx. Proteomic studies indicate that Fdx, long been known to be present in heterotrophic plant tissues, plays a primary role in enzyme regulation as a member of the Fdx/Trx system identified in amyloplasts, starch storing organelles resident in heterotrophic plant tissues (19).

B. Ferredoxin:thioredoxin reductase (FTR)

In transmitting the redox signal from Fdx to a Trx, FTR occupies a niche that is seemingly peculiar to oxygenic photosynthetic organisms (*i.e.*, prokaryotic cyanobacteria and chloroplasts) and, as found recently, amyloplasts of eukaryotes (19, 53, 257). The enzyme is completely different from the earlier known bacterial and mammalian (114) NADP-dependent Trx reductases (NTRs), as well as those later identified in plants (28), all of which are flavoproteins reduced by NADPH. By contrast, FTR is an iron–sulfur protein with a redox-active disulfide bridge that utilizes the [4Fe–4S] cluster to mediate electron transfer from a one-electron donor, the $[2Fe–2S]^{2+}$ cluster of Fdx, to a two-electron acceptor, the disulfide bridge of a Trx. FTR is a versatile enzyme in terms of reactivity: it efficiently reduces chloroplast *f*- and *m*-type Trxs. Owing to lack of specificity, FTR also catalyzes the reduction of extraplastidic Trx *h* and *E.coli* Trx *in vitro* (126). The extraplastidic NTR of plants, on the other hand, shows strict Trx specificity with the Trxs tested (180).

Originally thought to be present in all oxygenic photosynthetic cells, recent genome sequencing studies have demonstrated that FTR is apparently absent in several slow-growing cyanobacterial species that are considered to represent organisms from early epoch in evolution (73). The presence of NTR apparently meets the relatively limited needs of these organisms for photosynthetic redox regulation (204). In a recent study with a cyanobacterium, which contains both the NTR and FTR/Trx systems (*Synechocystis*), the authors concluded that the NTR/Trx system is linked to antioxidant reactions while the FTR/Trx system controls cell growth (112). These findings on the cyanobcteria raise the questions of the origin of FTR and the evolution of redox regulation. Knowledge in these areas would complement extensive studies on the phylogeny of Trxs in plants (see below).

FTR has been isolated and characterized from different sources such as cyanobacteria (*Nostoc, Synechocystis)*, maize, soy, and green algae (*Chlamydomonas reinhardtii)* (257). It is a protein of 20–25 kDa, composed of two nonidentical subunits. One of the subunits, the catalytic subunit, contains the [4Fe–4S] cluster, responsible for the yellowish-brown color of the protein, and the redox-active disulfide bridge, instrumental in the reduction of Trxs. The second subunit, designated the variable subunit due to variability in size and sequence among different types of organisms, ranges from 8 kDa in cyanobacteria to 13 kDa in eukaryotes. The evidence suggests that the variable subunit has a structural function (53).

1. Primary structures. The primary structure of FTR has been established by amino acid sequencing for the enzymes from spinach and maize (257). Many other primary structures have been deduced from nucleotide sequences.

An N-terminal extension of inconstant length in the variable subunit accounts for the size differences in FTR from prokaryotes and eukaryotes (Fig. 2). In addition, the enzyme shows less extensive size differences within each of these groups. The extension is present in the known eukaryotic enzymes, but absent from prokaryotic counterparts. In addition, the eukaryotic enzymes have a ~10 residue long insert toward the C-terminal end that appears to be situated in a loop structure (53). In spinach FTR, the N-terminal extension seems to be responsible for the reported instability of the protein (278). Removal of part of the N-terminal extension by site-directed mutation significantly stabilized spinach FTR without affecting its catalytic properties (173).

Two variable subunit genes have been isolated from both spinach and *Arabidopsis*. In spinach, the differences between the two are minor, one gene corresponds to the isolated protein whereas the second has an amino acid substitution in the transit peptide and an additional residue in the mature part (67, 81). In *Arabidopsis*, the two clones code for proteins that have only 61% overall identity, 69% when excluding the putative transit peptides (Fig. 2). Transcripts for both variable subunits were found in *Arabidopsis* WT plants. The analysis of *Arabidopsis* mutants, in which the gene for one of the variable subunits (A1) was disrupted, showed that only the transcript of the nondisrupted gene (A2) was present and that the protein was apparently expressed, although perhaps in less active form. This conclusion was based on indirect evidence—measurements of the activation state of NADP-MDH, whose activity is strictly dependent on redox state generated in reactions catalyzed by a functional FTR. Further, the mutant plants grew more slowly and were abnormally sensitive to oxidative stress (136). Although suggested by the absence of deletion mutants, additional experiments will be needed to find out whether the catalytic subunit is essential for survival. Further work is also required to demonstrate (a) that the two variable subunit genes (A1 and A2) are both expressed and that their products are equally able to form the heterodimeric complex with the catalytic subunit, yielding a fully functional enzyme, and (b) whether the two different variable subunits can provide specificity to enable FTR to interact with different Trxs. This latter possibility appears improbable in the light of the structural results discussed below.

The mature catalytic subunit of FTR from sources analyzed has a constant size of ~13 kDa and a highly conserved primary structure (Fig. 3). Among the strictly conserved residues are seven Cys, six of which are organized in two CPC- and one CHC-motifs. These six Cys are the functionally essential residues that form the redox active disulfide bridge and ligate the Fe–S cluster. This ligation, however, does not follow usual consensus motifs for [4Fe–4S] centers, but shows a novel arrangement with the fingerprint: **C**P*C*X_{16}**C**P**C**X_8**C**H*C* (cluster ligands are in **bold**). In spinach FTR, the solvent accessible Cys54 and the buried Cys84 form the active-site disulfide (shown above in *italic* font). The four remaining Cys, Cys52, Cys71, Cys73 and Cys82 are ligands to the iron center, positioning the cluster adjacent to the redox-active disulfide bridge (257), an essential structural feature of the enzyme (Fig. 3).

2. Expression. Fully active recombinant FTR expressed in *Escherichia coli* has been obtained from two sources, the eukaryotic enzyme from spinach (80) and the cyanobacterial en-

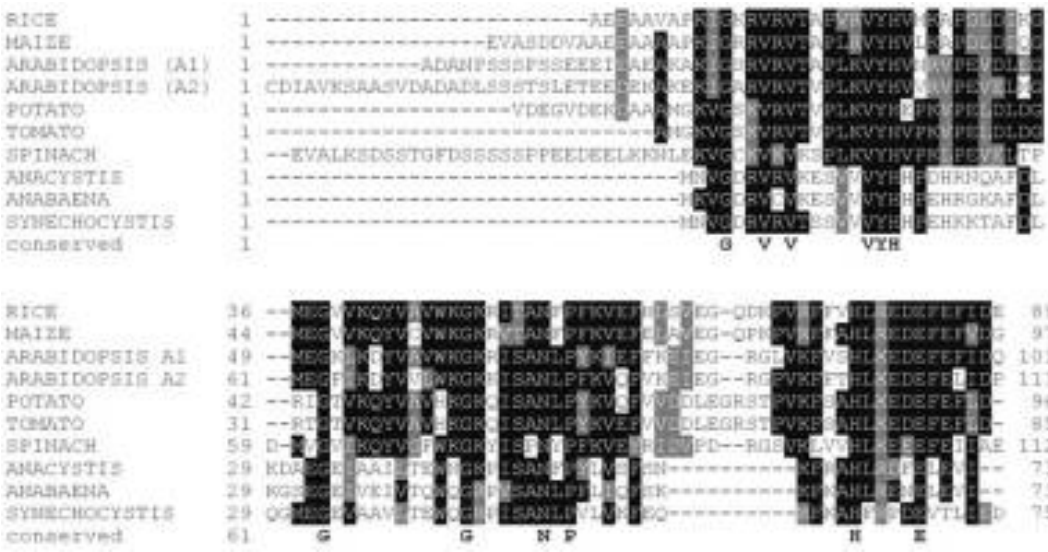

FIG. 2. Multiple sequence alignment of the variable subunit of FTR from different organisms. The sequences were aligned using CLUSTALW (http://www.ch.embnet.org/software/ClustalW.html) and formatted with BOXSHADE (http://www.ch.embnet.org/software/BOX_form.html). The unknown N-termini of the eukaryotic subunits were determined using ChloroP (http://www.cbs.dtu.dk/services/ChloroP/). The sequences retrieved from the SwissProt and the EMBL-EBI data banks have the following accession numbers: rice Q6H5V4, maize P80680, *Arabidopsis* A1 (Q9FHL4) and A2 (Q8LBP6), potato (Q94IK1), tomato (AW092527), spinach (P38365), *Anacystis* (P24018), *Anabaena* (Q8YU85), and *Synechocystis* (Q55781).

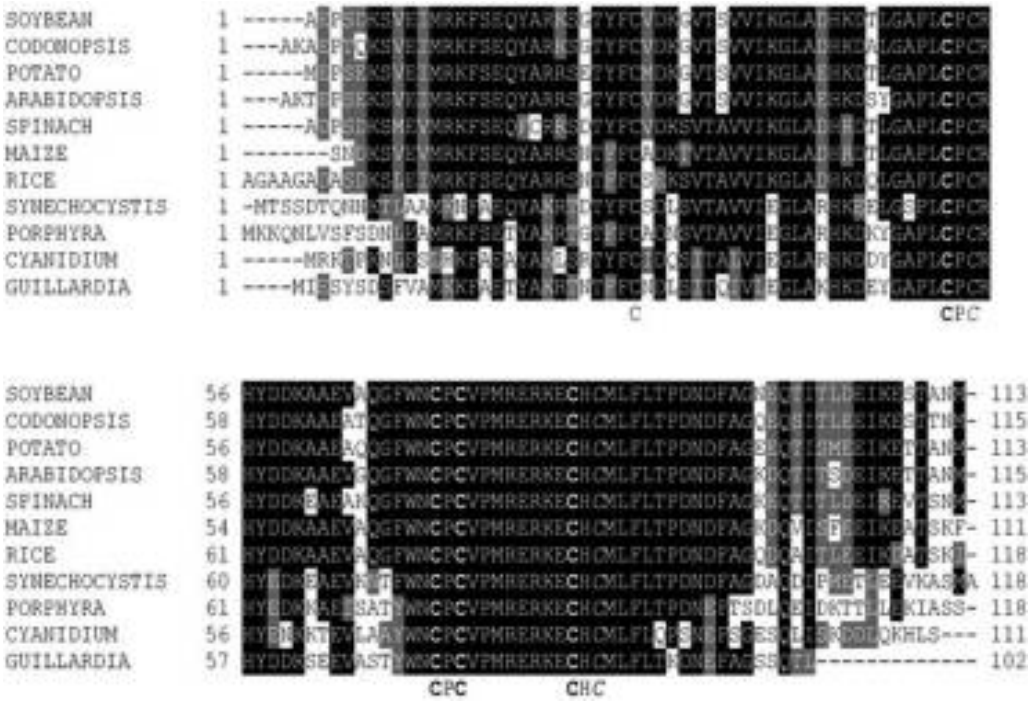

FIG. 3. Multiple sequence alignment of the catalytic subunit of FTR from different organisms. The four Cys holding the cluster are shown in **bold** and the two Cys forming the redox-active disulfide are in *italic*. The sequences were aligned and formatted as indicated for Fig. 2. The sequences retrieved from the SwissProt data bank have the following accession numbers: soybean (O49856), *Codonopsis* (Q6L8H7), potato (Q94IK0), *Arabidopsis* (Q9SJ89), spinach (P41348), maize (P41347), rice (Q6K471), *Synechocystis* (Q55389), *Porphyra* (P51386), *Cyanidium* (Q9TM25), and *Guillardia* (O78461).

zyme from *Synechocystis* sp PCC 6803 (254). The same expression strategy has been adopted for both recombinant proteins. The coding sequences for the two subunits were inserted in series in the expression vector, separated by a spacer region and a second ribosome binding site. These constructs yielded soluble, heterodimeric enzymes that contained the correctly inserted Fe–S cluster, documented by their spectral properties and catalytic activities. Likely owing to the prokaryotic nature of its genes, *Synechocystis* FTR is significantly better expressed than the spinach enzyme. The recombinant cyanobacterial enzyme was also more stable than that from spinach, apparently due to its shorter, more stable variable subunit. However, as mentioned above, the stability of the spinach FTR could be increased to values comparable to the cyanobacterial enzyme by truncation of the N-terminus of its variable subunit (173). Recombinant *Synechocystis* FTR proved to be ideal for structural studies by X-ray crystallography.

3. Crystal structure. *Synechocystis* FTR crystallized as dark brown, well diffracting crystals that allowed structural resolution to 1.6 Å (54). FTR has a rather unique molecular structure. It is a flat, disk-like molecule, with the catalytic subunit sitting on top of the heart-shaped variable subunit (Fig. 4A). The main body of the variable subunit consists of an open β-barrel with five antiparallel strands and two loops forming the upper, outer parts of the heart. The shape of the variable subunit shows striking similarities with PsaE, the Fdx binding protein of photosystem I, with the SH3 domain from mouse c-Crk and with the GroES type chaperone subunit Gp31, although there are no sequence similarities (53). The main function of the variable subunit seems to be the stabilization of the active site region of the catalytic subunit. This possibility can be deduced from the finding that expression of the catalytic subunit alone failed to yield a functional protein (79), an observation confirmed *in vivo* by disrupting the gene of the variable subunit (112).

Overall, the catalytic subunit is an α-helical structure with five helices and loops inserted between the helices containing the iron–sulfur ligands and the redox active Cys. The Fe–S center and the active-site disulfide bridge are both located in the catalytic subunit, in the center of the heterodimer, where the molecule is only 10 Å thick (Fig. 4B). The cubane [4Fe–4S] cluster is positioned on one side of the flat molecule, close to the surface, containing three positive charges. The redox active disulfide bridge is in a surface of more hydrophobic character on the opposite side (53). These surfaces, which are highly conserved, are ideally suited for simultaneous docking of negatively charged Fdx on one side and different Trxs on the opposite side of this unusually flat molecule.

4. FTR interactions: complex formation with ferredoxin and thioredoxin. To reduce Trx, FTR is able to interact simultaneously with both Fdx and Trx owing to the special structure of the FTR heterodimer—a thin, concave, disk-shaped molecule only 10Å across the center where the iron–sulfur cluster is located. Evidence has been published for the complexes between FTR and Fdx, between FTR and Trx, and between Fdx, FTR, and Trx (86), and the structures of all of these complexes have been solved by X-ray crystallography (50).

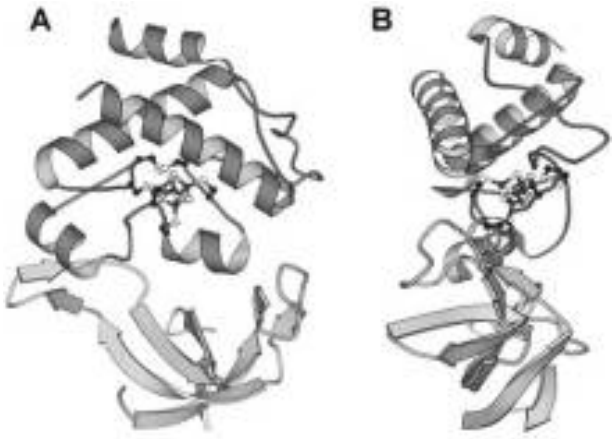

FIG. 4. Crystal structure of the FTR heterodimer in (A) face and (B) side view. The catalytic subunit has an overall α-helical structure and sits on top of the variable subunit with an open β-barrel structure. The [4Fe–4S] cluster and the redox-active disulfide bond are given in *ball and sticks*. Reproduced from ref. 53 with permission of Cambridge University Press.

Under low ionic strength, Fdx and FTR form a noncovalent 1:1 complex (86, 108) which has been crystallized and its structure determined at 2.6 Å (50). The structure shows that Fdx docks, as expected, on the side where a Cys-cisPro-Cys motif is located in which both Cys are ligands of the Fe–S cluster (Fig. 5). The complex is stabilized by a number of hydrogen bonds and salt bridges as well as by hydrophobic interactions between the two proteins. All intermolecular interactions occur with the catalytic subunit, and there appear to be no interactions between Fdx and the FTR variable subunit. The variable subunit, however, may act as an additional attractant to facilitate the binding of Fdx to FTR. On the Fdx binding side, the variable subunit exposes a negatively charged patch, which is complementary to a positively charged patch on Fdx (50). It will be of interest to find out whether the variable subunit plays a role in fitting the Fe-S cluster on the catalytic subunit.

Three possible electron transfer routes are proposed, one through space since the two clusters are only 11.3 Å distant, and the others, more probable, through hydrogen- and covalent-bonded pathways.

The shape of the highly conserved docking site is complementary to Fdx. Several positively charged residues in FTR and several negatively charged residues in Fdx surround the area where the two interact. The lone close interaction is between charged residues (Lys47 of FTR and Glu92 of Fdx; *Synechocystis* numbering). The charged surfaces thus serve mainly as general attractants rather than providing specificity for the interactions (50). It was shown by selective chemical modification of spinach Fdx that several carboxylates were protected from modification by interaction with homologous FTR (57). Among them was the residue corresponding to Glu92. The others are located close, but not in direct contact with FTR. It was demonstrated by mutagenesis studies with the corresponding residue in *Chlamydomonas reinhardtii* Fdx that Glu92 was essential for light activation of NADP-MDH as the mutated protein was no longer able to reduce Trxs via FTR (129).

Crystallographic analysis of the Fdx–FTR complex of the *Synechocystis* proteins also revealed that neither FTR nor Fdx undergoes major conformational change on complex formation. Recent NMR chemical shift mapping studies of the Fdx–FTR interaction (303) are consistent with the previous results obtained by differential chemical modification (57) and also with the crystal structure of the Fdx–FTR complex (50). The results emphasize the dependency of the interaction on polar as well as nonpolar residues, the latter forming a hydrophobic core. The NMR mapping results also underscore the importance of the C-terminal acidic patch (including Glu92) to the interaction observed in both crystallographic analysis (50) and site-directed mutagenesis studies (129).

The transient mixed disulfide formed during the reduction of Trx by FTR involves the surface-exposed active-site Cys of both proteins. This reaction intermediate can be stabilized by using mutated proteins in which the buried active-site Cys has been changed to Ala/Ser. By using mutant forms of Trxs *m* and *f* and WT FTR, covalent duplex complexes were generated (86) and their crystallographic structures determined. In both cases, the Trx molecules were positioned on the opposite side of the FTR Fdx-binding site [*i.e.*, where the redox-active disulfide covers the iron–sulfur cluster of the enzyme (Fig. 6A and B)]. The interaction with FTR is similar for both Trxs *m* and *f*. The complexes are stabilized by a number of specific interactions in addition to the intermolecular disulfide. Like Fdx, the Trx mutants interact exclusively with the catalytic subunit of FTR (50). Since it is not involved in interaction with the redox partners of the enzyme, it was concluded that the variable subunit of FTR possibly stabilizes the structure of the catalytic subunit or, alternatively, has a chaperone like function.

5. Spectroscopic characterization. Detailed spectroscopic characterization of WT spinach FTR and a chemi-

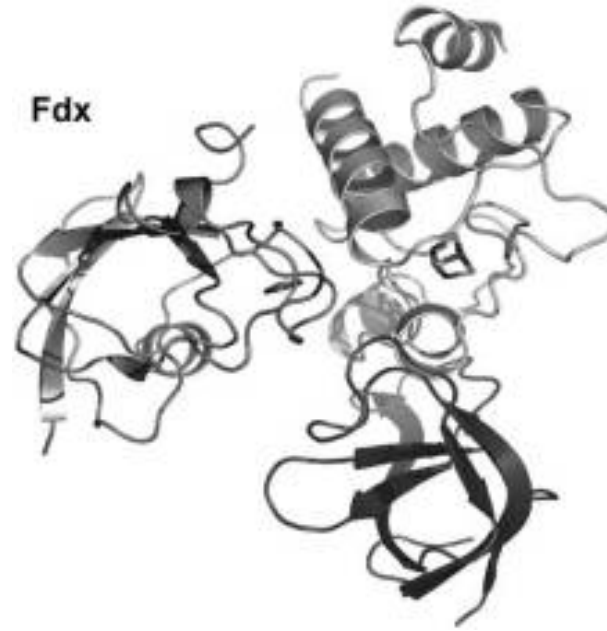

FIG. 5. Crystal structure of the noncovalent Fdx–FTR complex. The [2Fe–2S] cluster of Fdx (*structure to the left*) and the [4Fe–4S] cluster of FTR are represented in *sticks*. The structure clearly shows that there is no interaction between Fdx and the variable subunit of FTR. Reproduced from ref. 50.

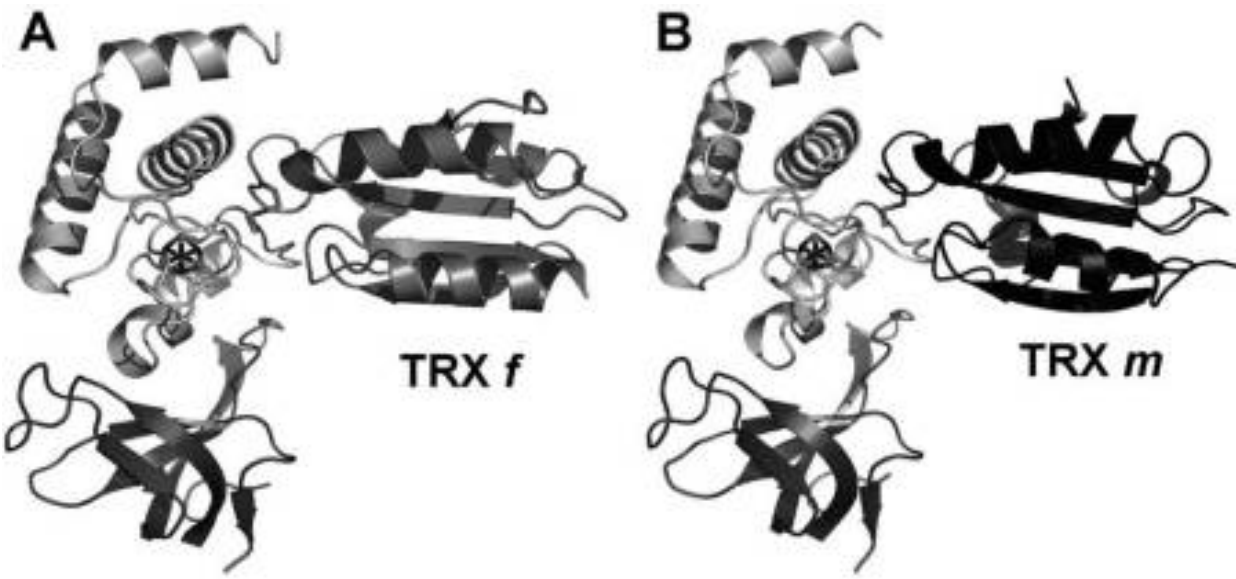

FIG. 6. Crystal structures of the covalent complexes between FTR and (A) Trx *f* (C49S) and (B) Trx *m* (C40S) representing the reaction intermediates. Trx structures are to the *right* and the disulfide bridge linking FTR and Trx is given in *sticks*. Reproduced from ref. 50.

cally modified inactive form in which Cys57 (*Synechocystis* numbering) was selectively alkylated with *N*-ethylmaleimide (NEM-FTR) has helped delineate the properties of the iron–sulfur center and its mechanistic role in the reduction of Trx (130, 268, 269, 285, 286). UV, visible, and CD spectra together, with the absence of an EPR signal, indicated the presence of an S = 0 $[4Fe–4S]^{2+}$ cluster in the resting enzyme. This cluster was found to exhibit unusual properties in being redox-inactive over a broad potential range, from –650 to +300 mV (pH 7) (268). The results suggested that the cluster is not directly involved in electron transfer from Fdx to Trx. While the oxidized (disulfide) and two-electron-reduced (dithiol) forms of FTR both contained S = 0 $[4Fe–4S]^{2+}$ clusters, a transient S = 1/2 species corresponding to a one-electron-reduced intermediate with a $[4Fe–4S]^{3+}$ cluster was observed in the oxidized NEM-FTR derivative (268). This species was also seen either upon reduction of WT FTR with stoichiometric amounts of reduced methyl viologen or during catalytic turnover in the presence of Trx (269). Hence, NEM–FTR represents a stable analogue of the one-electron-reduced reaction intermediate containing a novel type of S = 1/2 $[4Fe–4S]^{3+}$ cluster with an anomalously low redox potential for the $[4Fe–4S]^{3+/2+}$ couple (*i.e.*, lowered at pH 7 from +420 to –210 mV in the spinach enzyme and to –145 mV in the *Synechocystis* enzyme). Both values are significantly more positive than the redox potential reported for the active-site disulfide (–320 mV at pH 7) (110, 239, 268, 269). Similarly, an identical value for the cluster was obtained for the *Synechocystis* active-site mutant FTR C57S, which is an analogue of NEM-FTR, and an even more positive value of –60 mV (285) was found for the heteroduplex FTR-Trx *m*, the stabilized reaction intermediate (86). The cluster was proposed to be covalently attached to a Cys formed by reduction of the disulfide bridge in these intermediates (130, 285). Similar lowering of the redox potentials by 350–700 mV has been observed for synthesized penta-coordinated iron clusters compared to tetra-coordinated iron clusters (42). Due to the more positive redox potential, the one-electron-reduced intermediates are more easily reduced (86).

Mössbauer spectroscopy studies provided further insight into the catalytic mechanism of FTR (130, 285). Analysis of the resting enzyme revealed an interaction of the active-site disulfide with the Fe–S cluster (*i.e.*, partial bonding of the disulfide to a single Fe of the cluster), thereby promoting charge buildup at a unique Fe site, making it an electron donor. Concomitantly, the interaction between the unique Fe and an S of the active site polarizes the S–S bond, making the interacting S an electron acceptor. This state primes the active site to accept an electron from Fdx to break the disulfide bridge. Cleavage of the active-site disulfide is accompanied by attaching one of these Cys (Cys87) to the unique Fe site to yield a $[4Fe–4S]^{3+}$ cluster with a five-coordinate Fe ligated by two Cys residues—a structure seen with the NEM-modified enzyme (130). Analyses of active-site FTR mutants from *Synechocystis* corroborated the results obtained with NEM-modified FTR and defined specific functions of the two active-site Cys: Cys87 providing the cluster-interacting thiol important for the stability of the Fe–S cluster, and Cys57 providing the interchange thiol responsible for attacking the Trx disulfide (86, 285). In addition, structural analysis of NEM–FTR and of the FTR-Trx complexes provided clear evidence for the penta-coordinate Fe-S cluster with Cys87 and Cys55 ligating the same Fe atom of the cluster (Fig. 7) (50). It is noteworthy that such a five-membered coordinate Fe with five sulfur ligands is so far unique to FTR and has not previously been observed in biological systems.

The spectroscopic studies indicate that the function of the Fe–S cluster is more complex than simply to transfer an electron from Fdx to the disulfide bridge. It can fulfill its challenging task of reducing the disulfide group because of a unique structural organization that enables close contact between the Fe–S cluster and the disulfide bridge.

6. Mechanism of thioredoxin reduction. The task of FTR is to catalyze reduction of a disulfide bond with two

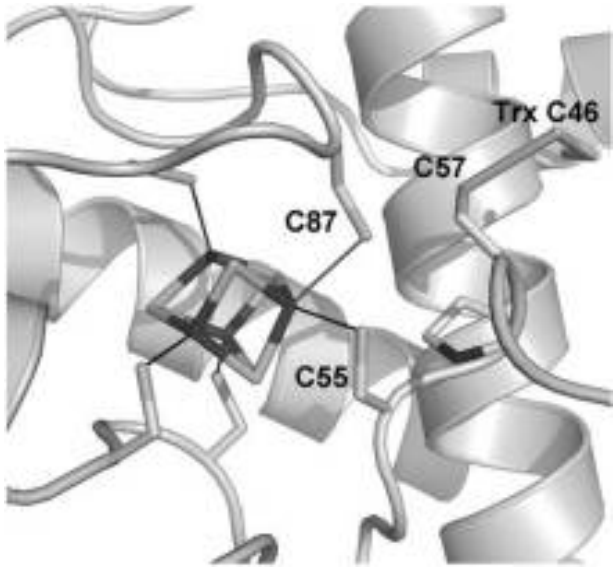

FIG. 7. Active site structure of FTR in the complex with Trx *f* showing the penta-coordinate Fe–S. The [4Fe–4S] cluster of FTR and the disulfide bridge linking FTR and Trx are represented in *sticks* and the cluster-ligations as *black lines*.

electrons transferred one at a time by a one-electron donor, thereby converting an electron-signal to a dithiol-signal that can be transmitted to Trx. Since Fdx, the principal electron donor, transports only a single electron and since only one Fdx molecule can dock with the enzyme at a time (see above), FTR has to mediate two consecutive one-electron transfers from Fdx and stabilize a one electron-reduced reaction intermediate in the process. The reaction scheme summarized in Fig. 8 has been proposed on the basis of spectroscopic analyses of native and active-site modified FTR (130, 268, 269, 285, 286) and structural models derived from crystallographic data (50, 51, 53).

In a first reduction step (Rx 1 → 2), an electron is delivered by Fdx and transferred via the Fe–S center directly to the disulfide (Cys87–Cys57) that is in close contact with the cluster (53). This cleaves the active-site disulfide of FTR and produces a solvent-accessible sulfhydryl (Cys57 in *Synechocystis*) and a solvent-inaccessible Cys-based thiyl radical (Cys87). The latter is stabilized by covalent attachment of the Cys to a unique Fe atom of the cluster as indicated from Mössbauer studies (130, 285), to form an iron–sulfur cluster with five Cys ligands unique to this enzyme. The formation of this derivative was confirmed by structural analyses (50). The Fe–S center then donates an electron to form the sulfur–Fe bond between Cys87 and the unique Fe atom. This results in an oxidation of the [4Fe—4S]$^{2+}$

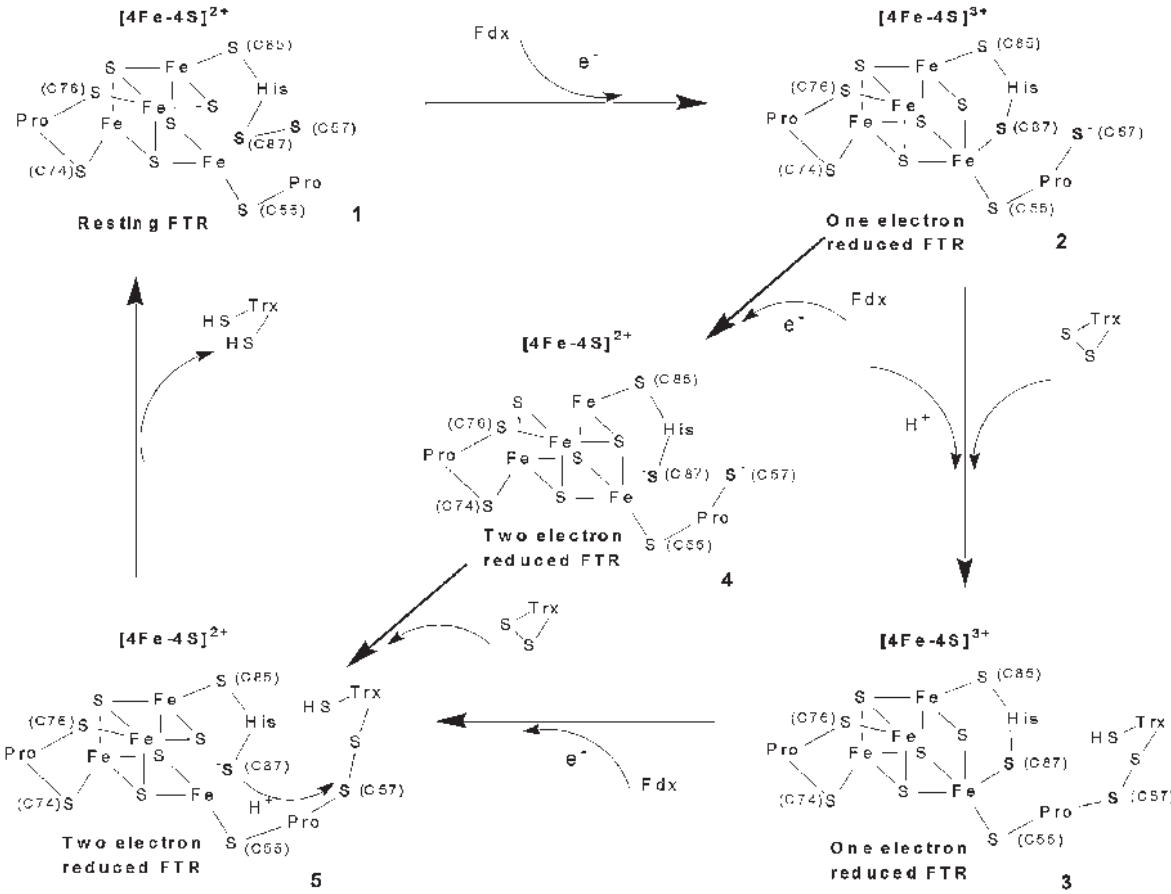

FIG. 8. Reaction scheme for the reduction of Trx by Fdx via FTR. This scheme is based on spectroscopic and structural evidence. Details of the reaction are described in the text. The S of the FTR–disulfide are given in **bold**. Adapted from ref. 50.

cluster, observed in the resting (EPR-silent) enzyme to a [4Fe—4S]$^{3+}$ cluster (268, 269, 286).

The exposed Cys57 can now act as an attacking nucleophile and cleave the disulfide of Trx. This nucleophilic attack results in the formation of a transient mixed disulfide between FTR and Trx, linked through an intermolecular disulfide bond (Rx 2 → 3). The FTR–Trx complexes have been stabilized using mutant Trxs (86) and their structures solved by X-ray crystallography, thus clearly showing the presence of a disulfide bond between Cys57 of FTR and the accessible active-site Cys of Trx *f* or *m* and providing structural confirmation of the mixed disulfide intermediate (Fig. 6A and B). These structures also document the penta-coordinated iron–sulfur cluster present in the one-electron reduced intermediate during the catalytic cycle (Fig. 7) (50).

This transient protein/protein mixed disulfide covers the Trx docking site on one side of the flat FTR molecule. However, the Fdx docking site, on the opposite side of the FTR, stays free for an incoming Fdx to deliver the second electron needed for the complete reduction of Trx. Thus, in a second reduction step, driven by an electron delivered by a second Fdx molecule (or an alternate suitable electron donor that can act under experimental conditions (86)) the bond between a cluster Fe and Cys87 is cleaved and the cluster is reduced to its original 2^{+} oxidation state (Rx 3 → 5). Cys87, which has been converted to the thiol state, or perhaps the thiolate anion state (the protonation state of the sulfur is not known), serves as a nucleophile and attacks the intermolecular disulfide releasing fully reduced Trx and returning the FTR active site to its disulfide state (Rx 5 → 1). His86 may increase the nucleophilicity of the attacking Cys87—a proposal supported by the mutational studies, showing that the H86Y mutant FTR is significantly less active (86).

The particular, disk-like structure of FTR enables simultaneous docking of Fdx and Trx on opposite sides of the molecule, as described in the sequence of interactions, and a rapid transfer of electrons across the thin center of the FTR. The evidence for the existence of a two-electron-reduced FTR in which the disulfide is reduced to a dithiol and which contains an unprecedented electron-rich [4Fe—4S]$^{2+}$ cluster prompted the proposal of an alternative reaction route (50, 285). According to this route (Fig. 8, center), FTR is first reduced to the two-electron-reduced state by two successive interactions with Fdx (Rx 1 → 2 → 4). It then interacts with oxidized Trx to form the transient mixed disulfide (Rx 4 → 5), which is immediately cleaved by the second thiol (Cys87) of the active site to release the reduced Trx. At present, evidence is not available to enable one to discriminate between the two reaction schemes and to determine if one scheme is more likely than the other. In fact, it is possible that both mechanisms function dependent on conditions. Thus, the mechanism described first above could function under conditions normally prevailing in the chloroplast, while the alternative mechanism could function under specialized conditions such as overreduction.

C. Thioredoxins

Following the discovery of a role for Fdx in the activation of chloroplast FBPase (29), several observations provided the foundation for the subsequent discovery of FTR and Trx as additional participants in linking light to enzyme activity in chloroplasts ((297); history reviewed in refs. 26 and 27). The finding that liver Trx was functionally interchangeable with a purified chloroplast protein fraction (115) was key to the realization that Trx was the active principle in earlier preparations used for enzyme activation. This link opened the door to much of the later work. It became clear that Trx is a low molecular weight protein, typically with the canonical active site sequence WCGPC, and is present in plants as well as animals and microorganisms (114, 157, 169). With time, Trx emerged as a ubiquitous protein functional not only as a reductant for enzymes such as ribonucleotide reductase and methionine sulfoxide reductase, but also as a regulatory element that plays a central role throughout biology.

In fulfilling its role, Trx catalyzes thiol–disulfide exchange reactions in partnership with a large number of enzymes and related proteins. Whereas bacterial (*E. coli*) and mammalian (human) cells contain only two types of Trx (in the latter case, one confined to the cytosol and the other to mitochondria (282)), plant cells contain a growing number of these proteins in the cytosol, the nucleus, mitochondria, endoplasmic reticulum, and chloroplasts (21, 175, 181). Cytoplasmic Trxs, designated the *h*-type, are found outside plastids in heterotrophic compartments of plant cells. The *h* group of Trxs is heterogenous and is now organized in three subgroups each containing several isoforms (181). Nucleoredoxin is a form of Trx found in the nucleus (156), and *o-type* Trxs are specific to mitochondria (152).

1. Chloroplast thioredoxins. Four types of typical Trxs are reported for plastids (chloroplasts), and three of these exist as isomers. The *m*– and *f*–types function as messengers in the Fdx/Trx system by transmitting the redox signal from FTR to target enzymes. The remaining two types of Trx, *x* and *y*, identified more recently in *Arabidopsis* and *Chlamydomonas* by genome analysis (160, 161, 179a, 181), appear not to be primarily involved in enzyme regulation, but in stress response. Trx *x*, which is inactive toward FBPase and NADP-MDH, is the most efficient reductant of 2-Cys peroxiredoxin. This property suggests that Trx *x* functions specifically in resisting oxidative stress (44). Trx *y* exists in two isoforms—one expressed mainly in leaves and the other in nonphotosynthetic organs, especially seeds. Peroxiredoxin Q, which has been reported to be an antioxidant (153, 232), was shown to be the best substrate of Trx *y* (45). Trx *y* was also reported to be an efficient electron donor to chloroplast glutathione peroxidase (198) and methionine sulfoxide reductase B2 (280). Finally, an atypical Trx designated CDSP32 (**c**hloroplastic **d**rought-induced **s**tress **p**rotein), a 32 kD protein, also appears to be involved exclusively in stress response (225).

The plant Trxs longest known, *f* and *m*, differ in phylogenetic origin (100, 238), primary structure and target specificity. Trx *f* is of eukaryotic origin, whereas Trx *m* is prokaryotic (as are the *x*- and *y*-forms). All photosynthetic eukaryotes analyzed contain *f*- and *m*-type Trxs, whereas, as expected, photosynthetic prokaryotes lack the *f*-type. Trx *f* was originally described as the activator protein for spinach FBPase and Trx *m* for NADP-MDH (26, 30, 126). An unequivocal functional distinction between the two types has, however, not always been consistently obtained in investigations under different *in vitro* conditions. Nonetheless, the two types can be clearly distinguished by their primary structures.

Both types of chloroplast Trxs appear to be reduced indiscriminately by FTR, although quantitative data are not available to support this conclusion. Their interaction with target proteins, however, displays specificity in most studies. This specificity necessitates recognition between Trx and target enzyme, perhaps on the basis of charge and shape complementarity. Some information has been gained on these points by site-directed mutagenesis. However, heterodimeric structures between chloroplast Trxs and target enzymes have not yet been reported although such complexes have been demonstrated at an analytical level (17, 24, 90, 91).

2. Thioredoxin m. The *m*-type Trx, originally described as an activator protein for chloroplast NADP-dependent MDH, is present in oxygenic prokaryotes, algae, and land plants. The protein strongly resembles Trx from heterotrophic and anoxygenic photosynthetic prokaryotes (26). In land plants and green algae, *m*-type Trxs are nuclear-encoded, whereas in red algae the gene is located on the chloroplast genome (224, 226), supporting its endosymbiotic origin. Functionally and structurally, Trx *m* strongly resembles bacterial Trxs such that the two can be used interchangeably for *in vitro* assays. Trxs of the *m*-type are, therefore, considered of the bacterial-type. As far as is known, all eukaryotic Trx *m* isoforms are confined to plastids.

a. Isomers, localization, and function. Sequencing of the *Arabidopsis* genome revealed the presence of four Trx *m* genes (181), whereas only a single gene was found in *Chlamydomonas* (160, 161) and *Synechocystis* PCC 6803 (164). *Arabidopsis* Trxs *m1*, *m2*, and *m4* are unable to activate FBPase but efficiently activate NADP-MDH and reduce 2-Cys peroxiredoxin A and B, as well as peroxiredoxin Q (44). Recently two functions have been identified for Trx *m3*—a protein whose function had been a mystery. Like other isoforms of *m*-type Trx, *m3* has been shown to regulate the activity of G6PDH (see below). Further, in an area previously unexplored, studies on symplasmic communication in plant development have linked Trx *m3* to protein movement through plasmodesmata (D. Jackson, M. Cilia and Y.Benitez, personal communication). According to evidence obtained with specific *Arabidopsis* mutants, Trx *m3* appears to regulate protein movement from the phloem to the meristematic cells of the root tip. Further details on this unsuspected function for Trx are awaited with interest.

Three of the four *m*-type Trxs in *Arabidopsis* have been directly implicated in antioxidant defense. By complementation assays with a mutant yeast strain, it was found that Trxs *m1*, *m2*, and *m4* (and the *x*-type Trx) induce hydrogen peroxide tolerance (123). Unexpectedly, the fourth *m*-type Trx, *m3*, had a hypersensitizing effect on oxidative stress, again highlighting its difference from other Trx *m* isoforms. On the basis of these results, it was concluded that the three *m*-type Trxs *m1*, *m2*, and *m4* (and the single *x*-type) can serve as electron donors for the reduction of hydroperoxides. In view of their high structural similarity, Trxs of the *m, x* and *y* types would be expected to be reduced by FTR because of its low substrate specificity. If reduced by FTR, a reaction still awaiting experimental proof, Trx *x* and *y* could then reduce the peroxiredoxins as has been shown for spinach Trx *f* and *m* and barley 2-Cys peroxiredoxin (144), although discussed below, there exists an alternate route for this reduction via NTRC that is of growing importance.

Analysis of the lumenal and peripheral thylakoid proteome in *Arabidopsis* revealed that three *m*-type Trxs (*m1*, *m2*, and *m4*) are loosely associated with the stromal face of the thylakoid membranes (75, 208). A preferential membrane location of the *m*-type Trxs could be favorable for the function of 2-Cys peroxiredoxins, which have also been associated with thylakoid membranes. Furthermore, the reaction cycle of the 2-Cys-type peroxiredoxins was proposed to involve oligomerization and attachment of the reduced dimer to the thylakoid membrane followed by detachment of the fully oxidized dimer (144, 145). Finally, peroxiredoxin Q attaches to the thylakoid membrane, particularly to photosystem II, and appears to have a specific function distinct from 2-Cys peroxiredoxin in protecting the photosynthetic apparatus against ROS (153). Recent evidence suggests that peroxiredoxin Q performs its function in the lumen (210).

b. Structure. Cloning and heterologous expression of Trx proteins from spinach leaves and *Chlamydomonas reinhardtii* cells have allowed their structural analysis by x-ray crystallography (33) and NMR (155, 199). The crystal structure of recombinant spinach Trx *m* has been solved for the oxidized and reduced states at 2.1 and 2.3 Å resolution, respectively (33). The three-dimensional structure is very similar to that of *E. coli* Trx (135) and the surface around the active-site Cys also largely resembles the *E. coli* counterpart. This arrangement corroborates biochemical evidence showing that the proteins are functionally interchangeable. The oxidized and reduced forms of Trx *m* show little difference in their active-site conformation. However, some slight structural changes in the main chain conformation of the active site renders the solvent-exposed Cys (Cys37 in the spinach protein) more accessible upon reduction (33). Structural analysis of oxidized Trx *m* by NMR essentially confirms the crystallographic results (199). However, the observation that the crystal structure of this protein contains two independent molecules per asymmetric unit was misinterpreted as evidence for the formation of dimers in solution. It was shown that the noncovalent arrangement of two monomers found in the crystals represents a "crystallization intermediate" formed under the conditions of crystal growth that has no relevance on the *in vivo* state of the protein (34).

3. Thioredoxin f. Trx *f* was originally described as a specific activator protein of chloroplast FBPase (26, 30). The *f*-type Trx is of eukaryotic origin and, in contrast to the *m*-type, its occurrence is restricted to eukaryotic organisms. There are at present fewer sequences available in the databases for the *f* relative to the *m* protein. Nonetheless, a comparison of the primary structures shows that the Trx *f* group is more homogeneous, having impressively extensive homologies around the active site and the carboxy terminal regions across species. The largest deviations in primary sequence are observed with the *Chlamydomonas* protein. The C-terminal part of these sequences resembles classical animal Trx in containing a third, strictly conserved Cys.

a. Isomers. Based on genome sequencing, two isomers, *f1* and *f2*, each with a chloroplast transit peptide sequence, have been identified in *Arabidopsis* (182) and *Chlamydomonas* (160). The two *Arabidopsis* proteins are very similar (44). There

is no information concerning difference in function between the two isoforms, nor is there a report of isomers from other plant sources.

b. Structure. Two different forms of recombinant Trx *f*, a "long form" closely resembling the *in vivo* protein (1) and a more soluble "short form" truncated at the N-terminus (58, 254) have been expressed in *E. coli* and their structures solved. The two structures are essentially identical, except for the presence of an additional α-helix in the long form and a difference in the conformation of their active-site regions. Whereas the overall structure of Trx *f* does not differ markedly from that of Trx *m*, its surface topology is unique and distinct. Trx *f* is more positively charged with some of these charges surrounding the active site where they must be instrumental in orienting the protein correctly upon interaction with its targets. The hydrophobic residues, also prominent in the contact area, may be more important in the less specific interaction with FTR which reduces various Trxs efficiently. A striking difference is the presence of a conserved third Cys in the C-terminal part of the Trx *f* sequence. This Cys (Cys73 in spinach) is structurally exposed on the surface, 9.7 Å away from the accessible Cys46 of the active site. Structural analysis also shows that the active-site Cys with the lower sequence number (Cys46 in spinach) is exposed, whereas its partner is buried, confirming biochemical experiments showing that Cys46 is the attacking nucleophile in the reduction of target disulfides (23). This mechanism is identical to the one originally worked out for *E.coli* Trx (134).

Another potentially important feature of Trx *f* is the apparent flexibility of its active-site region as evidenced by different conformations observed in the short and long forms. Trp45, which is part of the active-site sequence (WCGPC), can flip its indole ring away from the active site. This is possible as a result of the absence of a hydrogen bond between the indole ring and the carboxyl group of the neighboring aspartate that are observed in *m*-type and *E. coli* Trxs. Trp45 of Trx *f* cannot form such a hydrogen bond because the residue corresponding to aspartate is Asn74, whose side chain points in the opposite direction as it forms a hydrogen bond with the main chain nitrogen of Asn77. In what appears to be a distinctive feature of *f*-type Trx, Asn74 is followed by the insertion of a Gln75 that modifies the loop conformation (residues 74 to 77), keeping the Asn74 side chain away from Trp45. This distinctive local conformation appears to represent an important structural factor contributing to the specificity of Trx *f* (33).

c. Glutathionylation. The third conserved Cys located close to the active site of *f*-type Trxs is positioned on the putative contact surface similar to human Trx (292) in accord with their phylogenetic relationship (19, 238). Modification of this Cys was shown to reduce its capacity to activate FBPase and NADP-MDH (58). One of the conclusions drawn from this observation was that Cys73 (spinach numbering) might be involved in the interaction with target enzymes. Direct structural proof to this effect has, however, not been obtained. In human Trx 1 Cys73, which corresponds to the third Cys of Trx *f*, is subject to glutathionylation under oxidative stress conditions (37). Similar observations have recently been reported for chloroplast Trx *f* (183). The third Cys of *f*-type Trxs can be specifically glutathionylated in a reaction greatly accelerated by oxidants. However, based on current data, the glutathionylation reaction is rather slow compared to redox regulation, taking $\sim$1 h to reach 80% modification. When tested with NADP-MDH or GAPDH, the activation rate displayed by glutathionylated Trx *f* was 20–25% that of the control. Based on gel-shift assays, this decrease was suggested to be due primarily to impaired interaction with FTR rather than with individual target enzymes. Although Cys73 is not involved in docking (50), its glutathionylation could impair the formation of a nearby hydrogen bond and, through steric hindrance, prevent the proper approach between the two proteins.

If operative at the level of Trx-reduction, glutathionylation could be a way of decreasing Trx *f* activity under conditions of enhanced ROS production, thereby slowing down the Calvin–Benson cycle and freeing reducing power to cope with the offending oxidants (184). Further experiments are needed to assess the importance of this suggested role.

4. Specificity of thioredoxins. When tested under conditions approaching those occurring *in vivo*, Trxs *m* and *f* display selectivity in their interaction with target enzymes. Under these conditions. the Calvin–Benson cycle enzymes, FBPase (26, 44, 45, 49, 83), sedoheptulose 1,7-bisphosphatase (SBPase) (298), NADP-glyceraldehyde-3-P dehydrogenase (GAPDH) (26, 266), and phosphoribulokinase (PRK) (26), as well as Rubisco activase (312) and ATP synthase (CF_1) (260, 270), have been shown to be efficiently, and in some cases exclusively, activated by Trx *f*. Originally considered to be specifically light-regulated through Trx *m*, NADP-MDH was later shown to be even more efficiently activated by Trx *f* under certain conditions (44, 83, 113). Glucose 6-phosphate dehydrogenase (G6PDH), initially thought to be deactivated specifically by Trx *m* (293), is also efficiently modulated by Trx *f*, according to recent work with stable, homogeneous forms of the *Arabidopsis* enzyme (211). The data suggest that Trx *f* was most effective followed sequentially by Trxs *m*1 = *m2* and *m*3; Trx *m*4 was not tested. Trxs *x* and *y* were generally much less effective. Similar observations were made in activation (*i.e*., when the reduced enzyme was activated by oxidized Trx). In a more recent re-examination of the Trx-linked activation of PRK, a higher V_{max} was observed for Trx *m* than for Trx *f*, but similar $S_{0.5}$ values were reported for the two. From this study it was concluded that Trx *m* might be somewhat more efficient in activating PRK than Trx *f* (82). Taken together, present results suggest that, at least as far as photosynthetic carbohydrate metabolism is concerned, Trx *f* functions primarily in enzyme activation (*i.e*., enhancing the rate of biosynthesis in the light), whereas Trx *m* is less effective in this capacity. Both Trxs are active in enzyme deactivation (*i.e*., facilitating degradation in the dark).

During the past decade, several enzymes, including acetyl-CoA carboxylase, ADP-glucose pyrophosphorylase, and α-glucan water dikinase, have been shown to be redox regulated, each showing specificity for Trx *f*. Acetyl CoA carboxylase catalyzes the first committed step in fatty acid biosynthesis in chloroplasts (241), ADP-glucose pyrophosphorylase the first committed step in starch biosynthesis (12, 84), and α-glucan water dikinase catalyzes the phosphorylation of starch granules—a reaction considered essential for the initiation of starch degradation in leaves and tubers. Significantly, the redox state

of the dikinase enzyme affects binding to the starch granules in a selective and reversible manner (191).

In addition to its role in carbon metabolism discussed above, Trx *m* appears to function in processes such as translation (55, 167), removal of reactive oxygen species (8), and activation of enzymes of N-metabolism [*i.e.*, glutamine synthetase (72) and Fdx:glutamate synthase (GOGAT)] (168).

The observed specificity of plastid Trxs raises the question of the properties responsible for their interaction with target proteins. Since the overall structure and redox potential of chloroplast Trxs *m* and *f* (Table 1) are very similar and since they catalyze identical redox reactions, this specificity seemingly resides in the residues around the active site that form the docking area for target proteins. A comparison of the models of Trx *m* and *f* shows that their contact surfaces are clearly different with respect to surface topology as well as surface potentials. Trx *m* has a more electronegative surface potential (33, 44), whereas Trx *f* has more positive charges around the active site. However, not only the global charge, but also its precise location on the molecule surface, is important. As no structures of complexes between Trxs and target enzymes had been solved until recent work with the barley α-amylase inhibitor (172), answers have been sought by applying site-directed mutagenesis to Trxs. Sequence comparison based on the three-dimensional structure of *E. coli* Trx (64) and comparison of the surface potentials based on structural models (61, 193) revealed residues by which Trx *f* differs from other Trxs. Especially if a change in charge is involved, such residues could, at least in part, be responsible for the observed specificity. With spinach Trx *f*, certain relevant residues have been replaced experimentally to make the protein more similar to Trx *m* (82, 83). Contrariwise, in *E. coli* Trx (154, 193) and pea Trx *m* (171), residues typical of Trx *f* have been inserted and, toward this same end, Pro35 was replaced by Lys in rapeseed (61). In general, the modified proteins showed the expected properties. The conversion of Trx *f* to a more *m*-like protein decreased its capacity to activate FBPase, whereas modification of *E. coli* and *m*-type Trxs with residues typical of *f* improved their capacity to activate FBPase. As Trx *f* contains more positively charged residues on its surface than the *E. coli* or *m* counterparts, replacement of positively charged or neutral amino acids by negatively charged residues reduces the affinity of the mutated Trx *f* for FBPase and PRK. On the other hand, the introduction of positively charged residues into the surface of *E. coli* or *m*-type Trxs increased their capacity to activate FBPase, even though concentrations well beyond physiological level were required. It appears that electrostatic components play a critical role in the interaction of Trx with target proteins, but these are not the only factors. However beneficial with respect to activation of NADP-MDH, mutations made so far on Trx *f* have been counterproductive with respect to FBPase activation (83). Further, replacement of the surface exposed third Cys of Trx *f* by Ser, Ala, or Gly reduced its affinity for FBPase as well as NADP-MDH (58). The mutational studies show that the interplay of several factors, including charge, hydrophobic interactions and hydrogen bonds, are responsible for specificity in the interaction of Trxs with their target proteins.

The properties of the Trx protein complexes described above have been confirmed and extended in the recent structural analysis of the complex between Trx and the α-amylase inhibitor from barley (172). The work showed that a conserved hydrophobic motif of Trx was important for this interaction as were van der Waals contacts and backbone–backbone hydrogen bonds, particulary surrounding the disulfide. The work also revealed that Trx possesses a structural element that allows recognition of disulfides that distinguishes it from glutaredoxin and glutathione transferase. These features help explain the specificity that Trx shows for many proteins.

IV. TARGETS OF THE CHLOROPLAST SYSTEM

After the details of the ferredoxin/thioredoxin system became clear, the number of enzymes shown to be linked to Trx slowly but steadily increased. Most of the proteins originally described were identified either by chance or by following up on prior observations (*i.e.*, metabolite changes reported for *in vivo* light/dark transition experiments with chloroplasts or algal cells or increased enzyme activity found *in vitro* after adding DTT, a nonphysiological substitute for Trx). Studies during the first 25 years following the identification of chloroplast Trx (26) led to the identification of the 16 Trx-linked enzymes in chloroplasts discussed below (15). Interestingly, each of these targets has a specific set of conserved Cys and there is no evidence of a consensus regulatory sequence.

A. Classical target proteins with known regulatory sequences

1. Fructose 1,6-bisphosphatase. Chloroplast fructose 1,6-bisphosphatase (FBPase; EC 3.1.3.11) catalyzes the hydrolysis of fructose 1,6-bisphosphate to fructose 6-phosphate and P_i. The reaction has a high negative free energy, making it irreversible and an important point of regulation for reductive carbon dioxide fixation. A homotetramer of ~160 kDa, FBPase is one of the classical light-regulated enzymes and is generally used to determine Trx specificity. A review summarizing different aspects of the enzyme has been published (41). A comparison of the primary structures of chloroplast FBPase and its cytoplasmic counterpart shows that the available sequences are quite homologous. One major difference is that, unlike the cytosolic enzyme, chloroplast FBPases contain an insert in the middle of the primary structure that constitutes the regulatory disulfide site. This insert contains a number of negatively charged amino acids and three Cys residues. Two of these are separated by four predominantly hydrophobic residues (C_{173}IVNVC_{178} in pea) and the third, Cys153, is twenty residues upstream toward the N-terminus (Table 1). The possible involvement of each of the three Cys in a regulatory disulfide bridge has been probed by site-directed mutagenesis. Replacement of Cys153 resulted in a permanently fully active enzyme, whereas replacement of either remaining Cys (C173, C178) resulted in a partly active enzyme that still required reduction by Trx for full activity. These results suggested that Cys153 is an obligatory part of the regulatory disulfide, whereas the remaining two Cys (C173, C178) can act interchangeably to constitute the regulatory disulfide bridge (127, 128, 229).

TABLE 1. PROPERTIES OF PROTEINS ASSOCIATED WITH THE FERREDOXIN/THIOREDOXIN SYSTEM OF CHLOROPLASTS

Protein	*Organism*	*Redox-active disulfide*	$E_{m,7.0}$ *mV*	*Activator thioredoxin*	*References*
Ferredoxin/Thioredoxin System					
Ferredoxin	Spinach	—	−420	—	
Ferredoxin:thioredoxin reductase	Spinach	**−C54** X_{29} **C84−**	−320	—	110
Thioredoxin *m*	Spinach	**−C37** GP **C40−**	−300	—	110
Thioredoxin *f*	Spinach	**−C46** GP **C49−**	−290	—	110
Calvin-Benson Cycle					
Fructose 1,6-bisphosphatase	Spinach	**−C155** IVDSDHDDESQLSAEEQR **C174** VVNV C179−	−305	*f*	18
Glyceraldehyde 3-P dehydrogenase subunit B	Spinach	**−C349** KDNPADEE **C358−**	−300	*f*	266
Sedoheptulose 1,7-bis-phosphatase	Wheat	**−C52** GGTA **C57−**	−295[b]	*f*	117
Phosphoribulokinase	Spinach	**−C16** GKX_{34}VI **C55−**	−290	*m/f*	110
Rubisco activase	Arabidopsis	**−C392** TDPVAENFDPTARSDDGT **C411−**	−290	*f*	313
CP12[a]	Spinach	**−C21** SDDPVSGE **C30−**	n.d.	(*m/f*)	
		−C61 KDNPETDE **C70−**			
Chloroplast Energetics					
NADP-malate dehydrogenase	Sorghum	**−C365** VAHLTGEGNAY **C377−**	−330		
		−C24 FGVF **C29−**	−280	*f/m*	109
		−C24 — C207−	−310		
ATP synthase γ-subunit	Spinach	**−C199** DINGK **C205−**	−280[b]	*f*	117
Oxidative Pentose Phosphate Cycle					
Glucose 6-phosphate dehydrogenase	Potato	**−C149** RIDKRDN **C157−**	−300[c]	*m/f*	211, 257
Fatty Acid Synthesis					
Acetyl CoA carboxylase	Pea	**−αC267 — βC442−**	n.d.	*f*	149, 241
Starch Metabolism					
β-Amylase	Arabidopsis	**−C32 — C470−**	−302	*f*	264
α-Glucane water dikinase	Potato	**−C1004** FAT **C1008−**	−257	*f*	191
ADP-glucose pyrophosphorylase	Potato	**−αC12 — αC12−**	n.d.	*f*	12, 76
Protein Folding					
Peptidyl-prolyl cis-trans isomerase (Cyclophilin)	Arabidopsis	**−C53 — C170−**	n.d.	*m*	197
		−C128 — C175−			
Oxidative Stress					
2-Cys Peroxiredoxin	Barley	**−C64 — C185−**[d]	−315	*m/f*	144

The redox potentials have been normalized at pH 7.0 assuming a slope of E_m vs. pH of −59 mV/pH unit. The regulatory Cys are in bold and additional conserved residues are underlined. n.d., not determined.

[a]Has been shown to be reduced by DTT and Trx from *E. coli* (177), but not by chloroplast Trx.

[b]Potential determined for Tomato.

[c]Potential for Pea, estimated by ref. 150 based on results by ref. 249.

[d]The two Cys of the disulfide bridge in peroxiredoxin are located on separate homologous subunits (ref. 145).

a. Mechanism of activation. Early structural studies on the enzyme from spinach chloroplasts (281) provided little information on the nature of the regulatory disulfide as the structure of the insert was weakly organized, perhaps because the enzyme was in a reduced and active state (39). A more recent X-ray crystallographic analysis of the oxidized enzyme from pea clearly demonstrates the presence of a disulfide bridge between Cys153 and Cys173 and that Cys178 is located on an α-helix at the C-terminal border of the insert, oriented toward the interior of the protein structure (39). The model derived from the analysis also shows that the regulatory insert forms a partly flexible loop, sometimes called the '170 loop' (281), that extends out of the core structure of the enzyme and makes the disulfide bridge accessible to Trx. In the oxidized enzyme the loop is stabilized by the disulfide bridge, whereas in a C153S mutant, also analyzed by X-ray crystallography (39), the structure is more disordered—likely also a property of the reduced enzyme. The oxidized conformation of the loop has an allosteric effect on the 20 Å distant active site where it disrupts the catalytic Mg^{2+} binding site by the displacement of Glu105 (Fig. 9, Sketches 1–3). Through reduction of the regulatory disulfide, the loop structure is loosened, enabling the binding of Mg^{2+} and fructose bisphosphate substrate and allowing the active site to become catalytically competent (Fig. 9, Sketch 4) (39, 53).

An analysis of the Mg^{2+} dependence of WT and mutant spinach chloroplast FBPases provides experimental evidence for these proposals. The concentration of Mg^{2+} required for optimal activity of the enzyme decreased dramatically when the disulfide was reduced by Trx. Mutation of either one of the two regulatory Cys (Cys155 or Cys174 in spinach FBPase) produced an enzyme with a $S_{0.5}$ for Mg^{2+} identical to the value observed for the reduced WT enzyme and 20 times lower than for the oxidized WT enzyme (18). The nonphysiological *in vitro* conditions generally used to assay FBPase activity—high pH and a high Mg^{2+} concentration—largely bypass the requirement for reductive activation. These factors must have a similar effect on FBPase structure.

b. Mechanism of deactivation. The mechanism by which Trx-linked enzymes are deactivated in darkened chloroplasts has long remained an outstanding question. Advances made on the structure of FBPase during the past decade have enabled the interpretation of early published and certain other little known data and led to the description of a deactivation mechanism that should be further analyzed. In the original work (297), oxidized glutathione was found to accelerate deactivation of the enzyme. The subsequent finding that the redox state of glutathione did not differ in dark and illuminated chloroplasts (98) indicated that, while this mechanism could apply following a period of high light or other conditions generating ROS, additional factors are likely involved under normal conditions. An early study showed that the redox state of Fdx was critical to maintaining the fully active reduced enzyme under anaerobic conditions and that the enzyme was deactivated by oxygen and other oxidants (158). This work was confirmed and extended in experiments demonstrating that the addition of oxidized components of the Fdx/Trx system enhanced deactivation of the photochemically activated enzyme subjected to dark conditions (Table 2) (253). Admission of air (oxygen) or chloroplast thylakoids to the anaerobic assay gave similar results. Moreover, the addition of FBP substrate largely prevented deactivation (Fig. 10) (259). These results suggest that it is essential to maintain all components of the Fdx/Trx system in a highly reduced state to maintain enzyme activity. Once this "electron pressure" is relieved, the enzyme becomes highly susceptible to oxidation and can be deactivated by various oxidants. FBP binds to the active site via Mg^{++} and protects the active enyzme from oxidative deactivation that, according to present evidence, would occur preferentially via Trx and peroxiredoxin following the onset of dark conditions (Fig. 9, Sketches 5 and 6; also Equation insert and figure legend). Deactivation would be accelerated by the drop in stromal pH (from pH 8 to 7) and Mg^{++} concentration that accompany this transition (26). The lower pH could also possibly influence the ambient redox potential—a property of the stroma that remains undefined. In short, it appears that once photochemically reduced by Trx, the activated FBPase is stabilized by FBP and Mg^{++}. Following the hydrolysis of FBP, Trx oxidizes the enzyme (in the dark) and transfers the reducing equivalents either directly to oxygen or, more rapidly, via a peroxiredoxin to hydrogen peroxide. Deactivation of the enzyme is facilitated by the accompanying decrease in pH and Mg^{++} concentration. Evidence for a role for Trx *f* in enzyme deactivation was also found with NADP-GAPDH (266).

c. Cysteines of the redox site. Based on structural analysis of the WT and C153S mutant enzyme, the third Cys of the regulatory loop (Cys178 in pea) seems not normally to participate in forming a disulfide bond. However, it may form an artefactual disulfide bridge in the mutant proteins, thus explaining their partial dependency on Trx. It has been observed that upon aerobic storage of the C174S spinach mutant FBPase, a nonphysiological Cys155/Cys179 disulfide is formed, rendering the enzyme only partially dependent on activation by Trx (18). Mutation of the third Cys (Cys179 in spinach) produced an FBPase that behaved very much like WT enzyme, except for its more rapid activation by Trx *f*. This difference was probably the result of a shift of +15 mV in the redox potential of the regulatory disulfide in the mutant enzyme, making its redox potential equivalent to that of Trx *f* (18).

The function of the three Cys of the regulatory loop has essentially been independently confirmed in a study in which the FBPase from a land plant (spinach) was compared to the enzyme from a red alga, *Galdieria* (223). While containing the two Cys corresponding to the regulatory Cys conserved in the enzyme from land plants, the algal enzyme showed poor redox regulation (204). This behavior is possibly due to the shorter insert which precludes the formation of a disulfide bridge between the two Cys needed for regulation. The red algal FBPase may be an intermediate form between the cyanobacterial enzyme, that lacks a disulfide, and the enzyme from land plants that has acquired a full-length regulatory disulfide insert that renders the enzyme fully capable of redox regulation. Mass spectrometric evidence has also been presented for the nature of the physiological disulfide bond (Cys153–Cys173) in pea FBPase (301). Although the results await confirmation, there was an indication of a Cys173–Cys178 disulfide bond. There are four additional Cys residues conserved in the chloroplast FBPases that lie in well-defined secondary structures. Their replacement with Ser had no significant effect on either activation or catalysis (128, 229).

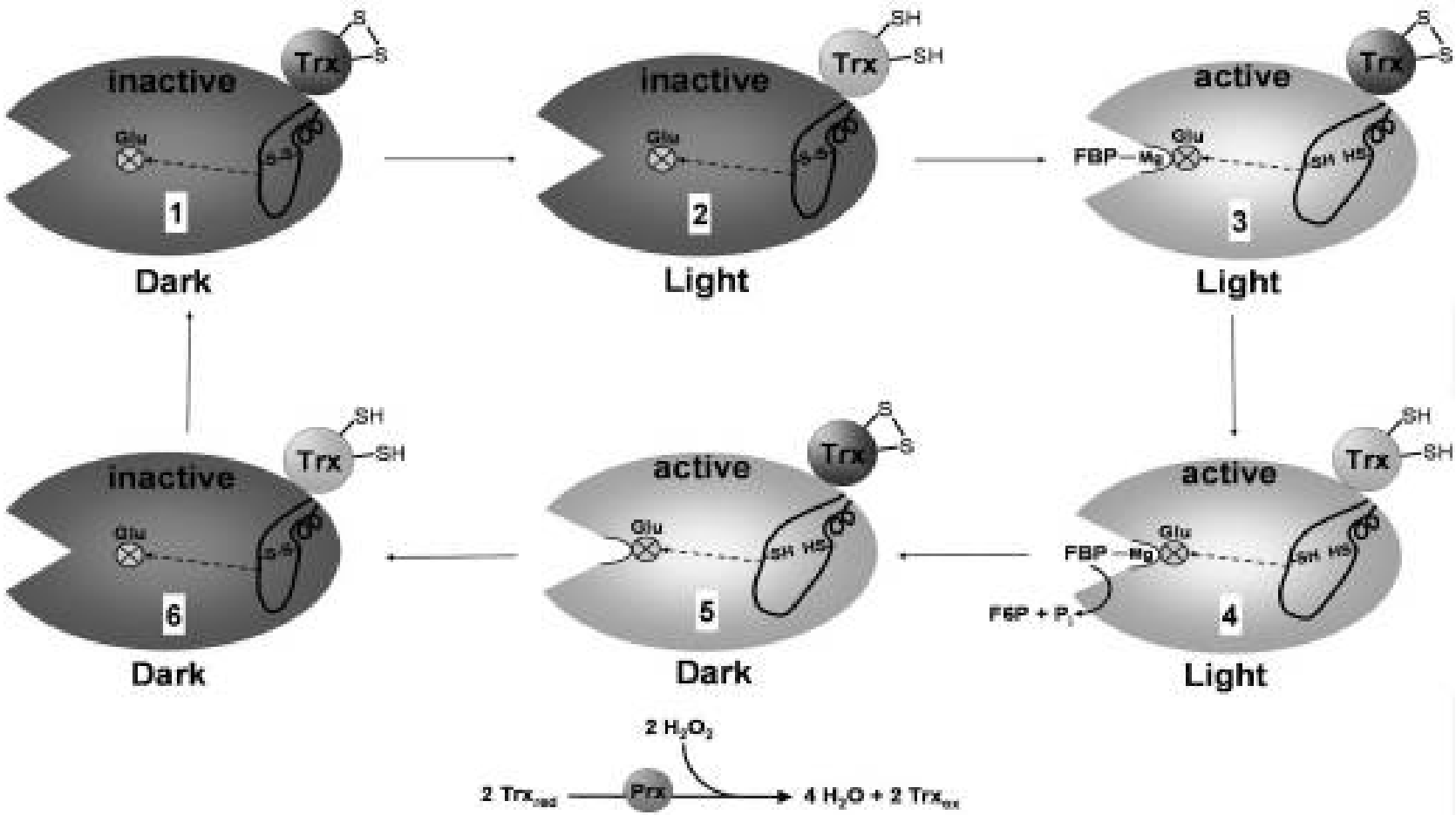

FIG. 9. A mechanism for the activation and deactivation of chloroplast FBPase by Trx *f*. In the inactive, oxidized enzyme [1], the 170-loop is stabilized by the regulatory disulfide bridge locking the active site in a noncompetent conformation in which the position of the catalytically essential glutamate is occupied by valine (53). Upon reduction of the regulatory disulfide by Trx in the light [2, 3], the loop becomes more disordered and shifts glutamate 105 into the active site (~20 Å away) through the movement of two β-strands to allow binding of Mg ions, thereby making the active site catalytically competent [3]. In the light, the active (reduced) enzyme hydrolyzes FBP to F6P and Pi [4] and is maintained active by reduced Trx and substrate. In the dark [5], the decreased concentration of substrate (and Mg^{++}) together with the change in pH favor deactivation of the enzyme by enabling the essential glutamate to be replaced by valine as the reduced enzyme interacts with oxidized Trx, resulting in oxidized deactivated enzyme and reduced Trx [6]. The reduced Trx is oxidized, thereby forming the original enzyme [1]. The Trx reduced in deactivation is preferentially oxidized by Prx, yielding inactive enzyme and reduced Prx. The Prx reduced is oxidized by hydrogen peroxide, regenerating oxidized Prx and forming water, thereby completing the deactivation phase. Alternatively, the enzyme can be oxidatively deactivated directly or indirectly with oxygen through interactions with reduced enzyme or reduced Trx, respectively. Certain elements of this mechanism for deactivation of FBPase are similar to the Prx-mediated water–water cycle of Dietz *et al.* (59).

TABLE 2. DEACTIVATION OF PHOTOCHEMICALLY ACTIVATED FBPASE BY OXIDANTS

Addition at beginning of dark period	*Half time of deactivation (min)*
None (Control)	8.0
H_2O (20 μl)	8.0
Air	2.5
FTR (9 μg)	2.0
Fdx (0.7 nmol)	2.0
Fdx (2.8 nmol)	1.0
Trx *f* (0.1 nmol)	2.0
Trx *f* (0.4 nmol)	1.0
Trx *m* (0.7 nmol)	1.0
Thylakoids	1.5

Activation mixture of 400 μl contained 20 μmol Tris-Cl, pH 7.9, 4 μmol Na-ascorbate, 0.04 μmol dichlorophenol indophenol, 1.4 μmol 2-mercaptoethanol, 2.8 nmol Fdx, 0.4 nmol Trx *f*, 9 μg FTR, 0.25 nmol FBPase, heated chloroplast thylakoids (20 μg chlorophyll). Results taken from ref. 253.

The question remains as to which of the regulatory Cys of FBPase is attacked by Trx *f* to form the transient mixed disulfide. Heterodimer formation between mutants of both proteins has been studied to answer this question (17). The results show that Cys155 is clearly part of the disulfide bridge between FBPase and Trx *f*, although the structure of the pea enzyme positions the sulfur atom corresponding to Cys174 closer to the surface (39). The fact that Cys155 (and not Cys174) is part of the mixed disulfide with Trx *f* suggests that there is a change in the conformation of the flexible regulatory loop that favors this residue as the target for the nucleophilic attack by Cys46 of interacting Trx *f*. Several groups have studied the interaction between the two proteins to pinpoint the responsible amino acids on each partner (58, 61, 83, 107, 154, 171, 193, 203, 288). The studies suggest that the interaction is electrostatic between positive charges on the Trx *f* surface (Lys58, Lys108 in spinach) and negative charges (Asp, Glu) on the FBPase regulatory loop. However, no mutations for these amino acids have been reported for the FBPase.

Recently an attempt was made to introduce the regulatory component of the pea chloroplast FBPase, either the C-termi-

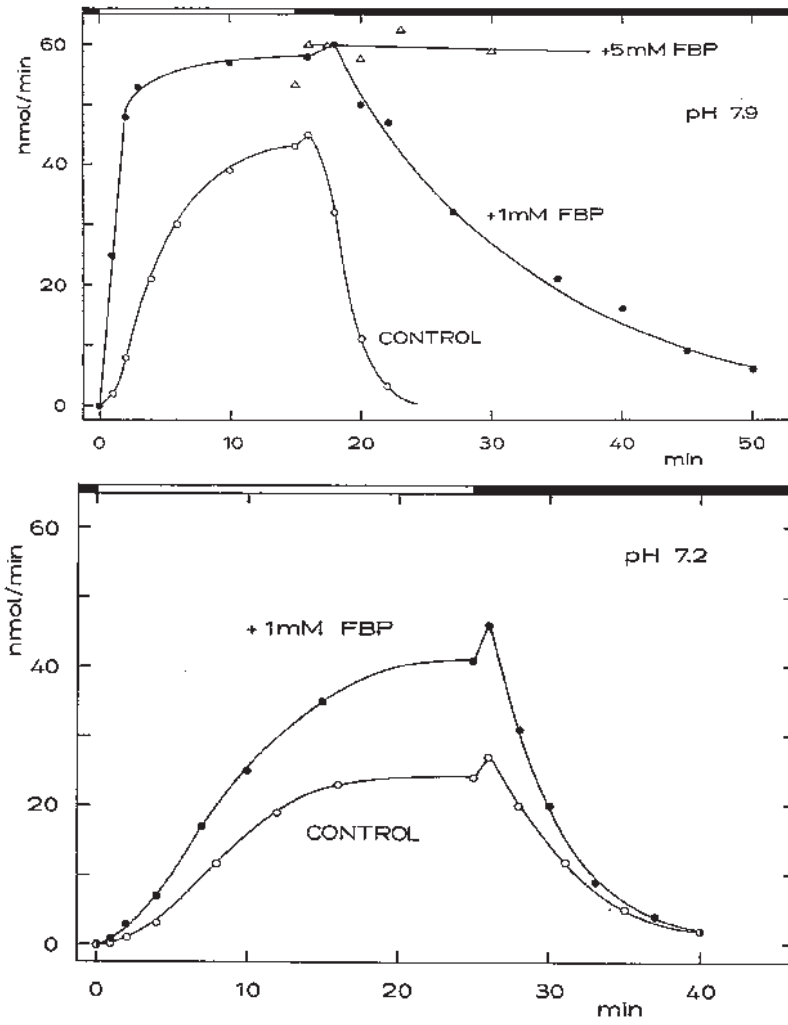

FIG. 10. Time-course of activation and deactivation of FBPase, under anaerobic conditions, in presence of different substrate concentrations (*top*) and at different pH values (*top vs. bottom*) (259).

nal half of the protein or only the '170 loop', into the human enzyme and the cytosolic counterpart from sugar beet. All the different chimera failed to respond to redox change and showed properties of the cytosolic enzyme, confirming that the regulatory loop is not the only essential element and that additional structural adaptations are required for redox regulation (38). As seen below, a similar conclusion has been reached for NADP-MDH.

2. Sedoheptulose 1,7-bisphosphatase. Sedoheptulose 1,7-bisphosphatase (SBPase; EC 3.1.3.37) catalyzes the dephosphorylation of sedoheptulose-1,7-bisphosphate in the regenerative phase of the Calvin–Benson cycle. Such a substrate-specific SBPase is found only in oxygenic photosynthetic eukaryotes and is unique to the Calvin–Benson cycle (220, 221).

SBPase is located in the chloroplast and is encoded in the nuclear genome. There is no cytosolic counterpart. Primary structures are known from five land plants (wheat: P46285 (Swiss-Prot acc. no), rice: Q84JG8, Arabidopsis: P46283, spinach: O20252, and the liverwort *Marchantia*: A3QSS2) and ten algae including *Chlamydomonas*: P46284. The primary structures of the land plants code for a protein of 387 to 396 residues that include a putative chloroplast transit peptide of ~60 residues.

Aside from putative transit peptide sequences, land plant SBPases are highly homologous (up to 98% similarity), whereas the algal sequences show greater variability. The mature enzyme is a homodimer of ~70 kDa. Its sequence and modeled three-dimensional structure show significant overall similarity with FBPase but lack the regulatory Cys insert. So far, an SBPase gene has not been found in cyanobacterial genomes. In these autotrophic prokaryotes, SBPase activity appears to be provided by an FBPase that recognizes both sugar bisphosphate substrates (272).

SBPase from different land plants contains a variable number of Cys residues with four found in pairs at strictly conserved positions in the N-terminal part. The most N-terminal pair is arranged in a CXXXXC motif (C_{52}GGTAC_{57} in wheat; Table 1). The two Cys in this motif have been shown to function in redox regulation by site-directed mutagenesis. When replaced by Ser, an active, redox-insensitive SBPase results (62). Like FBPase, the regulatory Cys residues of SBPase are not part of the catalytic site that is located in the C-terminal part of the primary structure. Based on structural similarities between the two enzymes, it has been proposed that the regulatory Cys are located on a flexible loop equivalent to the 70's loop described for the cytoplasmic FBPase. It is suggested that oxidation of the 70's loop in SBPase could fulfill a role analogous to that of the FBPase insertion, by acting on the nearby β-strands (39).

Like its FBPase counterpart, SBPase is specifically activated by Trx *f* and, once reduced, is also regulated by stromal pH and Mg^{++} level as well as by SBP substrate and the products of the reaction (252, 298). In contrast to FBPase, the SBPase shows an absolute requirement for a dithiol for activation—a property revealed when the enzyme was discovered (26, 200). The recent finding that overexpression of the enzyme enhances photosynthesis and growth of tobacco plants has highlighted its potential importance to agriculture (159).

3. Glyceraldehyde 3-phosphate dehydrogenase. Photosynthetic glyceraldehyde 3-phosphate dehydrogenase (NAD(P)-GAPDH; EC 1.2.1.13) catalyzes the freely reversible reduction of 1,3-bisphosphoglycerate to glyceraldehyde 3-phosphate in the presence of NAD(P)H in the sole reductive step of the Calvin–Benson cycle. This enzyme, which is specific to photosynthetic tissue, exhibits dual cofactor specificity toward pyridine nucleotides with a kinetic preference for NADP(H) (26, 66). After the finding of a link to Trx, the enzyme emerged as a special case with respect to understanding its mechanism of regulation, due both to its dual specificity for pyridine nucleotides and its interaction with metabolite effectors (26). As seen below, recent efforts by the Bologna group have elucidated many of these elusive regulatory details and a decades' old puzzle has largely been solved.

The NADH-dependent activity of the enzyme, which is probably needed for chloroplast dark metabolism, is constitutive and insensitive to regulation by Trx (276), whereas the NADPH-dependent activity is modulated. Two isoforms with different regulatory properties are found in the chloroplast stroma of land plants: a minor homotetrameric A_4-isoform known as the nonregulatory GAPDH and a major heterotetrameric A_2B_2-isoform that is modulated by Trx and metabolites (6, 26, 243, 266, 277). The two types of subunits of the A_2B_2-GAPDH are quite similar with ~80% identity in the N-terminal part. The major difference is the presence of a flexible, C-terminal extension (CTE) of ~30 residues in the B-subunit, containing two invariant Cys and a large number of negatively charged residues (25). This CTE is highly homologous to the C-terminal end of CP12, a small (8.5 kDa) nuclear-encoded chloroplast protein participant in the oligomerization of GAPDH (291) and also, as recently found, in regulating phosphoribulokinase (PRK) (see below).

GAPDH displays complex behavior that depends, at least in part, on illumination status (Fig. 11). In the dark, the enzyme appears as large aggregates of ~600 kDa that lack normal NADPH-dependent activity. The aggregates are composed of homo-oligomers consisting of hexadecamers of A_2B_2-GAPDH, and of hetero-oligomers, consisting either of A_4-GAPDH or A_2B_2-GAPDH, PRK, and CP12. Upon illumination the oligomers dissociate into 150 kDa tetrameric GAPDH (5, 6, 244). Disaggregation parallels the state of activation brought about by the combined action of a reductant (Trx *f*) and different effector molecules.

A_4-GAPDH, the nonregulatory isoform whose activity is not regulated *per se*, is fixed in a fully active conformation (276). However, it can be dark-deactivated through interaction with the small protein CP12, forming a supramolecular complex composed of two trimers, each containing a dimeric PRK, a tetrameric GAPDH, and CP12 (92, 290). Formation and dissociation of this supramolecular complex, which is controlled by Trx and pyridine nucleotides in concert with metabolite effectors, contributes to the light-dependent modulation of both enzyme activities and hence to the overall regulation of photosynthetic metabolism (93, 250, 273, 291). An additional mechanism of potential regulatory control and/or protection against oxidative damage is linked to glutathionylation of the A_4-GAPDH (309).

The heterotetrameric A_2B_2-enzyme was shown to be part of the supramolecular complexes with CP12 and PRK (43, 250, 291). In addition, it exhibits an autonomous type of regulation

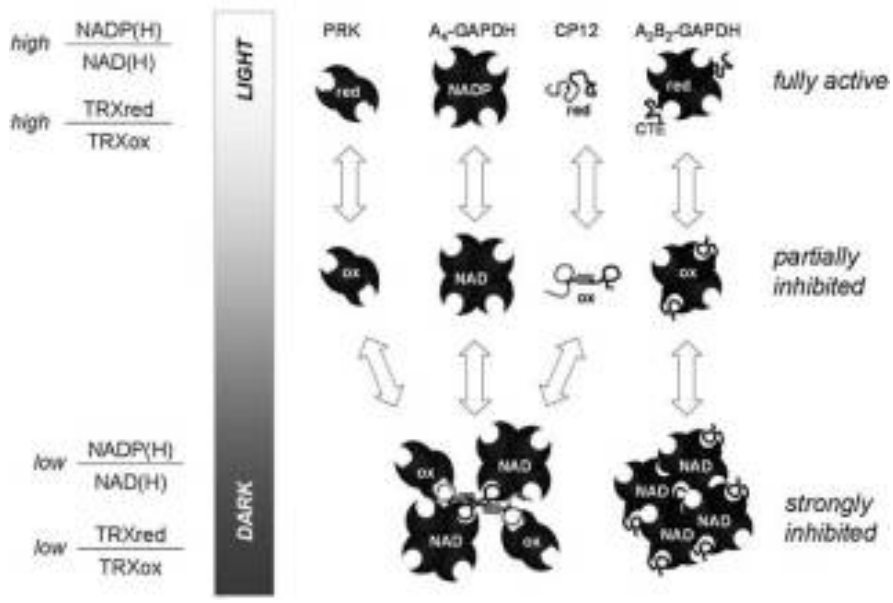

FIG. 11. Mechanism of regulation of chloroplast GAPDH. The increased level of reductants formed under light conditions (reduced Trx, NADPH/NADH) promotes the reduction and dissociation of the supramolecular complexes consisting of A_4-GAPDH, CP12 + PRK, and A_2B_2-GAPDH, yielding fully active GAPDH and PRK and free CP12. The decreased level of these reductants occurring under dark conditions brings about the oxidation (disulfide formation) of A_2B_2-GAPDH, PRK, and CP12, and favors the formation of less active supramolecular complexes. Although not shown, A_2B_2-GAPDH also forms a complex with CP12 and PRK, rendering it inactive. In these complexes, the activity of both NADPH-GAPDH and PRK is strongly suppressed. Reproduced from ref. 276 with kind permission of Springer Science and Business Media.

by Trx, pyridine nucleotides, and metabolites (6, 26, 266, 277). Moreover, the heterotetramer forms kinetically inefficient hexadecamers (A_8B_8) in darkened chloroplasts without PRK or CP12. This conversion strictly depends on the presence of the CTE on the B-subunits (7, 247) which harbors the two invariant Cys shown to form a disulfide bond (219).

Recent mutational and structural studies, comprehensively discussed in refs. 267 and 276, have greatly improved our understanding of GAPDH regulation. Three-dimensional structures have been determined for the enzyme from spinach chloroplasts [*i.e.*, oxidized A_2B_2-GAPDH (69) and A_4-GAPDH both alone and complexed with $NADP^+$ (68)], for the recombinant spinach A_4-GAPDH complexed with NAD^+ (66) and for different mutants and the wild-type recombinant A_4-GAPDH (265). The three-dimensional structure of the apo-enzyme isolated in a different crystalline form from spinach has also been reported (32). The overall structures are comprised of four subunits that are very similar to those of glycolytic GAPDH. Each subunit contains an N-terminal coenzyme-binding domain and a C-terminal catalytic domain, that includes the binding site for the substrate 1,3-bisphosphoglycerate.

Five Cys present in the regulatory isoform of spinach GAPDH, that are potentially involved in regulation together with two residues (Thr33 and Ser188) responsible for coenzyme specificity (66), have been replaced by site-directed mutagenesis and the modified proteins characterized (265, 266). The results provide clear evidence that the two invariant Cys of the CTE, Cys349 and Cys358 (spinach enzyme numbering), are responsible for the redox-sensitivity of the enzyme ($E_{m,\ pH\ 7.0} = -300$ mV). Further, in the presence of oxidized Trx *f*, the disulfide formed between these two residues enables the protein to form higher oligomers that are stabilized by NADH and show inhibited activity with NADPH. Completely dependent on subunit B, redox regulation selectively affects activity with NADPH and leaves NADH activity unchanged. The kinetic parameters determined for the different mutants prompt the conclusion that the CTE can only inhibit the enzyme and not activate it. The oxidized extension acts as an autoinhibitory domain, which, by lowering the k_{cat} through a two- to threefold decrease of V_{max} in oxidized *versus* reduced enzyme, lowers the catalytic efficiency with NADPH as co-substrate (266, 267). In addition, structural studies suggest that this flexible CTE, which carries nine negatively charged residues, might interact with five positively charged Arg on a long S-shaped loop, the S-loop, of the catalytic domain in the oxidized enzyme, in keeping with an idea proposed earlier (222). In the tetramer this S-loop protrudes toward the cofactor binding domain of the adjacent subunit, thereby contributing to the formation of the coenzyme binding site and perhaps sensing the type of cofactor bound. Mutants in which Ser188 was replaced with Ala underwent a decrease in catalytic activity with NADPH. Structural analysis demonstrated that the mutant enzyme relaxed to a less compact, enlarged conformation with respect to wild-type. A similar drop in activity was observed when the A_2B_2-GAPDH was treated with oxidized Trx *f* (265).

Structural studies also provide clues on how the coenzyme binding site can accommodate either NADP or NAD depending on the activation state of the enzyme (66, 68). Further mutational and structural experiments showed that residues Ser188 and Arg77 interact specifically with the 2′-phosphate group of NADP and are therefore responsible for the selectivity of the enzyme for NADP. In addition, mutating Arg77 completely abolished redox regulation, showing that this residue is also needed in this capacity (265, 267).

The mutational and structural results can be explained by a model in which elevated NADPH-dependent GAPDH activity depends on an optimal conformation adopted by the enzyme when NADPH is properly bound and held in place in the coenzyme site. In any other case, catalytically less effective (relaxed) conformations will predominate [*e.g.*, with NADH or with NADPH following disulfide formation in the Trx-regulated CTE accompanied by an approximate twofold drop in k_{cat} of

NADPH-dependent activity (267)]. Recent structural studies with the oxidized A_2B_2-isoform suggest that the inhibition of the NADPH-dependent activity is due to the docking of the disulfide-structured, negatively-charged CTE into a positively-charged cleft delimited by A/B-subunits (69). In this position, the CTE appears to interfere with recognition of bound NADP by the critical Arg77 and Ser188 residues, thus leaving the tetramer in a kinetically inhibited conformation unable to use NADPH efficiently. Reduction of the disulfide bridge on the CTE by Trx *f* seemingly releases the CTE allowing recognition of NADP, via a mechanism reminiscent of that described for Rubisco activase and NADP-MDH (see below). It is interesting to note that construction of a chimeric A_4-GAPDH mutant containing the CTE from subunit B conferred redox sensitivity to this normally redox-independent isoform, thereby providing additional evidence for the regulatory function of the CTE (265).

The specificity of the enzyme for Trx has not been further examined. However, the negative charges clustered on the CTE harbouring the regulatory disulfide (25) may be instrumental in determining specificity by selectively favoring an interaction with Trx *f*, which has a positively charged interaction surface.

4. Phosphoribulokinase. Phosphoribulokinase (PRK; EC 2.7.1.19), one of three enzymes unique to the Calvin–Benson cycle, catalyzes the phosphorylation of ribulose 5-phosphate to ribulose 1,5-bisphosphate, the CO_2 acceptor for Rubisco. PRK was long known to be redox regulated by the Fdx/Trx system, and in early work was most effectively activated by Trx *f* (26). Trx *m* was later reported to be more efficient than *f* by effecting a 40% higher V_{max} with a similar $S_{0.5}$ (82). PRK is a nuclear encoded, homodimeric enzyme of ~80 kDa in its mature form. Each subunit contains four conserved Cys residues, two close to the N-terminus and two near the C-terminus. The two Cys in the N-terminal region (Cys16 and Cys55, in spinach, Table 1) constitute the regulatory disulfide (215) with a redox potential of $E_{m,\ pH\ 7.0} = -290$ mV (spinach PRK) (110). Both Cys are located in the nucleotide binding domain of the active site and Cys55 was proposed to play a facilitative role in catalysis (213, 214). Cys55 was shown to form a transient heterodisulfide with Cys46 of Trx *f* during reductive activation (24), suggesting that it is surface exposed. PRK is the only known example of a Trx-dependent enzyme with a regulatory Cys as part of its active site.

As the structure of chloroplast PRK has not been determined, functional considerations depend on the structure of the enzyme from *Rhodobacter sphaeroides*, which is an octameric enzyme, a form that lacks a regulatory disulfide and is not regulated by Trx (99). The mechanism by which Trx possibly regulates the eukaryotic enzyme was deduced from the structure of the P-loop of the prokaryotic counterpart. Although the P-loop is disordered in the structure, it was estimated that the α-carbons of two specific residues are within 15 Å of each other. To achieve a disulfide bridge in the eukaryotic enzyme, the two Cys residues at these positions would need to move at least 5 Å, distorting the P-loop and making it incapable of binding ATP.

In addition to decisive direct regulation via the regulatory disulfide, PRK aggregates in the dark (212), forming inactive, high molecular weight complexes with GAPDH and CP12 (291). These complexes dissociate in illuminated chloroplasts when the enzymes become active (Fig. 11). Trx, reduced by DTT, was reported to dissociate the *Arabidopsis* GAPDH/PRK/CP12 complex quantitatively and to activate PRK fully (177). CP12 contains two disulfide bridges that are responsible for the formation of an N- and a C-terminal peptide loop. The N-terminal peptide loop was shown to be essential for the molecular interaction between CP12 and PRK (291). Reduction of one or both disulfide bridges is probably linked to the dissociation of the GAPDH/PRK/CP12 complex.

Although PRK from the marine diatom, *Odontella sinensis*, was found to possess the two conserved Cys functional in Trx-dependent regulation of PRK in other organisms, the enzyme is equally active in light- or dark-adapted cells. Further, when isolated from the parent cells or from *E. coli* after heterologous expression, the enzyme is also fully active and does not require reduction. This may be due, in part, to the more positive redox potential of the conserved disulfide of the diatom PRK ($E_{m,\ pH\ 7.0} = -257$ *vs.* -290 mV for the spinach counterpart) (185). Alternatively, the structure of the diatom enzyme could differ and protect the relevant sulfhydryls from oxygen which, as seen below, is also the case for the enzyme from cyanobacteria (142). A comparison of the structures of the PRKs from the diatom and a land plant could give clues to this conundrum which is reminiscent of the situation with the FBPase of the red alga, *Galdieria*, discussed above.

Present results suggest that, while FBPase and SBPase are redox regulated in *O. sinensis* (185), this may not be essential for PRK under normal conditions, because of the apparent absence of an oxidative pentose phosphate pathway in the algal chloroplasts. Regulation could be important under some conditions, however [*e.g.*, in times of oxidative stress (15)]. Along similar lines, PRK of the cyanobacterium, *Synechococcus* sp. PCC 7942, was found to contain a pair of cysteinyl residues corresponding to Cys16 and Cys55 of the spinach homologue, but lacked 17 of the residues between the Cys found in the enzyme from vascular plants. Further, while the *Synechococcus* enzyme responded to Trx-linked redox changes *in vitro*, it was less redox sensitive than its spinach counterpart (142), again raising the possibility that the main function of Trx may be linked not to light/dark but to oxidative regulation (Fig. 12) (15).

5. Ribulose 1,5-bisphosphate carboxylase/oxygenase (via Rubisco activase). Ribulose 1,5-bisphosphate carboxylase/oxygenase (Rubisco; EC 4.1.1.39), which catalyzes the sole carboxylation reaction in the Calvin–Benson cycle has long been known to be activated by light, based on several lines of evidence (26). In certain plants (312), light acts via the Fdx/Trx system in regulating activity, but not directly on the enzyme. Rather, aside from increasing Mg^{++} concentration, the light activation of Rubisco requires Rubisco activase—a nuclear-encoded chloroplast protein that consists of two isoforms arising from alternative splicing, one linked to Trx. In these plants, after reductive activation by Trx *f*, this regulatory enzyme brings about the dissociation of a wide variety of inhibitory sugar phosphates bound to the active site of Rubisco, thereby restoring full activity. The activation by Trx *f* takes place at physiological ADP/ATP ratios. The discovery of Rubisco activase and the current status of research on the structure, regulation, mechanism, and importance of this enzyme

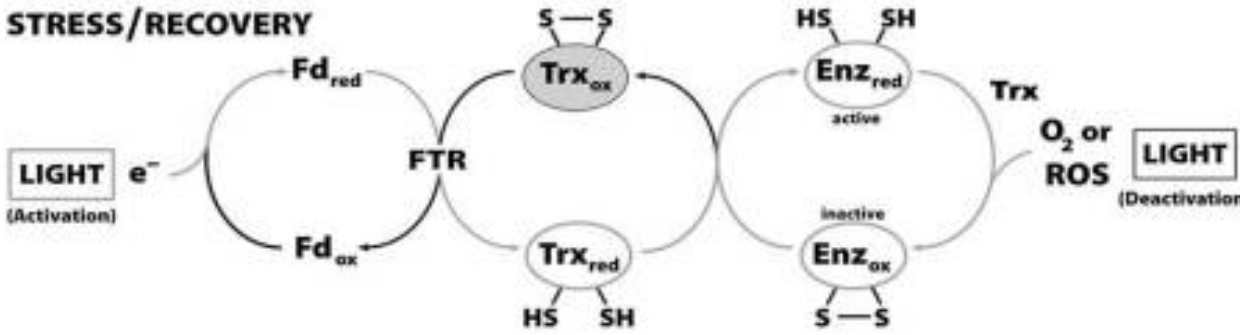

FIG. 12. Role of Trx in oxidative regulation. Under oxidative stress (*e.g.*, presence of ROS), Trx target proteins appear to be oxidized (protected), leading to their deactivation. Once the oxidants are removed (*e.g.*, by Trx-linked peroxiredoxins), the targets are reduced, thereby restoring enzyme activity. Adapted from ref. 28.

have been reviewed (216, 217). Rubisco activase was recognized as a member of the AAA^+ protein family (**A**TPases **a**ssociated with diverse cellular **a**ctivities) that constitute a novel type of molecular chaperone, typically acting as disruptors of molecular or macromolecular structures. This property accurately describes the activity of the activase, which disrupts Rubisco-inhibitor complexes, resulting in activation of the Rubisco enzyme.

In many plants (*e.g.*, spinach, *Arabidopsis*, barley, cotton, and rice), Rubisco activase is present as two isoforms of 41–43 kDa and 45–46 kDa, differing only at the carboxy-terminus. The larger of the two isoforms contains two Cys in the C-terminal domain (C392 and C411 in *Arabidopsis*, Table 1) that were shown to form a redox active disulfide ($E_{m,\,pH\,7.0} = -291$ mV) linked to Trx *f* (312, 313). Through the reduction of the disulfide bond in the larger isoform, the one more sensitive to ADP (261), the sensitivity of the activase to ADP inhibition is greatly diminished, thereby increasing activity. The redox changes in the larger isoform can also alter the activity of the smaller isoform, presumably through cooperative interactions. The main function of the larger isoform is thus to regulate the activity of both isoforms (313).

Although no structural information is available for Rubisco activase, recent experiments support an early model (313), describing the mechanism by which the larger isoform confers redox sensitivity to the CTE of the enzyme (Fig. 13). A redox change in the two Cys residues in the CTE is accompanied by conformational change (287), probably rendering the extension more flexible when reduced. The extension carries the two regulatory Cys as well as a number of negative charges. On one hand, these negative charges might be responsible for the reported specificity of activase for Trx *f* (312). On the other, they could stabilize a docking conformation that makes activase less accessible to ATP through electrostatic interactions with one or more positive residues on or close to the ATP-binding site (287, 313). Cross-linking studies provide strong evidence that the CTE of the oxidized large isoform is located near the ATP binding site and selectively interferes with the binding of ATP (but not ADP) and its associated hydrolysis (287). Furthermore, the observed extensive intersubunit cross-linking suggests that the interactions between the two isoforms include the CTE, which may explain how the larger isoform can regulate both isoforms *in vitro* and *in vivo* (311, 312). The proposed mechanism of activation of activase by Trx *f* (*i.e.*, removal of CTE blocking the binding site for ATP), is reminiscent of the situation described for GAPDH and NADP-MDH. Structural studies should reveal further details of the proposed mechanism.

6. ATP synthase. Chloroplast ATP synthase or CF_oCF_1 (CF_1-ATPase; EC 3.6.3.14) is a membrane-associated enzyme complex that synthesizes ATP from ADP and P_i at the expense of a proton-motive force across the thylakoid membrane. It is composed of the integral membrane portion CF_o and the hydrophilic CF_1, the latter consisting of five subunits (α, β, γ, δ, ε). ATP synthase is a latent enzyme whose activity is linked *in vivo* to the transmembrane electrochemical proton gradient that induces a conformational rearrangement and alters the activity of the enzyme (206). The potential gradient thus acts not only as driving force for phosphorylation, but also as a means for controlling the reversible conversion of the complex to catalytic

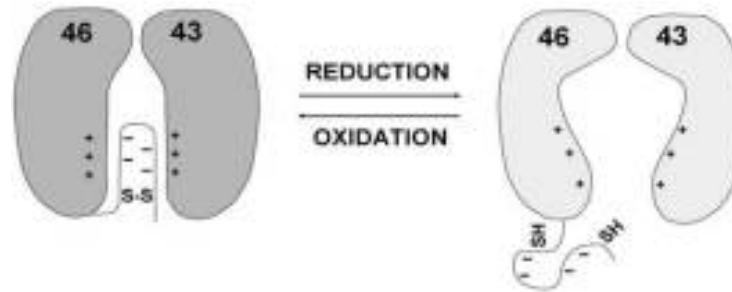

FIG. 13. Model for the activation of Rubisco activase. In the oxidized, deactivated state, the C-terminal extension is stabilized by a disulfide bridge and is fixed by charge interactions close to the ATP-binding site, thereby blocking access. Reduction of the disulfide by Trx is accompanied by conformational changes and probably renders the C-terminal extension more flexible, giving the ATP substrate access to the binding pocket. Adapted from ref. 313.

competence. In addition to the electrochemical activation, ATP synthase is subject to redox regulation by the Fdx/Trx system. Trx was shown early on to reduce the enzyme from higher plants and thereby modulate its activity (26, 206).

The structural element allowing for thiol modulation is a nine residue sequence motif in the CF_1 γ-subunit with two Cys residues that form a disulfide bond in the oxidized enzyme (between Cys199 and Cys205 in the spinach enzyme; Table 1). The role of this regulatory element has been confirmed by introduction of mutations into the sequence motif (230, 231) and by insertion of the regulatory element into the γ-subunit of a cyanobacterial, thiol-insensitive CF_1 (296). This motif, which is contained in an extra peptide, is present in the enzyme of land plants (190) and green algae (308) but not in the counterpart of cyanobacteria (48, 179, 295), diatoms (207), or mitochondria. Recent results indicate that the interaction between the γ- and ε-subunits is important for redox regulation (146). It appears that the regulatory disulfide bridge of the γ-subunit is shielded from reduction by part of the C-terminus of the ε-subunit. The formation of the ΔpH (transmembrane proton concentration difference) elicits structural changes that include movement of the C-terminus of the ε-subunit so as to expose the regulatory disulfide, thereby giving access to Trx (201). The effects of regulation on the rotation of the γ-subunit has also been studied by the single enzyme molecule technique (10, 279), but can not yet be interpreted without structural background. The structure of the CF_1-ATPase from spinach chloroplasts has been solved, however, the γ- and ε-subunits responsible for regulation are not clearly resolved, and the results obtained so far give no structural insight in the mechanism of redox regulation (95).

Early experiments showed that Trx *f* is able to activate thylakoid-bound ATPase effectively in the light (192) and that *m*-type and *E. coli* Trxs were more efficient than human Trx (78). A strict comparison of the efficiencies of spinach chloroplast and *E. coli* Trxs clearly showed that Trx *f* is the most efficient activator of CF_oCF_1. DTT alone showed $<0.01\%$ the effectiveness of Trx *f* (260). Its higher efficiency compared to the other Trxs tested could be due to a more favorable interaction between Trx *f* and ATP synthase made possible by the presence of a number of negatively charged residues in the regulatory insert in the γ-subunit. The importance of the protein–protein interaction between Trx and CF_1 in facilitating disulfide reduction has also been noted with Trx derivatives, that, despite a mutated active site, were able to enhance thiol activation with DTT through noncatalytic interactions with CF_1 (270).

Reduction of CF_1 is very rapid, even in weak light that enables the enzyme to synthesize ATP actively with the onset of photosynthesis. This high rate may be due to the redox potential of the regulatory disulfide, which is relatively oxidizing, approximately equal to that of Trx *f* or even slightly more positive (Table 1). The main purpose of reduction is seemingly not to modulate enzyme activity, but rather to permit a higher rate of ATP formation at limiting electrochemical potential. Regulation linked to Trx also allows the enzyme to be switched off in the dark so as to avoid wasteful hydrolysis of ATP. Analysis of the structural changes brought about by reduction of the regulatory disulfide should give new information on how this gain of efficiency is achieved. In organisms such as cyanobacteria in which CF_1 serves a dual function in oxidative and photophosphorylation, the enzyme should remain active in the dark. Thus, in such organisms, CF_1 lacks the regulatory disulfide segment seen with the chloroplast counterpart (48, 179, 295).

7. Glucose 6-phosphate dehydrogenase. Glucose 6-phosphate dehydrogenase (G6PDH; EC 1.1.1.49) catalyzes the first committed step of the oxidative pentose phosphate cycle—the oxidation of glucose 6-phosphate to 6-phosphogluconate with concomitant reduction of NADP. Two major isoforms have been reported in potato plants, one in the chloroplast (283) and the other in the cytosol (94). In contrast to enzymes of the Calvin–Benson cycle, chloroplast G6PDH is reductively deactivated in the light by the Fdx/Trx system to provide differential control of the two carbon pathways. Deactivation is reversible so that the reduced enzyme becomes oxidized and catalytically active in the dark. In this way, the plastid minimizes the simultaneous occurrence of carbohydrate synthesis (via the Calvin–Benson cycle) and degradation (via the oxidative pentose phosphate cycle). More recently a third, plastid-targeted isoform, which shares 77% identity with the chloroplast enzyme and which is also inhibited by reduction, has been identified (294). A recent in-depth study revealed the presence of six members of the G6PDH gene family in *Arabidopsis*, four encoding plastidic and two cytosolic isoforms (284). Five genes were found to encode active G6PDH—three plastidic and two cytosolic. Consistent with earlier findings, the chloroplast enzyme forms contained conserved Cys, were sensitive to reduction by dithiothreitol and resisted efforts of stabilization—a feature that impeded progress in understanding the enzyme for many years. However, as discussed above, a recent report indicates that isoforms of the overexpressed *Arabidopsis* enzyme can be stabilized and purified. Homogeneous preparations of the *Arabidopsis* enzyme were found to be regulated reductively by Trx *f* as well as Trx *m* (211). One of the plastid isoforms was present throughout the plant (284).

So far, G6PDH is the only enzyme of carbohydrate metabolism found to be deactivated by reduction with Trx. Redox modulation has been demonstrated for G6PDH from cyanobacteria (46, 87), as well as chloroplasts (26, 246). The chloroplast form contains four to six Cys residues at positions not conserved in the cytosolic isoform. Despite their similar response to light, the redox-modulated cyanobacterial and plastid G6PDH show considerable overall sequence differences. The cyanobacterial enzymes contain fewer Cys and the two conserved putative regulatory Cys are far apart, separated by almost 300 residues at positions entirely different from the plant counterpart. There is no experimental evidence that these two Cys form the regulatory disulfide.

The possible function of the different Cys residues in the recombinant chloroplast enzyme of potato has been investigated by site-directed mutagenesis (293). This enzyme contains six Cys residues, all located within the NADP-binding domain in the N-terminal half of the protein. The activity was inhibited by reduction with DTT in a reaction specifically accelerated by Trx *m*, but not by Trx *f*. Only the mutants C149S and C157S could no longer be inhibited by reduction, suggesting that these two Cys are engaged in a regulatory disulfide bridge ($\mathbf{C}_{149}$RIDKREN$\mathbf{C}_{157}$; see Table 1) in the active enzyme. Breaking the regulatory disulfide bond by either mutation with the recombinant enzyme or reduction with the wild-type enzyme inhibits

the activity through a 30- to 40-fold increase of the K_m for G6P substrate. The basis for the Trx specificity difference displayed by the *Arabidopsis* and potato G6PDH remains to be elucidated.

In the cyanobacterium *Nostoc punctiforme* ATCC 29133, a protein, OpcA, was described as an allosteric effector that appears also to play a role in the redox modulation of G6PDH. This protein was required for optimal catalytic activity and for deactivation of G6PDH by reduced Trx. The function of OpcA in redox modulation is not yet clear. However, the results are consistent with the idea that OpcA, which itself contains five conserved Cys residues, might also be reductively inactivated by Trx (97).

Since structural information is not available for photosynthetic G6PDH, there is no molecular basis for deactivation by Trx. By homology modeling with the crystal coordinates of the *Leuconostoc* enzyme, which is not redox regulated, the regulatory Cys were found to be located on an exposed loop, sufficiently close to accommodate a disulfide bridge and freely accessible to interact with Trx (293). It is hoped that the recent availability of stable, pure preparation described above will enable future studies on its structure.

8. NADP-dependent malate dehydrogenase. NADP-dependent malate dehydrogenase (NADP-MDH; EC 1.1.1.82)—an enzyme present in chloroplasts of green algae and different types of land plants [C3, C4, Crassulacean Acid Metabolism or (CAM)], but not diatoms, red algae or cyanobacteria (202)—catalyzes the reduction of oxaloacetate to malate with NADPH as reductant. This enzyme differs from the constitutively active NAD-dependent MDH of the cytoplasm by a strict dependence on activation by light via the Fdx/Trx system. In C3 plants, NADP-MDH is not directly involved in carbon fixation, but functions in a shuttle mechanism to export surplus reducing equivalents in the form of malate from chloroplasts to the cytosol under highly reducing conditions (245). In C4 plants of the NADP-malic enzyme type (maize, sugarcane, or sorghum), NADP-MDH functions as a member of a carbon trapping and transport system of mesophyll cells to reduce the oxaloacetate that has been transported to the chloroplast following its formation from phosphoenolpyruvate and CO_2 in the cytosol (102). The newly formed malate is then transported via plasmodesmata into chloroplasts of the bundle-sheath cells where it is decarboxylated by malic enzyme, thereby generating NADPH and releasing CO_2. The CO_2 is fixed by Rubisco and the NADPH is used in the Calvin–Benson cycle together with ATP generated by photophosphorylation. In land plants, the activity of NADP-MDH is strictly controlled by reversible reduction of the two redox active disulfide bridges through the Fdx/Trx system.

C4 plants which trap CO_2 as malate contain a significantly higher level of NADP-MDH than their C3 counterparts (71). Although its mechanism of redox regulation is rather complex, NADP-MDH is the best understood of the light-activated enzymes of chloroplasts. Details of its regulation have been extensively discussed in excellent reviews (4, 187–189).

Primary structures of NADP-MDH show a high degree of homology (80–90% identical residues). The chloroplast enzyme, a homodimer of 85 kDa, differs from its NAD-dependent cytosolic homolog by the presence of eight Cys and N- and C-terminal extensions that together accommodate four Cys residues at strictly conserved positions. In the oxidized enzyme, four of these Cys form disulfide bridges located in each of the extensions. The remaining four Cys are located in the core of the protein. One of them may also participate in the activation mechanism by forming an intermediary disulfide with one of the N-terminal Cys (91, 237). The N-terminal disulfide is located entirely in the ~40 residue long N-terminal extension in a CY/FGV/IFC motif. The C-terminal disulfide forms the bridge between one Cys in the 18–19 residue long extension and a second Cys eleven residues distant in the last helix in the common MDH core (Table 1 and Fig. 14). The two regulatory disulfides are not equivalent but exert differential effects on the activity of the enzyme (103, 119, 227, 236). Both need to be reduced for full activation of the enzyme. The function of the five Cys considered to participate in regulation has been extensively explored using chemical modification and site-directed mutagenesis. The determination of three-dimensional structures of two enzyme preparations—one in the native state and the other with NADP bound to the active site—has corroborated the biochemical results and placed the proposed activation mechanism on a structural basis (36, 132).

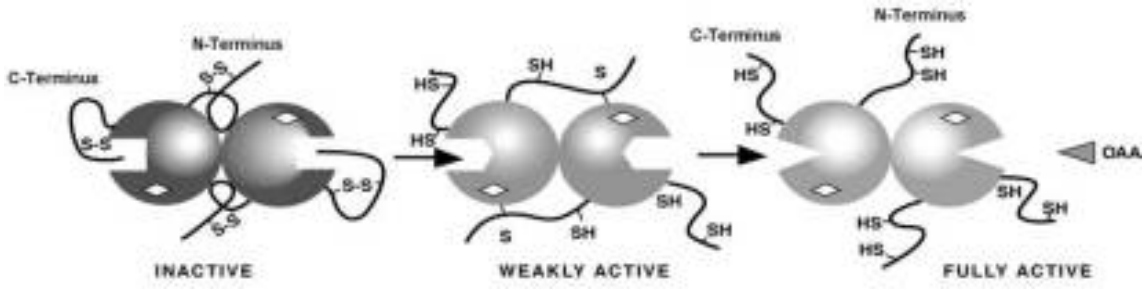

FIG. 14. Model for activation of NADP-MDH by Trx. In the inactive enzyme, the N-terminal extensions are located at the dimer interface holding the two subunits tightly together. The CTEs, forced by their disulfides, loop back into the active sites, blocking access. Upon reduction by Trx, the regulatory disulfides are broken, and the CTEs are loosened and move out of the active sites. The N-terminal extensions also move, changing enzyme conformation toward better catalytic efficiency and perhaps forming a new (still hypothetical) N-terminal disulfide that links the two monomers. After reduction of this transient disulfide, the interaction between the subunits is loosened, and the active site adopts its high-activity conformation. Adapted from ref. 189 and reproduced with kind permission of Springer Science and Business Media.

Both disulfides are located on the surface of the protein in a position easily accessible for reduction by Trx. Removal of the N-terminal disulfide does not yield fully active enzyme, but accelerates the activation rate by Trx considerably (120). Removal of the C-terminal disulfide has no effect on activation rate, but eliminates the inhibition of activation by NADP. Unlike the reduced form, the oxidized enzyme displays weak activity and a high Km for oxaloacetate (121, 227). The observed effects of reduction can be understood on the basis of molecular structures. The N-terminal extension is highly flexible and the two Cys of the N-terminal disulfide are positioned approximately in the middle of the extension. This extension is located at the interface between subunits where it makes a number of mainly hydrophobic interactions with both the catalytic domain of one subunit and the coenzyme-binding domain of the other. The reduction of the disulfide is thought to relax this rigid structure and free the catalytic domain to adopt its active conformation (51). This is in line with the observed increased activation rate.

The CTE of the oxidized enzyme is held against the core structure of the protein by the disulfide bridge and is believed to shield the entrance to the active site by occupying the position of the natural oxaloacetate substrate. Negative charges at the tip of the extension, a penultimate glutamate and the C-terminal carboxylate, are instrumental in this inhibitory action by mimicking the dicarboxylic substrate. The negative charges can also interact with $NADP^+$ and, in this way, inhibit the enzyme. When cofactor specificity is changed from NADPH to NADH, the inhibitory effect is shifted from $NADP^+$ to NAD^+ (251). Trx reduction of the C-terminal disulfide eventually destabilizes the extension and renders it very mobile based on its behavior in NMR (151). This change relieves the intrasteric inhibition of the active site and permits access to the oxaloacetate substrate.

Studies on the formation of transient mixed disulfides between NADP-MDH and Trx demonstrated that the nucleophilic attack of Trx on the C-terminal bridge proceeds through the formation of a disulfide with the most external Cys (90). Results obtained with the N-terminal bridge were not as clear-cut and supported the hypothesis of the involvement of an internal Cys in a transient heterodisulfide with an N-terminal Cys, as suggested earlier (91). Since, for practical reasons, an *h*-type Trx was used in these experiments, the results provide no information with respect to the Trx specificity of the enzyme which, as mentioned above, can be activated by either Trx *f* or Trx *m in vitro*. As it is more efficient under certain conditions (44, 83, 113), Trx *f* has been proposed to be the primary activator (257, 258). The redox potential of the N-terminal disulfide of the enzyme (~280 mV, pH 7.0) is 10 mV more positive than that of Trx *f*, while the C-terminal disulfide is more electronegative (~330 mV, pH 7.0), thus prompting the requirement of an excess of reduced Trx for activation (109). This requirement is consistent with the role of the enzyme in transporting excess reducing equivalents from the chloroplast to the cytosol in C3 plants.

Research on the NADP-MDH of *Chlamydomonas reinhardtii* suggests that the enzyme of eukaryotic green algae is an evolutionary precursor of the counterpart of land plants (165). Although activity is light-regulated, the mechanism of regulation of the algal enzyme is less complex and does not allow the fine tuning observed with the plant enzyme. The algal NADP-MDH has N- and C-terminal extensions (88), but only one regulatory disulfide (in the CTE) that appears to operate as in the C4 (sorghum) enzyme. The unique regulatory disulfide has a potential that is 15 mV more positive (~315 mV, pH 7.0) than the sorghum counterpart. It appears to be reduced by Trx *f* of *Chlamydomonas*, which also has a more positive redox potential than the higher plant homologue (165).

An effort has been successfully made to confer the redox regulatory properties of the sorghum NADP-MDH to the constitutively active NAD-MDH from the thermophilic bacterium, *Thermus flavus*. Grafting the C- and N-terminal regulatory extensions of the sorghum enzyme to that of the bacterium yielded a hybrid that was reductively activated (122). The results also demonstrated that grafting the two disulfide-containing extensions to the bacterial enzyme alone is not sufficient for redox regulation. Specific hydrophobic residues seemingly involved in interactions between the monomers have to be introduced into the core of the protein. Such a transformed NAD-MDH became redox regulated and displayed kinetic parameters much like the native chloroplast NADP-MDH (122).

B. Related target proteins identified by biochemical approaches

In addition to the members of the Calvin–Benson cycle and related reactions identified in early experiments, enzymes functional in diverse processes of chloroplasts were found to be linked to Trx using biochemical approaches. These enzymes are discussed in the following section.

1. Lipid synthesis

a. Acetyl CoA carboxylase. Acetyl CoA carboxylase (ACCase; EC 6.4.1.2) catalyzes the first committed step in *de novo* fatty acid synthesis in chloroplasts—the carboxylation of acetyl CoA to malonyl CoA. This enzyme is considered to be important for the regulation of fatty acid biosynthesis—a process long been known to be linked to light (242, 263). Most plants contain two types of ACCase: a heteromeric, prokaryotic form in plastids and a homodimeric, eukaryotic form in the cytosol (240, 241). The prokaryotic form, isolated from pea chloroplasts, was found to be redox regulated, whereas the cytosolic counterpart from the same source was not. The activity of the enzyme was significantly increased *in vitro* by millimolar concentrations of DTT or by micromolar concentrations of reduced Trx. Of the three different Trxs tested in the activation of ACCase—*E. coli*, spinach *m* and *f*—Trx *f* was the most efficient, suggesting a role as specific activator *in vivo* (241).

These studies were extended to determine the oxidation state of the enzyme in chloroplasts in the dark or after illumination. The results showed that there is more reduced (active) enzyme in the light than in the dark (148), corroborating experiments that demonstrated higher ACCase activity in light- than dark-treated chloroplasts (116).

The prokaryotic heteromeric ACCase is a multi-enzyme complex consisting of four different polypeptides—namely, biotin carboxylase, biotin carboxyl carrier protein, and the carboxyltransferase made up of two nuclear-encoded α- and two chloroplast-encoded β-subunits (205, 240). Sequences of all of these polypeptides from different species reveal varying numbers of

conserved Cys residues that could be responsible for the observed redox sensitivity, but only the carboxyltransferase reaction was found to be linked to redox (148). When overexpressed from pea, recombinant tetrameric pea carboxyltransferase was activated by Trx *f* (147) comparably to WT enzyme. Two Cys residues located on separate subunits function in redox regulation as determined by site-directed mutagenesis: Cys267, a conserved residue on the α-subunit, and Cys442, a residue present in the β-subunit of the pea enzyme (Table 1). These regulatory Cys form an intermolecular disulfide bridge in the inactive enzyme, based on electrophoretic analyses of the recombinant enzyme and of the WT enzyme in extracts from dark- and light-adapted plants (149). However, since one of the proposed regulatory Cys is absent in all other sequences available in the database, further experiments are needed to clarify whether this is a general mechanism operational in all redox responsive ACCases and which Cys are involved in other plants.

b. Monogalactosyldiacylglycerol (MGDG) synthase. Monogalactosyldiacylglycerol (MGDG) synthase (EC 2.4.1.46), an enzyme of lipid metabolism with nine conserved Cys, also appears to be redox regulated. This enzyme provides MGDG, a plant lipid required both for the biogenesis and integrity of plastids and for photosynthetic activity. It has long been known that a thiol reagent such as DTT is necessary to maintain activity of the solubilized enzyme isolated from spinach chloroplasts (47, 176). Additionally, light and cytokinin were found to regulate MGDG synthesis cooperatively in greening cucumber cotyledons (304). Recent experiments with the recombinant cucumber enzyme showed that inhibition with an oxidant such as $CuCl_2$ is accompanied by the formation of a disulfide bridge. Activity could be recovered by reduction with DTT, or more efficiently with reduced spinach Trx *f* or *m* (305). However, since the recombinant enzyme is present in reduced active form, further experiments will be needed to determine whether reduction is a mechanism essential for classical regulation or rather is a means to achieve oxidative regulation of the enzyme in response to stress or after oxidative damage. MGDG synthase is predicted to be localized on the inner envelope, possibly facing the intermembrane space (186). As an *m*-type Trx is also associated with the envelope membrane (70), it is of interest to know whether a Trx of this type is the physiological regulator of the bound MGDG synthase, and, if so, how it is reduced in activating the enzyme.

2. Starch synthesis and degradation.

a. ADP-glucose pyrophosphorylase. ADP-glucose pyrophosphorylase (AGPase; EC 2.7.7.27) catalyzes the first committed step of starch synthesis in plastids, converting glucose 1-phosphate and ATP to ADP-glucose and PP_i. AGPase is a heterotetramer that contains two distinct subunits—a smaller, highly conserved catalytic α-subunit and a slightly larger, less conserved modulatory β-subunit. In leaves and potato tubers, AGPase activity is allosterically regulated by ultrasensitive interactions with metabolic effectors, 3-phosphoglycerate is an activator, and P_i an inhibitor (13, 218). More recent reports have revealed that AGPase from both sink and source tissues is also regulated by Trx. The enzyme from potato tubers (12) and pea leaf chloroplasts (84) is activated via reversible cleavage of the intermolecular disulfide bridge connecting the two catalytic α-subunits. The disulfide bridge, which is formed between Cys12 of the two (small) α-subunits in the potato tuber enzyme (Table 1) (76), is slightly more efficiently reduced by Trx *f* than by Trx *m* and its reduction leads to increased sensitivity to activation by 3PGA (12). There is evidence for a role for this redox modulation of AGPase in regulating starch synthesis in potato tubers *in vivo* (274) as well as in leaves of several plants—potato, pea, and *Arabidopsis* (106).

Recent experiments have given new insight into the regulation of AGPase. Incubation of intact isolated pea chloroplasts with trehalose 6-phosphate significantly and specifically increased the reductive activation of the enzyme. The evidence suggests that trehalose 6-phosphate, which is synthesized in the cytosol, acts as a messenger to report cytosolic metabolic status to the plastid by promoting the Trx-mediated activation of AGPase in response to sugar levels in the cytosol (143). In this way, the activity of the enzyme can be linked to the metabolic status of the cytosol, and hence to sucrose synthesis, in addition to light. In view of this evidence, AGPase has become more important in determining resource allocation between plastid and cytosol.

b. α-Glucan water dikinase. α-Glucan water dikinase (GWD; EC 2.7.9.4) is a plastid enzyme that catalyzes the phosphorylation of starch in a reaction required for normal degradation of the polymer. GWD from potato tuber was found to be activated in a reductive reaction in which Trx *f* was more efficient (higher V_{max} and a lower $S_{0.5}$) than Trx *m* (191). Deactivation of the enzyme resulted from the formation of an intermolecular disulfide bridge between two Cys in a regulatory sequence $C_{1004}FATC_{1008}$ (Table 1) that is conserved in other chloroplast-targeted GWDs. The redox potential of this disulfide is the most positive value among known Trx-activated enzymes ($E_{m,\ pH\ 7.0} = -257$ mV). In addition to controlling activity, the redox state of GWD appears to affect binding of the enzyme to the starch granules in a selective and reversible manner. In chloroplasts from dark adapted potato plants, GWD was found mainly in an inactive oxidized state when attached to starch granules. By contrast, in chloroplasts from light-adapted plants, the enzyme was soluble and fully active in the reduced state (191). It seems that GWD is needed to initiate starch granule degradation at the onset of darkness. However, contrasting views have been presented recently (63).

c. β-Amylase. β-Amylase (EC 3.2.1.2) catalyzes the hydrolytic release of maltose from polyglucans in the degradation of starch. Genome sequencing revealed the presence of nine genes coding for β-amylase isoenzymes in the *Arabidopsis* genome. Three are predicted to be located in plastids, one of which (At3g23920) has been linked to redox regulation *in vitro* by Trx (264). The enzyme, TR-BAMY (Trx-regulated β-amylase), is a monomeric 60 kDa protein with a conserved region corresponding to the typical $(\alpha/\beta)_8$ barrel of β-amylases and eight Cys. Recombinant TR-BAMY was active only after reduction by either DTT or reduced homologous, plastid Trxs. Among the isoforms tested (*f*1, *m*1, and *y*1), Trx *f*1 was the most effective (264).

Redox titrations revealed a redox potential of $E_{m,pH\ 7.0} = -302$ mV (Table 1) for the putative regulatory disulfide of TR-

BAMY (264). A comparison of the activity of the enzyme from WT and Cys to Ser mutants showed that two of the eight Cys are responsible for redox sensitivity. The implicated Cys are far apart in the primary structure, Cys32 close to the N-terminus and Cys470 in the C-terminal region, reminiscent of the spacing in PRK (see above). TR-BAMY transcripts were detected in plastids throughout the plant, in leaves, roots, flowers, pollen, and seeds. Aside from TR-BAMY, none of the other eight β-amylase genes contained the two putative regulatory Cys. Interestingly, TR-BAMY seems not to be universally distributed among plants. While present in dicotyledons—*Brassica napus* (GenBank AAL37169), tomato (*Lycopersicon esculentum*; TIGR TC163705), and potato (TIGR TC118938)—the enzyme is noticeably absent in cereals (The Institute for Genomic Research [TIGR] databases, www.tigr.org).

The function of TR-BAMY is not yet clear. The situation is unusual in that, in leaves, chloroplast-targeted β-amylases are generally considered to act in the dark in the degradation of starch. The situation is, however, not without precedent: the activation of TR-BAMY has much in common with the recently described redox regulation of GWD (191)—a chloroplast enzyme also involved in starch degradation (see above). Overall, the findings suggest the existence of a redox-regulated, stress-induced pathway of starch degradation in leaves (264). It will be of interest to see whether the enzyme is activated in the light via the Fdx/Trx system as was the case with Trx and DTT (264). An additional unanswered question relates to how the activity of reductively activated enzymes functional in the synthesis and degradation of starch is physiologically coordinated by the chloroplast Trx system (11, 19, 262).

3. Nitrogen metabolism. Over the years, a number of reports have implicated Trx in the regulation of two enzymes of chloroplast algal metabolism that incorporate nitrite-derived ammonia into amino acids—glutamine synthetase and Fdx:glutamate synthase—references in (257). More recently, *in vitro* evidence suggests that these enzymes are also Trx-dependent in land plants (40, 168). Proteomic studies discussed below have provided independent evidence that glutamine synthetase is a Trx target in spinach (15, 196), *Chlamydomonas* (162), and *Arabidopsis* (174, 306). In *Synechocystis* Fdx:glutamate synthase was reported as a potential Trx target using a similar approach (170).

a. Glutamine synthetase. Glutamine synthetase (GS; EC 6.3.1.2), the enzyme catalyzing the ATP-dependent formation of glutamine from glutamate and ammonia, is encoded by a small multigene family that shows organ-specific patterns of expression. Both a cytosolic (GS1) and a chloroplast (GS2) isoform are found in leaves. The chloroplast isoform differs from the cytosolic counterpart in containing two additional, conserved Cys residues per subunit (40), which appear to account for its susceptibility to sulfhydryl reagents (72). Site-directed mutagenesis of the recombinant GS from *Canavalia lineata* showed that these two unique Cys (C306 and C371) are responsible for activation by monothiols or DTT (40). Although no Trx was tested in these experiments, earlier reports showed that reduced Trxs are significantly more efficient than DTT in the activation of GS from *Chlamydomonas reinhardtii* (72) or from *Chlorella fusca* (168).

However, the problem needs further work. The recombinant enzyme from *Canavalia* was active after isolation (DTT reduction increased activity only ~2.3-fold), thus raising the question whether this behavior is peculiar to the overexpressed enzyme or whether reduction is necessary *in vivo* and under what conditions. The issue is further complicated by the finding that mutating the active Cys residues decreased activity to a minor degree (ca. 30%)—an effect opposite to that usually observed with redox activated enzymes. Future work with the glutamine synthetase isolated from *Canavalia* leaves would help clarify the situation. Additionally, determination of the redox potential of the putative disulfide bridge could provide some information as could assessment of enzyme activity under stress (oxidizing) conditions.

b. Fdx:glutamate synthase. Fdx:glutamate synthase (Fdx-GOGAT; EC 1.4.7.1) catalyzes the conversion of glutamine and α-ketoglutarate to two glutamate molecules. In preparations from spinach and soybean chloroplasts, the enzyme was found to be significantly activated by DTT or reduced Trx, but not by GSH. The enzyme was more effectively stimulated by spinach Trx *m* than by two other Trxs tested (*E. coli* and spinach *f*-type). The main effect of reduction was an increase in reaction velocity, and there was little effect on the affinity of the enzyme for its substrates (168). Further experiments are needed to identify the disulfide(s) active in regulating this enzyme. Fdx-glutamate synthase provides an example of an enzyme that uses Fdx both directly as a substrate and indirectly as a regulator. Such a dual response to Fdx may help insure that the activity of the enzyme, which plays a central role in photorespiration, is closely tied to the illumination status of the plastid.

c. 3-Deoxy-D-arabino-heptulosonate 7-phosphate (DAHP) synthase. 3-Deoxy-D-arabino-heptulosonate 7-phosphate (DAHP) synthase (EC 2.5.1.54) is the first enzyme of the shikimate pathway that leads to the synthesis of chorismate, the precursor of branched amino acids (Phe, Trp, and Tyr) and various secondary metabolites derived from them. It catalyzes the condensation of phosphoenolpyruvate and erythrose-4-phosphate, yielding DAHP and inorganic phosphate. The activity of recombinant *Arabidopsis* DAHP synthase was shown to be redox dependent (65). A comparison of different reducing agents revealed that Trx *f* was the most efficient activator. The Cys involved in regulation are not yet known, however their alkylation with iodoacetamide yielded a permanently active enzyme, confirming that the enzyme is redox regulated. It is noteworthy that a proteomic approach indicated that an enzyme forming erythrose-4-phosphate in chloroplasts—transketolase—is also regulated by Trx (15). Thus, the carbon flow into the shikimate pathway appears also to be redox regulated via Trx.

4. Hydrogen metabolism

a. NiFe-hydrogenase. The green alga *Scenedesmus obliquus* possesses a chloroplast NiFe-hydrogenase that, under anaerobic conditions, can be used for either light-dependent hydrogen production or hydrogen uptake (photoreduction of CO_2). This hydrogenase was shown to be inhibited by reduced Trx *f* (302), thereby downregulating the production of hydrogen—a process that would compete for electrons (reducing equivalents) with

the Calvin–Benson cycle. Based on comparison of known structures of NiFe-hydrogenases, two surface-exposed Cys are proposed as possible candidates for the interaction with Trx. Recently, the crystal structures of three proteins involved in the maturation of an archael NiFe-hydrogenase have been published. Interestingly, the environment of the [4Fe–4S] cluster in one of these proteins, HypD, shows similarity to FTR, suggesting a comparable reaction pathway for the reduction of the disulfides (289). This work also poses the question of whether the Fe–S cluster of FTR had its origin in such an enzyme from an organism considered to be ancient.

5. Translation. The synthesis of certain chloroplast proteins is known to be enhanced up to 50- to 100-fold by illumination resulting from an increase in the rate of translation mediated, at least in part, by Trx. Although few specific targets have been biochemically confirmed, translation has emerged as a process extensively associated with Trx based on proteomic studies (28). One target that has been studied centers on psbA, the gene encoding the D1 protein of the photosystem II reaction center. Its protein product shows a dramatic increase in translation in the light. Initially, the translation of psbA RNA by *Chlamydomonas reinhardtii* preparations was found to be enhanced by the addition of dithiol compounds such as dithiothreitol (DTT), most effectively in the presence of Trx from *E. coli* (55). Subsequent findings indicated that translation is regulated via a Trx-mediated signal in the light in a manner proportional to the reducing potential generated by photosystem I (2, 275). According to current knowledge, the redox signal is transferred from Trx to a 60 kDa RNA binding protein (RB60)—an atypical redox-active protein disulfide isomerase (138) that contains two Trx-like domains with putative catalytic sites of Cys–Gly–His–Cys (137). Reduced RB60 interacts with high affinity specifically with RB47, forming mixed disulfides that have been experimentally identified (2). Together with RB47, RB60 is part of the psbA mRNA binding complex, which, once reduced, binds to the 5′ untranslated region of the psbA messenger RNA, thereby accelerating synthesis of the protein product.

It is not yet known which type of Trx is involved in RB60 reduction in chloroplasts, but, since Trx from *E. coli* was used in the early experiments, it would appear that *m*-type isoforms are active *in vivo*. The proposed regulatory mechanism provides a direct link between light and translation of the D1 protein—a component of the PS II reaction center known to undergo very high turnover during illumination. Regulation by the Fdx/Trx system makes it possible to adjust the rate of replacing reaction centers commensurate with the rate with which they are destroyed by photooxidation.

6. Light-harvesting antenna complex II phosphorylation. Redox regulation through Trx has been proposed to be implicated in phosphorylation of the light-harvesting antenna complex II (LHCII) of photosystem II (35) by reduction of a disulfide bond in a LHCII kinase (228). The Fdx/Trx system would provide a possible mechanism for the observed downregulation of LHCII phosphorylation at high irradiance. However, recent results raise questions as to the contribution of the Fdx/Trx system in this signaling network as it has assumed additional complexity (104, 178, 310).

7. Thylakoid electron transport chain. A model involving thiols has been proposed for the regulation (inhibition) of electron transport in chloroplasts, probably at the level of the cyt b_6/f complex. Experiments with isolated spinach thylakoids revealed that high concentrations of DTT inhibited electron transport rapidly and reversibly (133). A redox potential, $E_{m,\ pH\ 7.9} = -385$ mV with a pH dependence of about -90 mV/pH unit, was determined for the component susceptible to inhibition. Trx was suggested to be the transmitter of the thiol signal *in vivo* and was envisioned to act jointly with the "malate valve" (248) to decrease overreduction in the chloroplast under certain conditions. The "malate valve" and related electron transport were also recently found to be influenced by photoperiod, adjusting acclimation from more efficient light usage in short days to prevent oxidative damage under long-day conditions (22).

8. Detoxification.

a. 2-Cys peroxiredoxin and peroxiredoxin Q. The subject of several recent reviews (59, 234, 300), these redox-active enzymes of chloroplasts function as ubiquitous antioxidants to reduce a broad range of peroxides by intermolecular thiol–disulfide transition. One type, the 2-Cys peroxiredoxins, was found to be reduced by Trxs (196), suggesting that FTR may provide the reducing equivalents to remove peroxides *in vivo*. With a midpoint potential $E_{m,pH\ 7.0}$ of -315 mV (Table 1), it was shown that 2-Cys peroxiredoxin (from barley) can be reduced by chloroplast Trxs *f* and *m* (144) which, in turn, were reduced by FTR. However, the most efficient substrate appears to be DTT-reduced Trx *x* (see above (44)). Peroxiredoxin Q was reported to be present in the thylakoid lumen and to be most actively reduced by Trx *y*, as noted above. It has been proposed that 2-Cys peroxiredoxin reduced by Trx via Fdx and FTR could function as part of a water-to-water cycle independently of the one originally described for ascorbate (59). The route by which this could happen in the lumen remains to be identified.

Recently, a light-independent reduction of 2-Cys peroxiredoxin by a chloroplast NADPH thioredoxin reductase (NTRC) was described in rice. NTRC is a bimodular enzyme constituted of a NTR-like module at the N-terminus and a Trx-like module at the C-terminus (209). This enzyme showed higher efficiency in the reduction of 2-Cys peroxiredoxin than Trx *x* or CDSP32. This system, which can work in the light and in the dark, might be the primary reduction system for 2-Cys peroxiredoxins in stress response. In this way, harmful oxidants could be removed irrespective of illumination conditions and of the redox state of Fdx.

C. Target proteins identified by proteomic approaches

The advent of proteomics and new screening techniques, particularly Trx mutant affinity chromatography (Fig. 15) developed by Hisabori and co-workers for chloroplasts (196) has greatly extended the role of Trx in photosynthesis and beyond. The affinity procedure takes advantage of the mechanism by which Trx reduces a specific regulatory disulfide as originally shown for Trx from *E. coli* (134). As discussed above, the mechanism requires the formation of a transient heterodisulfide bond

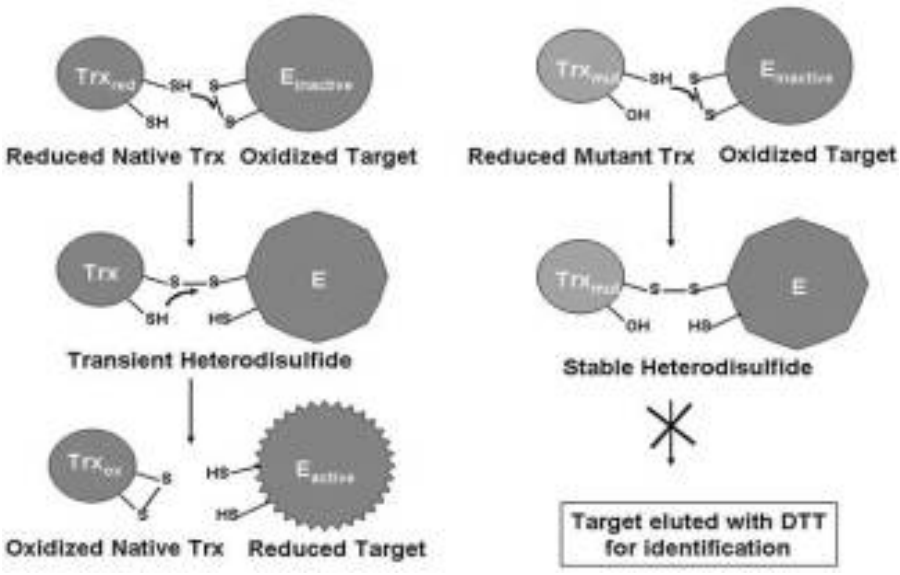

FIG. 15. The physiological mechanism by which Trx reduces a target enzyme is shown on the *left*, and the mutant Trx affinity chromatography procedure for isolating potential Trx target proteins is on the *right*. The less accessible (buried; (131, 134)) Cys of Trx is mutagenized to a serine prior to binding to an affinity column. A preparation containing Trx target proteins is applied to the column which is successively washed first with buffer, then with buffer plus NaCl, and finally with buffer plus DTT. The heterodisulfide formed between Trx and the target proteins is cleaved by the DTT, releasing the targets which are then separated on 2D IEF/SDS-PAGE gels and identified by proteomic procedures.

between Trx and enzyme prior to complete reduction of the targeted disulfide. Mutation of one of the two Cys of the Trx active site (the one buried in the molecule) stabilizes the normally transient heterodisulfide, thereby covalently linking the target protein to Trx via a bond that can be cleaved by DTT (Fig. 15). With this approach, it has been possible to confirm more than half of the known soluble Trx-regulated enzymes and to more than double the number of potential Trx-interacting proteins in chloroplasts. Most of the potential targets trapped by the column contain conserved Cys and function in chloroplast processes not previously linked to Trx (15, 196). The proteins identified function in 10 new processes (isoprenoid, tetrapyrrole, and vitamin biosynthesis, protein assembly/folding, protein and starch degradation, glycolysis, HCO_3^-/CO_2 equilibration, plastid division, and DNA replication/transcription), in addition to the five processes earlier known to be regulated by Trx (Calvin–Benson cycle, nitrogen metabolism, translation, and reductive pentose phosphate cycle).

At least three candidate targets identified in the study by Balmer *et al*. (15) have been confirmed as Trx targets in biochemical assays. One that functions in chlorophyll biosynthesis, magnesium chelatase (118), and another, β-amylase, active in the degradation of starch as discussed above. A third potential target identified with the mutant column approach, a stromal cyclophilin active as a peptidyl-prolyl cis-trans isomerase (PPIase) in protein folding (196), also appears to be linked to Trx on the basis of subsequent biochemical evidence (197). PPIase activity associated with the cyclophilin from *Arabidopsis* (AtCYP20-3), a homologue of the spinach protein identified with proteomics, was shown to be suppressed following oxidation by copper chloride and to be significantly increased by reduction via Trx *m*. Two disulfide bridges, located between Cys53-Cys170 and Cys128-Cys175 (Table 1), are responsible for its redox sensitivity. However, in contrast to these confirmatory findings, a Calvin–Benson cycle target identified using the mutant affinity technique, ribose 5-phosphate isomerase (174), has proven more problematic. Using the overexpressed enzyme, it has not been possible to demonstrate redox regulation on the basis of activity (111). It could be that the presence of a redox-active pair of conserved Cys is fortuitous or that the enzyme was trapped on the column by its association with an authentic target protein. Alternatively, the enzyme could be regulated by glutathionylation or by Trx in a process such as protein folding (28).

A fluorescent gel approach to identify potential Trx target proteins was developed, initially for seeds, in parallel with the mutant affinity column procedure (Fig. 16) (307). In several subsequent studies the two approaches were found to be complementary [*i.e*., approximately one-third of the potential targets were identified using the affinity column approach, another one-third by the fluorescent/gel approach, and the final third by both approaches (3, 19, 299)]. As with the column, almost all targets identified by the gel procedure contained conserved Cys.

The availability of these approaches has not only greatly increased the number of possible Trx-linked proteins of chloroplasts, but also extended the search for targets to other photosynthetic organisms, namely, algae (162) and cyanobacteria (170). It is significant that many of the target proteins identified in these studies were unique to each group, and, surprisingly, there were relatively few targets in common between these groups and land plants. Further, considerable information has also become available relative to the role of Trx in compartments of the plant cell such as mitochondria (20). To date, ~300 candidate targets have been identified in land plants, their organs, and organelles (3, 19, 28). Of these, ~10% have been confirmed as targets using biochemical or genetic approaches. Apropos this point, in a recent study with germinating seeds of the legume, *Medicago truncatula*, more than half of the 43 potential Trx targets identified with the mBBr labeling procedure were reduced during germination (3). In addition to extending the role of Trx to the germination of dicotyledons, the results provide evidence of the validity of the fluorescent/gel approach to identify Trx-linked proteins. It is anticipated that, as with chloroplasts, the Trx targets that are classified as "candidates" in other sources will eventually be tested to determine whether they contain Cys that are redox active and qualify as authentic

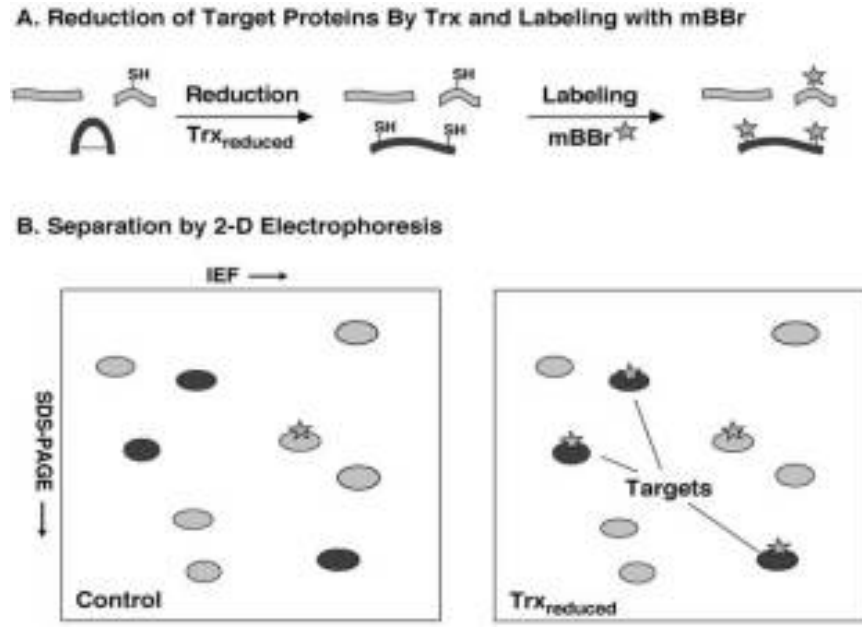

FIG. 16. Fluorescent/gel procedure for isolating potential Trx target proteins. (**A**) Preparations containing Trx target proteins are reduced by Trx, itself reduced by NADPH and NTR, and labeled with the sulfhydryl probe, mono-bromobimane (mBBr) designated by a *star*. (**B**) The preparation is then subjected to IEF and SDS-PAGE. Proteins with sulfhydryl groups form a covalent bond with mBBr. One protein shown with a sulfhydryl group prior to reduction is designated in *light gray*; proteins with sulfhydryl groups resulting from Trx reduction are *dark colored*. mBBr-labeled proteins are designated by a *star*. This procedure is often used to distinguish between proteins with intramolecular *versus* intermolecular disulfide bonds. Reproduced from ref. 307.

Trx targets. In these studies, the investigators should recall the multiple ways proteins can respond to Trx in addition to the classical regulation of enzyme activity uncovered in the early work with chloroplast FBPase (15). Finally, it is noted that in a related application of the affinity column procedure, the use of native Trx, rather than the mutant form bound to the resin, identified a number of chloroplast proteins that interact electrostatically with Trx *f* (*i.e*., without forming a covalent bond) in addition to the long known FBPase target (16).

V. REDOX REGULATION IN THE CHLOROPLAST THYLAKOID LUMEN

Recent advances in proteomics and genomics have led to the unexpected finding that the lumen, the site of oxygen evolution in chloroplast thylakoids, contains numerous enzymes in addition to those directly associated with the light reactions (208). Prominent among the lumen inhabitants are more than a dozen immunophilins, proteins that, as noted above, have PPIase activity (105). One member of this group, FKBP13, was found to contain a unique pair of disulfide bonds that is absent in animal homologs (89). In contrast to the stromal cyclophilin discussed above, these disulfides were reduced by Trx in a reaction that led to loss of the associated PPIase activity. It was suggested that FKBP13, which is synthesized in the cytosol as a precursor protein (96), is reduced by Trx on entering and traversing the stroma, perhaps to render it inactive. Once imported in the thylakoid lumen, the enzyme is converted to the active form by oxidation and interacts with the Rieske protein (31, 89). Independent evidence for the effectiveness of the oxidizing environment of the chloroplast lumen to promote disulfide bond formation has been obtained in a recent study with bacterial alkaline phosphatase (14). Both the yield and activity of this classical disulfide enzyme were greater when it was overexpressed in the lumen relative to the stroma.

Another recent study has added new information on redox regulation in the thylakoid lumen. HFC164 is a thylakoid membrane-bound protein thought to be involved in the assembly of the cytochrome b_6f complex. It is anchored by a membrane-spanning sequence and contains in the C-terminal part on the lumenal side a Trx-like CXXC motif that possesses disulfide reductase activity (166). Further analysis of this protein revealed that it is present in oxidized form in intact thylakoids and that reduced Trx *m* is able to transfer reducing equivalents across the membrane by a yet to be determined carrier to reduce its disulfide bridge ($E_{m,\,pH\,7.0} = -224$ mV). Affinity chromatography with column bound mutant HFC164 identified several thylakoid membrane proteins as possible targets (195). It will be of interest to learn whether lumenal Trx targets such as peroxiredoxin Q (210) are associated with this mechanism of transmembrane redox transfer.

VI. THE AMYLOPLAST FERREDOXIN/THIOREDOXIN SYSTEM AND ASSOCIATED TARGET PROTEINS

Heterotrophic plant tissues contain organelles that carry out many of the biosynthetic activities of chloroplasts. In starch-storing tissues, this function is served by amyloplasts—organelles that, among other activities, catalyze the synthesis and storage of copious amounts of starch. In view of their similarity to chloroplasts, the question arises whether amyloplasts also contain a Fdx/Trx system. Several earlier lines of evidence led to this possibility. (a) In contrast to long-prevailing dogma, Fdx and the enzyme catalyzing its reduction with NADPH, Fdx: NADP reductase, are not restricted to chloroplasts and occur in nonphotosynthetic tissues; (b) isolated amyloplasts contain these proteins in addition to enzymes capable of generating the NADPH needed for reduction of Trx—namely, G6PDH and 6-phosphogluconate dehydrogenase; (c) amyloplasts also contain

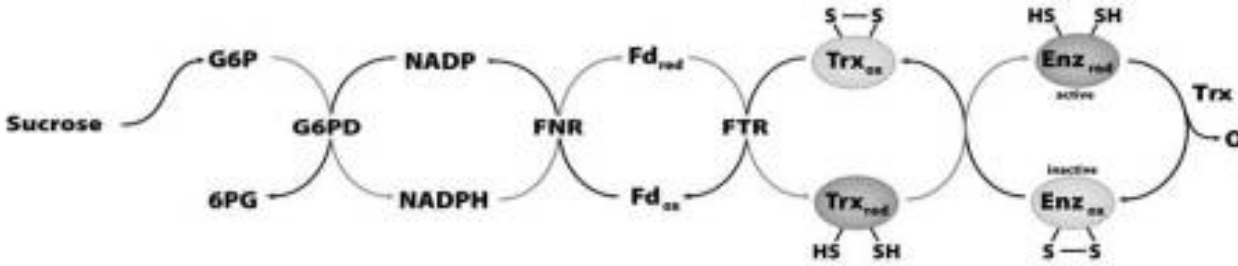

FIG. 17. Regulation of amyloplast enzymes by the Fdx/Trx system. Sucrose formed in leaves is transported to sink tissues where it is broken down to glucose-6-phosphate, generating NADPH via glucose-6-phosphate dehydrogenase (G6PDH). The NADPH is used to reduce Trx via ferredoxin:NADP reductase (FNR), ferredoxin (Fd), and FTR, similar to the mechanism identified in cyanobacterial heterocysts. Once reduced, Trx activates target enzymes as in chloroplasts. Reproduced from ref. 19.

enzymes known to be established Trx targets in chloroplasts, including AGPase and GWD; and, finally, (d) based on analysis of their proteome, isolated amyloplasts contain numerous other enzymes reported to be potential Trx targets [references in (19)].

In a recent study, Balmer *et al*. (19) built on this information (that had its origin with the Osaka group) and applied proteomic and immunological methods to identify the components of the Fdx/Trx system (Fdx, FTR, and Trx *m*) in amyloplasts isolated from wheat starchy endosperm. The authors proposed a regulatory variant in which Fdx is reduced not by light, as in chloroplasts, but by metabolically generated NADPH via Fdx:NADP reductase as established for cyanobacteria (Fig. 17). Once reduced, Fdx appears to act as in chloroplasts (*i.e*., via FTR and a Trx). The mutant column proteomics procedure in combination with the fluorescent gel approach led to the identification of 42 potential Trx target proteins in amyloplasts, 13 not previously recognized, including a major membrane transporter—Brittle-1 or ADP-glucose transporter that has since been found to be regulated by redox in physiological studies (139). Certain members of the Fdx/Trx system were earlier reported to occur in etioplasts based on proteomic analyes (140)—work that has been independently confirmed and extended in recent reports showing the presence of Trxs *m* and *f* in nonphotosynthetic organs throughout the plant (56).

The proteins identified in the amyloplast Trx study function in a range of processes in addition to starch metabolism: biosynthesis of lipids, amino acids, and nucleotides; protein folding; and several miscellaneous reactions. The results suggest a long distance communication mechanism whereby light is recognized initially as a thiol signal in chloroplasts, then as a sugar during transit to the sink, and, finally, again as a thiol signal in amyloplasts (Fig. 18). In this way, reactions of the amyloplast can be coordinated with photosynthesis taking place in leaves. The Trx-linked buildup of sucrose in illuminated leaves would increase the NADPH/NADP ratio after its transport to sink tissues, such as seeds, thereby increasing the extent of Trx reduction and, in effect, informing amyloplasts that the plant is illuminated and that associated biochemical processes should be adjusted accordingly (carbohydrate and nitrogen metabolism, and alteration of protein structure). In this way, metabolic processes in amyloplasts could be adjusted in keeping with photosynthetic activity.

VII. CONCLUSIONS AND OUTLOOK

The past five years have witnessed striking progress on the Fdx/Trx system. The structures of the members of the system have been described, including, most recently, that of FTR—the capstone of decades of effort. In addition to revealing a previously unrecognized path by which an electron signal from Fdx is converted to a thiol in Trx, this study broke new ground in our understanding not only of FTR, but also of iron–sulfur proteins and their mechanism of action in general. In experiments that complement earlier results with Trx, genetic studies

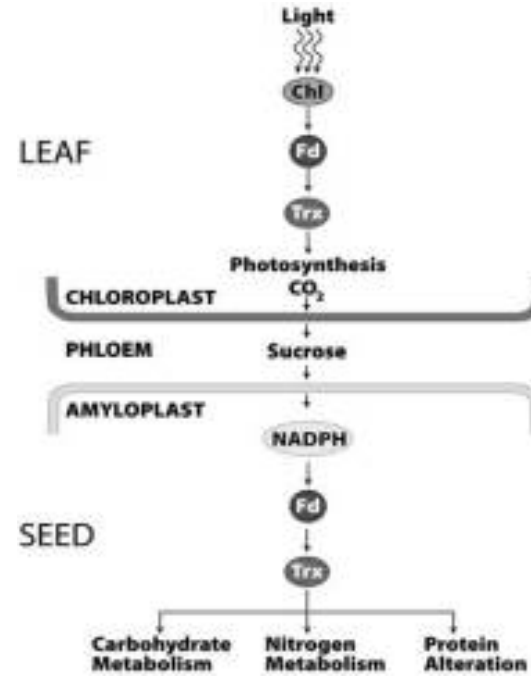

FIG. 18. Trx as a regulatory link between photosynthesis and metabolic processes in amyloplasts. The Trx-linked buildup of sucrose in illuminated leaves is envisaged to increase the NADPH/NADP ratio after transport to sink tissues, thereby increasing the extent of Trx reduction. In this way, amyloplasts are informed that the plant is illuminated such that Trx-linked biochemical processes can be adjusted accordingly. Reproduced from ref. 19.

have demonstrated a requirement for FTR for photosynthetic growth—an effect that is amplified under oxidative conditions. As a result of these findings, it becomes of interest to understand the origin of this special enzyme and how it became an integral part of oxygenic photosynthesis, seemingly at some point after the appearance of early cyanobacteria.

An advance has also been made with the elucidation of the structure and mode of regulation of GAPDH, a classical Trx target of the Calvin–Benson cycle, again after many years of research. This work has aided our understanding not only of the regulation of the Calvin–Benson cycle, but also of the function of CP12 and its deep evolutionary roots in oxygenic photosynthesis.

With respect to function, the availability of proteomic approaches has extended the potential role of the Fdx/Trx system to an extent unimaginable when the initial studies were carried out in the 1960s and 1970s. It remains an open question as to whether Trx acts in transcription in plants akin to its well-established role in animal cells. In all likelihood, new functions of plant Trxs will continue to emerge as the future unfolds, especially as additional mutants are analyzed. Research on redox regulation in the thylakoid lumen will also occupy a central position in the future.

On a related front, the elucidation of the structures of additional redox-regulated enzymes should reveal interesting details on how disulfide reduction modifies enzyme activity. As it is possible to obtain stabilized complexes between Trxs and target enzymes by the use of mutant proteins, analysis of these structures would provide valuable insight into the specificity of Trxs for their target proteins. Related studies may also answer the longstanding question of how structural Cys residues evolved to form a disulfide bond capable of responding to redox change so as to become a fundamental mechanism of enzyme regulation.

Finally, knowledge of the role of the Fdx/Trx system in amyloplasts is in its infancy and awaits further exploration. It is anticipated that major strides will be made on the role of Trx in this organelle—a problem that assumes special significance in view of the importance of the organelle to the world's food supply. A related question concerns the presence and possible function of Trx in chromoplasts, the pigmented plastids of fruits and flowers. Further research in these and related areas may lead to potential applications of the Fdx-linked Trx system similar to those identified for the NADP-linked counterpart that shows promise in solving societal problems ranging from medicine and human disease to the production and improvement of food.

In short, while our knowledge of the Fdx/Trx system has reached a certain level of maturity, it seems likely that the intriguing problems remaining will attract the attention of inquisitive scientists for years to come. Current evidence portends that decisive progress will be made on remaining problems in the next 10 years—when the redox biology field celebrates its 50th birthday in 2017.

Note added in proof:

Two relevant articles have come to our attention since this manuscript was submitted. One, a review, gives an update on glutaredoxins and thioredoxins, including those in chloroplasts (181a). The other article provides *in situ* evidence that the thioredoxin-linked regulatory disulfides of the chloroplast ATP synthase γ-subunit modulate the proton electrochemical gradient potential energy requirement for activation of the enzyme (300a).

ACKNOWLEDGMENTS

The authors thank Drs. Guido Capitani, Shaodong Dai, Hans Eklund, and David Knaff for helpful discussions, Shaodong Dai for providing Fig. 7, and Drs. Myroslawa Miginiac–Maslow and Paolo Trost for providing originals for Figs. 14 and 11, respectively. Research by PS was supported by the Schweizerischer Nationalfonds. He also thanks Dr. Jean–Marc Neuhaus for generously providing post-retirement office and laboratory space. BBB received research support from the United States Department of Agriculture, National Science Foundation, and the California Agricultural Experiment Station. He also acknowledges receipt of a Humboldt Research Award from the Alexander von Humboldt Foundation.

ABBREVIATIONS

ACCase, acetyl CoA carboxylase; AGPase, ADP-glucose pyrophosphorylase; CDSP32, **c**hloroplastic **d**rought-induced **s**tress **p**rotein; CF_1-ATPase, chloroplast ATP synthase or CF_oCF_1; CTE, C-terminal extension; DAHP, 3-deoxy-D-arabino-heptulosonate 7-phosphate; DTT, dithiothreitol; FBP, fructose 1,6-bisphosphate; FBPase, fructose 1,6-bisphosphatase; Fdx, ferredoxin; FTR, ferredoxin:thioredoxin reductase; G6PDH, glucose 6-phosphate dehydrogenase; GAPDH, NAD(P)-dependent glyceraldehyde 3-phosphate dehydrogenase; GOGAT, ferredoxin:glutamate synthase; GS, glutamine synthetase; GWD, α-glucan water dikinase; LHCII, light-harvesting antenna complex II; MGDG, monogalactosyldiacylglycerol; NADP-MDH, NADP-dependent malate dehydrogenase; NTR, NADP-thioredoxin reductase; NTRC, chloroplast NADPH thioredoxin reductase; PPIase, peptidyl-prolyl cis-trans isomerase; PRK, phosphoribulokinase; ROS, reactive oxygen species; Rubisco, ribulose 1,5-bisphosphate carboxylase/oxygenase; SBPase, sedoheptulose 1,7-bisphosphatase; TR-BAMY, Trx-regulated β-amylase; Trx, thioredoxin.

REFERENCES

1. Aguilar F, Brunner B, Gardet–Salvi L, Stutz E, and Schürmann P. Biosynthesis of active spinach-chloroplast thioredoxin *f* in transformed *E. coli*. *Plant Mol Biol* 20: 301–306, 1992.
2. Alergand T, Peled–Zehavi H, Katz Y, and Danon A. The chloroplast protein disulfide isomerase RB60 reacts with a regulatory disulfide of the RNA-binding protein RB47. *Plant Cell Physiol* 47: 540–548, 2006.
3. Alkhalfioui F, Renard M, Vensel WH, Wong J, Tanaka CK, Hurkman WJ, Buchanan BB, and Montrichard F. Thioredoxin-linked proteins are reduced during germination of Medicago truncatula seeds. *Plant Physiol* 144: 1559–1579, 2007.
4. Ashton AR, Trevanion SJ, Carr PD, Verger D, and Ollis DL. Structural basis for the light regulation of chloroplast NADP malate dehydrogenase. *Physiol Plant* 110: 314–321, 2000.

5. Baalmann E, Backhausen JE, Kitzmann C, and Scheibe R. Regulation of NADP-dependent glyceraldehyde 3-phosphate dehydrogenase activity in spinach chloroplasts. *Bot Acta* 107: 313–320, 1994.
6. Baalmann E, Backhausen JE, Rak C, Vetter S, and Scheibe R. Reductive modification and nonreductive activation of purified spinach chloroplast NADP-dependent glyceraldehyde-3-phosphate dehydrogenase. *Arch Biochem Biophys* 324: 201–208, 1995.
7. Baalmann E, Scheibe R, Cerff R, and Martin W. Functional studies of chloroplast glyceraldehyde-3-phosphate dehydrogenase subunits A and B expressed in *Escherichia coli*: formation of highly active A_4 and B_4 homotetramers and evidence that aggregation of the B_4 complex is mediated by the B subunit carboxy terminus. *Plant Mol Biol* 32: 505–513, 1996.
8. Baier M and Dietz KJ. The costs and benefits of oxygen for photosynthesizing plant cells. *Prog Bot* 60: 282–314, 1999.
9. Baier M and Dietz KJ. Chloroplasts as source and target of cellular redox regulation: a discussion on chloroplast redox signals in the context of plant physiology. *J Exp Bot* 56: 1449–1462, 2005.
10. Bald D, Noji H, Yoshida M, Hirono–Hara Y, and Hisabori T. Redox regulation of the rotation of F1-ATP synthase. *J Biol Chem* 276: 39505–39507, 2001.
11. Ball SG and Morell MK. From bacterial glycogen to starch: understanding the biogenesis of the plant starch granule. *Annu Rev Plant Biol*. 54: 207–233, 2003.
12. Ballicora MA, Frueauf JB, Fu Y, Schürmann P, and Preiss J. Activation of the potato tuber ADP-glucose pyrophosphorylase by thioredoxin. *J Biol Chem* 275: 1315–1320, 2000.
13. Ballicora MA, Iglesias AA, and Preiss J. ADP-glucose pyrophosphorylase: a regulatory enzyme for plant starch synthesis. *Photosynth Res* 79: 1–24, 2004.
14. Bally J, Paget E, Droux M, Job C, Job D, and Dubald M. Both the stroma and thylakoid lumen of tobacco chloroplasts are competent for the formation of disulphide bonds in recombinant proteins. *Plant Biotechnol J* 6: 46–61, 2008.
15. Balmer Y, Koller A, del Val G, Manieri W, Schürmann P, and Buchanan BB. Proteomics gives insight into the regulatory function of chloroplast thioredoxins. *Proc Natl Acad Sci USA* 100: 370–375, 2003.
16. Balmer Y, Koller A, del Val G, Schürmann P, and Buchanan BB. Proteomics uncovers proteins interacting electrostatically with thioredoxin in chloroplasts. *Photosynth Res* 79: 275–280, 2004.
17. Balmer Y and Schürmann P. Heterodimer formation between thioredoxin *f* and fructose 1,6-bisphosphatase from spinach chloroplasts. *FEBS Letters* 492: 58–61, 2001.
18. Balmer Y, Stritt–Etter A–L, Hirasawa M, Jacquot J–P, Keryer E, Knaff DB, and Schürmann P. Oxidation-reduction and activation properties of chloroplast fructose 1,6-bisphosphatase with mutated regulatory site. *Biochemistry* 40: 15444–15450, 2001.
19. Balmer Y, Vensel WH, Cai N, Manieri W, Schürmann P, Hurkman WJ, and Buchanan BB. A complete ferredoxin/thioredoxin system regulates fundamental processes in amyloplasts. *Proc Natl Acad Sci USA* 103: 2988–2993, 2006.
20. Balmer Y, Vensel WH, Tanaka CK, Hurkman WJ, Gelhaye E, Rouhier N, Jacquot JP, Manieri W, Schürmann P, Droux M, and Buchanan BB. Thioredoxin links redox to the regulation of fundamental processes of plant mitochondria. *Proc Natl Acad Sci USA* 101: 2642–2647, 2004.
21. Baumann U and Juttner J. Plant thioredoxins: the multiplicity conundrum. *Cell Mol Life Sci* 59: 1042–1057, 2002.
22. Becker B, Holtgrefe S, Jung S, Wunrau C, Kandlbinder A, Baier M, Dietz KJ, Backhausen JE, and Scheibe R. Influence of the photoperiod on redox regulation and stress responses in *Arabidopsis thaliana* L. (Heynh.) plants under long- and short-day conditions. *Planta* 224: 380–393, 2006.
23. Brandes HK, Larimer FW, Geck MK, Stringer CD, Schürmann P, and Hartman FC. Direct identification of the primary nucleophile of thioredoxin *f*. *J Biol Chem* 268: 18411–18414, 1993.
24. Brandes HK, Larimer FW, and Hartman FC. The molecular pathway for the regulation of phosphoribulokinase by thioredoxin *f*. *J Biol Chem* 271: 3333–3335, 1996.
25. Brinkmann H, Cerff R, Salomon M, and Soll J. Cloning and sequence analysis of cDNAs encoding the cytosolic precursors of subunits GapA and GapB of chloroplast glyceraldehyde-3-phosphate dehydrogenase from pea and spinach. *Plant Mol Biol* 13: 81–94, 1989.
26. Buchanan BB. Role of light in the regulation of chloroplast enzymes. *Annu.Rev.Plant Physiol*. 31: 341–374, 1980.
27. Buchanan BB. Thioredoxin: an unexpected meeting place. *Photosynth Res* 92: 145–148, 2007.
28. Buchanan BB and Balmer Y. Redox regulation: a broadening horizon. *Annu Rev Plant Biol* 56: 187–220, 2005.
29. Buchanan BB, Kalberer PP, and Arnon DI. Ferredoxin-activated fructose diphosphatase in isolated chloroplasts. *Biochem Biophys Res Commun* 29: 74–79, 1967.
30. Buchanan BB, Schürmann P, Wolosiuk RA, and Jacquot J–P. The ferredoxin/thioredoxin system: from discovery to molecular structures and beyond. *Photosynth Res* 73: 215–222, 2002.
31. Buchanan BB and Luan S. Redox regulation in the chloroplast thylakoid lumen: a new frontier in photosynthesis research. *J Exp Bot* 56: 1439–1447, 2005.
32. Cámara–Artigas A, Hirasawa M, Knaff DB, Wang M, and Allen JP. Crystallization and structural analysis of GADPH from *Spinacia oleracea* in a new form. *Acta Crystallograph Sect F Struct Biol Cryst Commun* 62: 1087–1092, 2006.
33. Capitani G, Markovic–Housley Z, del Val G, Morris M, Jansonius JN, and Schürmann P. Crystal structures of two functionally different thioredoxins in spinach chloroplasts. *J Mol Biol* 302: 135–154, 2000.
34. Capitani G and Schürmann P. On the quaternary assembly of spinach chloroplast thioredoxin *m*. *Photosynth Res* 79: 281–285, 2004.
35. Carlberg I, Rintamäki E, Aro E–M, and Andersson B. Thylakoid protein phosphorylation and the thiol redox state. *Biochemistry* 38: 3197–3204, 1999.
36. Carr PD, Verger D, Ashton AR, and Ollis DL. Chloroplast NADP-malate dehydrogenase: Structural basis of light-dependent regulation of activity by thiol oxidation and reduction. *Structure* 7: 461–475, 1999.
37. Casagrande S, Bonetto V, Fratelli M, Gianazza E, Eberini I, Massignan T, Salmona M, Chang G, Holmgren A, and Ghezzi P. Glutathionylation of human thioredoxin: a possible crosstalk between the glutathione and thioredoxin systems. *Proc Natl Acad Sci USA* 99: 9745–9749, 2002.
38. Cazalis R, Chueca A, Sahrawy M, and Lopez–Gorge J. Construction of chimeric cytosolic fructose-1,6-bisphosphatases by insertion of a chloroplastic redox regulatory cluster. *J Physiol Biochem* 60: 7–21, 2004.
39. Chiadmi M, Navaza A, Miginiac–Maslow M, Jacquot J-P, and Cherfils J. Redox signalling in the chloroplast: structure of oxidized pea fructose-1,6-bisphosphate phosphatase. *EMBO J* 18: 6809–6815, 1999.
40. Choi YA, Kim SG, and Kwon YM. The plastidic glutamine synthetase activity is directly modulated by means of redox change at two unique cysteine residues. *Plant Sci* 149: 175–182, 1999.
41. Chueca A, Sahrawy M, Pagano EA, and López Gorgé J. Chloroplast fructose-1,6-bisphosphatase: structure and function. *Photosynth Res* 74: 235–249, 2002.
42. Ciurli S, Carrie M, Weigel JA, Carney MJ, Stack TDP, Papaefthymiou GC, and Holm RH. Subsite-differentiated analogs of native iron sulfide $[4Fe\text{-}4S]^{2+}$ clusters: preparation of clusters with five- and six-coordinate subsites and modulation of redox potentials and charge distributions. *J Am Chem Soc* 112: 2654–2664, 1990.
43. Clasper S, Easterby JS, and Powls R. Properties of two high-molecular-mass forms of glyceraldehyde-3-phosphate dehydrogenase from spinach leaf, one of which also possesses latent phosphoribulokinase activity. *Eur J Biochem* 202: 1239–1246, 1991.
44. Collin V, Issakidis–Bourguet E, Marchand C, Hirasawa M, Lancelin JM, Knaff DB, and Miginiac–Maslow M. The *Arabidopsis* plastidial thioredoxins: new functions and new insights into specificity. *J Biol Chem* 278: 23747–23752, 2003.
45. Collin V, Lamkemeyer P, Miginiac–Maslow M, Hirasawa M, Knaff DB, Dietz KJ, and Issakidis–Bourguet E. Characterization of plastidial thioredoxins from *Arabidopsis* belonging to the new y-type. *Plant Physiol* 136: 4088–4095, 2004.

46. Cossar JD, Rowell P, and Stewart WDP. Thioredoxin as a modulator of glucose-6-phosphate dehydrogenase in a N_2-fixing cyanobacterium. *J Gen Microbiol* 130: 991–998, 1984.
47. Covès J, Block MA, Joyard J, and Douce R. Solubilization and partial purification of UDP-galactose:diacylglycerol galactosyltransferase activity from spinach chloroplast envelope. *FEBS Lett* 208: 401–406, 1986.
48. Cozens AL and Walker JE. The organization and sequence of the genes for ATP synthase subunits in the cyanobacterium *Synechococcus* 6301. Support for an endosymbiotic origin of chloroplasts. *J Mol Biol* 194: 359–383, 1987.
49. Crawford NA, Yee BC, Hutcheson SW, Wolosiuk RA, and Buchanan BB. Enzyme regulation in C4 photosynthesis: purification properties and activities of thioredoxins from C4 and C3 plants. *Arch Biochem Biophys* 244: 1–15, 1986.
50. Dai S, Friemann R, Glauser DA, Bourquin F, Manieri W, Schürmann P, and Eklund H. Structural snapshots along the reaction pathway of ferredoxin:thioredoxin reductase. *Nature* 448: 92–96, 2007.
51. Dai S, Hallberg K, Schürmann P, and Eklund H. Light/dark regulation of chloroplast metabolism. *Adv Photosyn Respir* 23: 221–236, 2006.
52. Dai S, Johansson K, Miginiac–Maslow M, Schürmann P, and Eklund H. Structural basis of redox signaling in photosynthesis: structure and function of ferredoxin:thioredoxin reductase and target enzymes. *Photosynth Res* 79: 233–248, 2004.
53. Dai S, Schwendtmayer C, Johansson K, Ramaswamy S, Schürmann P, and Eklund H. How does light regulate chloroplast enzymes? Structure–function studies of the ferredoxin/thioredoxin system. *Quart Rev Biophys* 33: 67–108, 2000.
54. Dai S, Schwendtmayer C, Schürmann P, Ramaswamy S, and Eklund H. Redox signaling in chloroplasts: Cleavage of disulfides by an iron–sulfur cluster. *Science* 287: 655–658, 2000.
55. Danon A and Mayfield SP. Light-regulated translation of chloroplast messenger RNAs through redox potential. *Science* 266: 1717–1719, 1994.
56. de Dios Barajas–Lopez J, Serrato AJ, Olmedilla A, Chueca A, and Sahrawy M. Localization in roots and flowers of pea chloroplastic thioredoxin f and thioredoxin m proteins reveals new roles in nonphotosynthetic organs. *Plant Physiol* 145: 946–960, 2007.
57. De Pascalis AR, Schürmann P, and Bosshard HR. Comparison of the binding sites of plant ferredoxin for two ferredoxin-dependent enzymes. *FEBS Lett* 337: 217–220, 1994.
58. del Val G, Maurer F, Stutz E, and Schürmann P. Modification of the reactivity of spinach chloroplast thioredoxin *f* by site-directed mutagenesis. *Plant Sci* 149: 183–190, 1999.
59. Dietz KJ, Jacob S, Oelze ML, Laxa M, Tognetti V, de Miranda SM, Baier M, and Finkemeier I. The function of peroxiredoxins in plant organelle redox metabolism. *J Exp Bot* 57: 1697–1709, 2006.
60. Dietz KJ, Link G, Pistorius EK, and Scheibe R. Redox regulation in oxigenic photosynthesis. *Prog Bot* 63: 207–245, 2002.
61. Duek PD and Wolosiuk RA. Rapeseed chloroplast thioredoxin-*m*—modulation of the affinity for target proteins. *Biochim Biophys Acta Protein Struct Mol Enzymol* 1546: 299–311, 2001.
62. Dunford RP, Durrant MC, Catley MA, and Dyer T. Location of the redox-active cysteines in chloroplast sedoheptulose-1,7-bisphosphatase indicates that its allosteric regulation is similar but not identical to that of fructose-1,6-bisphosphatase. *Photosynth Res* 58: 221–230, 1998.
63. Edner C, Li J, Albrecht T, Mahlow S, Hejazi M, Hussain H, Kaplan F, Guy C, Smith SM, Steup M, and Ritte G. Glucan, water dikinase activity stimulates breakdown of starch granules by plastidial beta-amylases. *Plant Physiol* 145: 17–28, 2007.
64. Eklund H, Gleason FK, and Holmgren A. Structural and functional relations among thioredoxins of different species. *Proteins* 11: 13–28, 1991.
65. Entus R, Poling M, and Herrmann KM. Redox regulation of Arabidopsis 3-deoxy-D-arabino-heptulosonate 7-phosphate synthase. *Plant Physiol* 129: 1866–1871, 2002.
66. Falini G, Fermani S, Ripamonti A, Sabatino P, Sparla F, Pupillo P, and Trost P. Dual coenzyme specificity of photosynthetic glyceraldehyde-3-phosphate dehydrogenase interpreted by the crystal structure of A_4 isoform complexed with NAD. *Biochemistry* 42: 4631–4639, 2003.
67. Falkenstein E, von Schaewen A, and Scheibe R. Full-length cDNA sequences for both ferredoxin-thioredoxin reductase subunits from spinach (*Spinacia oleracea* L.). *Biochim Biophys Acta* 1185: 252–254, 1994.
68. Fermani S, Ripamonti A, Sabatino P, Zanotti G, Scagliarini S, Sparla F, Trost P, and Pupillo P. Crystal structure of the non-regulatory A_4 isoform of spinach chloroplast glyceraldehyde-3-phosphate dehydrogenase complexed with NADP. *J Mol Biol* 314: 527–542, 2001.
69. Fermani S, Sparla F, Falini G, Martelli PL, Casadio R, Pupillo P, Ripamonti A, and Trost P. Molecular mechanism of thioredoxin regulation in photosynthetic A_2B_2-glyceraldehyde-3-phosphate dehydrogenase. *Proc Natl Acad Sci USA* 104: 11109–11114, 2007.
70. Ferro M, Salvi D, Brugiere S, Miras S, Kowalski S, Louwagie M, Garin J, Joyard J, and Rolland N. Proteomics of the chloroplast envelope membranes from *Arabidopsis thaliana*. *Mol Cell Proteomics* 2: 325–345, 2003.
71. Ferté N, Jacquot J–P, and Meunier JC. Structural, immunological and kinetic comparisons of NADP-dependent malate dehydrogenases from spinach (C3) and corn (C4) chloroplasts. *Eur J Biochem* 154: 587–595, 1986.
72. Florencio FJ, Gadal P, and Buchanan BB. Thioredoxin-linked activation of the chloroplast and cytosolic forms of *Chlamydomonas reinhardtii* glutamine synthetase. *Plant Physiol Biochem* 31: 649–655, 1993.
73. Florencio FJ, Pérez–Pérez ME, López–Maury L, Mata–Cabana A, and Lindahl M. The diversity and complexity of the cyanobacterial thioredoxin systems. *Photosynth Res* 89: 157–71, 2006.
74. Follmann H. Light-dark and thioredoxin-mediated metabolic redox control in plant cells. In: *The Redox State and Circadian Rhythms*, edited by Vanden Driessche T, Guisset J-L, and Petiaude Vries GM. Netherlands: Kluwer Academic Publishers, 2000, pp. 59–83.
75. Friso G, Giacomelli L, Ytterberg AJ, Peltier JB, Rudella A, Sun Q, and Wijk KJ. In-depth analysis of the thylakoid membrane proteome of *Arabidopsis thaliana* chloroplasts: new proteins, new functions, and a plastid proteome database. *Plant Cell* 16: 478–499, 2004.
76. Fu Y, Ballicora MA, Leykam JF, and Preiss J. Mechanism of reductive activation of potato tuber ADP-glucose pyrophosphorylase. *J Biol Chem* 273: 25045–25052, 1998.
77. Fukuyama K. Structure and function of plant-type ferredoxins. *Photosynth Res* 81: 289–301, 2004.
78. Galmiche JM, Girault G, Berger G, Jacquot J-P, Miginiac–Maslow M, and Wollman E. Induction by different thioredoxins of ATPase activity in coupling factor 1 from spinach chloroplasts. *Biochimie* 72: 25–32, 1990.
79. Gaymard E. 1996. *Clonage et expression de la ferrédoxine:thiorédoxine réductase de chloroplastes d'épinard*. Ph.D. thesis. University of Neuchâtel, 1–232.
80. Gaymard E, Franchini L, Manieri W, Stutz E, and Schürmann P. A dicistronic construct for the expression of functional spinach chloroplast ferredoxin:thioredoxin reductase in *E. coli*. *Plant Sci* 158: 107–113, 2000.
81. Gaymard E and Schürmann P. Cloning and expression of cDNAs coding for the spinach ferredoxin:thioredoxin reductase. In: *Photosynthesis: from Light to Biosphere*, Dordrecht: Kluwer Academic Publishers, 1995, pp. 761–764.
82. Geck MK and Hartman FC. Kinetic and mutational analyses of the regulation of phosphoribulokinase by thioredoxins. *J Biol Chem* 275: 18034–18039, 2000.
83. Geck MK, Larimer FW, and Hartman FC. Identification of residues of spinach thioredoxin *f* that influence interactions with target enzymes. *J Biol Chem* 271: 24736–24740, 1996.
84. Geigenberger P, Kolbe A, and Tiessen A. Redox regulation of carbon storage and partitioning in response to light and sugars. *J Exp Bot* 56: 1469–1479, 2005.
85. Gelhaye E, Rouhier N, Navrot N, and Jacquot JP. The plant thioredoxin system. *Cell Mol Life Sci* 62: 24–35, 2005.
86. Glauser DA, Bourquin F, Manieri W, and Schürmann P. Characterization of ferredoxin:thioredoxin reductase (FTR) modified by site-directed mutagenesis. *J Biol Chem* 279: 16662–16669, 2004.

87. Gleason FK. Glucose-6-phosphate dehydrogenase from the cyanobacterium, *Anabaena* sp PCC 7120: Purification and kinetics of redox modulation. *Arch Biochem Biophys* 334: 277–283, 1996.
88. Gomez I, Merchan F, Fernandez E, and Quesada A. NADP-malate dehydrogenase from *Chlamydomonas*: prediction of new structural determinants for redox regulation by homology modelling. *Plant Mol Biol* 48: 211–221, 2002.
89. Gopalan G, He Z, Balmer Y, Romano P, Gupta R, Heroux A, Buchanan BB, Swaminathan K, and Luan S. Structural analysis uncovers a role for redox in regulating FKBP13, an immunophilin of the chloroplast thylakoid lumen. *Proc Natl Acad Sci USA* 101: 13945–13950, 2004.
90. Goyer A, Decottignies P, Issakidis–Bourguet E, and Miginiac–Maslow M. Sites of interaction of thioredoxin with sorghum NADP-malate dehydrogenase. *FEBS Letters* 505: 405–408, 2001.
91. Goyer A, Decottignies P, Lemaire S, Ruelland E, Issakidis–Bourguet E, Jacquot J-P, and Miginiac–Maslow M. The internal Cys207 of sorghum leaf NADP-malate dehydrogenase can form mixed disulfides with thioredoxin. *FEBS Letters* 444: 165–169, 1999.
92. Graciet E, Gans P, Wedel N, Lebreton S, Camadro JM, and Gontero B. The small protein CP12: a protein linker for supramolecular complex assembly. *Biochemistry* 42: 8163–8170, 2003.
93. Graciet E, Lebreton S, and Gontero B. Emergence of new regulatory mechanisms in the Benson–Calvin pathway via protein-protein interactions: a glyceraldehyde-3-phosphate dehydrogenase/CP12/phosphoribulokinase complex. *J Exp Bot* 55: 1245–1254, 2004.
94. Graeve K, von Schaewen A, and Scheibe R. Purification, characterization, and cDNA sequence of glucose- 6-phosphate dehydrogenase from potato (*Solanum tuberosum* L.). *Plant J* 5: 353–361, 1994.
95. Groth G and Pohl E. The structure of the chloroplast F_1-ATPase at 3.2 Å resolution. *J Biol Chem* 276: 1345–1352, 2001.
96. Gupta R, Mould RM, He Z, and Luan S. A chloroplast FKBP interacts with and affects the accumulation of Rieske subunit of cytochrome *bf* complex. *Proc Natl Acad Sci USA* 99: 15806–15811, 2002.
97. Hagen KD and Meeks JC. The unique cyanobacterial protein OpcA is an allosteric effector of glucose-6-phosphate dehydrogenase in *Nostoc punctiforme* ATCC 29133. *J Biol Chem* 276: 11477–11486, 2001.
98. Halliwell B and Foyer C. Properties and physiological function of a glutathione reductase purified from spinach leaves by affinity chromatography. *Planta* 139: 9–17, 1978.
99. Harrison DH, Runquist JA, Holub A, and Miziorko HM. The crystal structure of phosphoribulokinase from *Rhodobacter sphaeroides* reveals a fold similar to that of adenylate kinase. *Biochemistry* 37: 5074–5085, 1998.
100. Hartman H, Syvanen M, and Buchanan BB. Contrasting evolutionary histories of chloroplast thioredoxins f and m. *Mol Biol Evol* 7: 247–254, 1990.
101. Hase T, Schürmann P, and Knaff DB. Ferredoxin and ferredoxin-dependent enzymes. *Adv Photosyn Resp* 24: 477–498, 2006.
102. Hatch MD. C4 photosynthesis: A unique blend of modified biochemistry, anatomy and ultrastructure. *Biochim Biophys Acta* 895: 81–106, 1987.
103. Hatch MD and Agostino A. Bilevel disulfide group reduction in the activation of C_4 leaf nicotinamide adenine dinucleotide phosphate-malate dehydrogenase. *Plant Physiol* 100: 360–366, 1992.
104. Hazra A and DasGupta M. Phosphorylation-dephosphorylation of light-harvesting complex II as a response to variation in irradiance is thiol sensitive and thylakoid sufficient: modulation of the sensitivity of the phenomenon by a peripheral component. *Biochemistry* 42: 14868–14876, 2003.
105. He Z, Li L, and Luan S. Immunophilins and parvulins. Superfamily of peptidyl prolyl isomerases in *Arabidopsis*. *Plant Physiol* 134: 1248–1267, 2004.
106. Hendriks JH, Kolbe A, Gibon Y, Stitt M, and Geigenberger P. ADP-glucose pyrophosphorylase is activated by posttranslational redox-modification in response to light and to sugars in leaves of *Arabidopsis* and other plant species. *Plant Physiol* 133: 838–849, 2003.
107. Hermoso R, Lázaro JJ, Chueca A, Sahrawy M, and López–Gorgé J. Purification and binding features of a pea fructose-1,6-bisphosphatase domain involved in the interaction with thioredoxin *f*. *Physiol Plant* 105: 756–762, 1999.
108. Hirasawa M, Droux M, Gray KA, Boyer JM, Davis DJ, Buchanan BB, and Knaff DB. Ferredoxin-thioredoxin reductase: Properties of its complex with ferredoxin. *Biochim Biophys Acta* 935: 1–8, 1988.
109. Hirasawa M, Ruelland E, Schepens I, Issakidis-Bourguet E, Miginiac-Maslow M, and Knaff DB. Oxidation-reduction properties of the regulatory disulfides of sorghum chloroplast nicotinamide adenine dinucleotide phosphate-malate dehydrogenase. *Biochemistry* 39: 3344–3350, 2000.
110. Hirasawa M, Schürmann P, Jacquot J-P, Manieri W, Jacquot P, Keryer E, Hartman FC, and Knaff DB. Oxidation-reduction properties of chloroplast thioredoxins, ferredoxin:thioredoxin reductase and thioredoxin *f*-regulated enzymes. *Biochemistry* 38: 5200–5205, 1999.
111. Hisabori T, Motohashi K, Hosoya–Matsuda N, Ueoka–Nakanishi H, and Romano PG. Towards a functional dissection of thioredoxin networks in plant cells. *Photochem Photobiol* 83: 145–151, 2007.
112. Hishiya S, Hatakeyama W, Mizota Y, Hosoya–Matsuda N, Motohashi K, Ikeuchi M, and Hisabori T. Binary reducing equivalent pathways using NADPH-thioredoxin reductase and ferredoxin-thioredoxin reductase in the cyanobacterium *Synechocystis* sp. strain PCC 6803. *Plant Cell Physiol* 49: 11–18, 2008.
113. Hodges M, Miginiac–Maslow M, Decottignies P, Jacquot J–P, Stein M, Lepiniec L, Crétin C, and Gadal P. Purification and characterization of pea thioredoxin *f* expressed in *Escherichia coli*. *Plant Mol Biol* 26: 225–234, 1994.
114. Holmgren A. Thioredoxin. *Annu.Rev.Biochem.* 54: 237–271, 1985.
115. Holmgren A, Buchanan BB, and Wolosiuk RA. Photosynthetic regulatory protein from rabbit liver is identical with thioredoxin. *FEBS Letters* 82: 351–354, 1977.
116. Hunter SC and Ohlrogge JB. Regulation of spinach chloroplast acetyl-CoA carboxylase. *Arch Biochem Biophys* 359: 170–178, 1998.
117. Hutchison RS, Groom Q, and Ort DR. Differential effects of low temperature induced oxidation on thioredoxin mediated activation of photosynthetic carbon reduction cycle enzymes. *Biochemistry* 39: 6679–6688, 2000.
118. Ikegami A, Yoshimura N, Motohashi K, Takahashi S, Romano PG, Hisabori T, Takamiya K, and Masuda T. The CHLI1 subunit of *Arabidopsis thaliana* magnesium chelatase is a target protein of the chloroplast thioredoxin. *J Biol Chem* 282: 19282–19291, 2007.
119. Issakidis E, Lemaire M, Decottignies P, Jacquot J–P, and Miginiac–Maslow M. Direct evidence for the different roles of the N- and C-terminal regulatory disulfides of sorghum leaf NADP-malate dehydrogenase in its activation by reduced thioredoxin. *FEBS Letters* 392: 121–124, 1996.
120. Issakidis E, Miginiac–Maslow M, Decottignies P, Jacquot J–P, Crétin C, and Gadal P. Site-directed mutagenesis reveals the involvement of an additional thioredoxin-dependent regulatory site in the activation of recombinant sorghum leaf NADP-malate dehydrogenase. *J Biol Chem* 267: 21577–21583, 1992.
121. Issakidis E, Saarinen M, Decottignies P, Jacquot J–P, Crétin C, Gadal P, and Miginiac–Maslow M. Identification and characterization of the second regulatory disulfide bridge of recombinant sorghum leaf NADP-malate dehydrogenase. *J Biol Chem* 269: 3511–3517, 1994.
122. Issakidis–Bourguet E, Lavergne D, Trivelli X, Decottignies JP, and Miginiac–Maslow M. Transferring redox regulation properties from sorghum NADP-malate dehydrogenase to *Thermus* NAD-malate dehydrogenase. *Photosynth Res* 89: 213–223, 2006.
123. Issakidis–Bourguet E, Mouaheb N, Meyer Y, and Miginiac–Maslow M. Heterologous complementation of yeast reveals a new putative function for chloroplast *m*-type thioredoxin. *Plant J* 25: 127–135, 2001.

124. Jacquot JP, Gelhaye E, Rouhier N, Corbier C, Didierjean C, and Aubry A. Thioredoxins and related proteins in photosynthetic organisms: molecular basis for thiol dependent regulation. *Biochem Pharmacol* 64: 1065–1069, 2002.
125. Jacquot JP, Rouhier N, and Gelhaye E. Redox control by dithiol-disulfide exchange in plants: I. The chloroplastic systems. *Ann NY Acad Sci* 973: 508–519, 2002.
126. Jacquot J-P, Lancelin J–M, and Meyer Y. Thioredoxins: structure and function in plant cells. *New Phytol* 136: 543–570, 1997.
127. Jacquot J-P, López–Jaramillo J, Chueca A, Cherfils J, Lemaire S, Chedozeau B, Miginiac–Maslow M, Decottignies P, Wolosiuk RA, and Gorgé JL. High-level expression of recombinant pea chloroplast fructose-1,6-bisphosphatase and mutagenesis of its regulatory site. *Eur J Biochem* 229: 675–681, 1995.
128. Jacquot J–P, López–Jaramillo J, Miginiac–Maslow M, Lemaire S, Cherfils J, Chueca A, and Lopez–Gorge J. Cysteine-153 is required for redox regulation of pea chloroplast fructose-1,6-bisphosphatase. *FEBS Letters* 401: 143–147, 1997.
129. Jacquot J–P, Stein M, Suzuki K, Liottet S, Sandoz G, and Miginiac–Maslow M. Residue Glu-91 of *Chlamydomonas reinhardtii* ferredoxin is essential for electron transfer to ferredoxin-thioredoxin reductase. *FEBS Letters* 400: 293–296, 1997.
130. Jameson GNL, Walters EM, Manieri W, Schürmann P, Johnson MK, and Huynh BH. Spectroscopic evidence for site specific chemistry at a unique iron site of the [4Fe–4S] cluster in ferredoxin:thioredoxin reductase. *J Am Chem Soc* 125: 1146–1147, 2003.
131. Jeng M–F, Campbell AP, Begley T, Holmgren A, Case DA, Wright PE, and Dyson HJ. High-resolution solution structures of oxidized and reduced *Escherichia coli* thioredoxin. *Structure* 2: 853–868, 1994.
132. Johansson K, Ramaswamy S, Saarinen M, Lemaire–Chamley M, Issakidis–Bourguet E, Miginiac–Maslow M, and Eklund H. Structural basis for light activation of a chloroplast enzyme. The structure of sorghum NADP-malate dehydrogenase in its oxidized form. *Biochemistry* 38: 4319–4326, 1999.
133. Johnson GN. Thiol regulation of the thylakoid electron transport chain–a missing link in the regulation of photosynthesis? *Biochemistry* 42: 3040–3044, 2003.
134. Kallis G and Holmgren A. Differential reactivity of the functional sulfhydryl groups of cysteine-32 and cysteine-35 present in the reduced form of thioredoxin from *Escherichia coli*. *J Biol Chem* 255: 10261–10265, 1980.
135. Katti SK, LeMaster DM, and Eklund H. Crystal structure of thioredoxin from *Escherichia coli* at 1.68 Å resolution. *J Mol Biol* 212: 167–184, 1990.
136. Keryer E, Collin V, Lavergne D, Lemaire S, and Issakidis–Bourguet E. Characterization of *Arabidopsis* mutants for the variable subunit of ferredoxin:thioredoxin reductase. *Photosynth Res* 79: 265–274, 2004.
137. Kim J and Mayfield SP. The active site of the thioredoxin-like domain of chloroplast protein disulfide isomerase, RB60, catalyzes the redox-regulated binding of chloroplast poly(A)-binding protein, RB47, to the 5' untranslated region of psbA mRNA. *Plant Cell Physiol* 43: 1238–1243, 2002.
138. Kim JM and Mayfield SP. Protein disulfide isomerase as a regulator of chloroplast translational activation. *Science* 278: 1954–1957, 1997.
139. Kirchberger S, Leroch M, Huynen MA, Wahl M, Neuhaus HE, and Tjaden J. Molecular and biochemical analysis of the plastidic ADP-glucose transporter (ZmBT1) from *Zea mays*. *J Biol Chem* 282: 22481–22491, 2007.
140. Kleffmann T, von Zychlinski A, Russenberger D, Hirsch–Hoffmann M, Gehrig P, Gruissem W, and Baginsky S. Proteome dynamics during plastid differentiation in rice. *Plant Physiol* 143: 912–923, 2007.
141. Knaff DB. Oxidation-reduction properties of thioredoxins and thioredoxin-regulated enzymes. *Physiol Plant* 110: 309–313, 2000.
142. Kobayashi D, Tamoi M, Iwaki T, Shigeoka S, and Wadano A. Molecular characterization and redox regulation of phosphoribulokinase from the cyanobacterium *Synechococcus* sp. PCC 7942. *Plant Cell Physiol* 44: 269–276, 2003.
143. Kolbe A, Tiessen A, Schluepmann H, Paul M, Ulrich S, and Geigenberger P. Trehalose 6-phosphate regulates starch synthesis via posttranslational redox activation of ADP-glucose pyrophosphorylase. *Proc Natl Acad Sci USA* 102: 11118–11123, 2005.
144. König J, Baier M, Horling F, Kahmann U, Harris G, Schürmann P, and Dietz KJ. The plant-specific function of 2-Cys peroxiredoxin-mediated detoxification of peroxides in the redox hierarchy of photosynthetic electron flux. *Proc Natl Acad Sci USA* 99: 5738–5743, 2002.
145. König J, Lotte K, Plessow R, Brockhinke A, Baier M, and Dietz KJ. Reaction mechanism of plant 2-Cys peroxiredoxin. Role of the C terminus and the quaternary structure. *J Biol Chem* 278: 24409–24420, 2003.
146. Konno H, Suzuki T, Bald D, Yoshida M, and Hisabori T. Significance of the epsilon subunit in the thiol modulation of chloroplast ATP synthase. *Biochem Biophys Res Commun* 318: 17–24, 2004.
147. Kozaki A, Kamada K, Nagano Y, Iguchi H, and Sasaki Y. Recombinant carboxyltransferase responsive to redox of pea plastidic acetyl-CoA carboxylase. *J Biol Chem* 275: 10702–10708, 2000.
148. Kozaki A and Sasaki Y. Light-dependent changes in redox status of the plastidic acetyl-CoA carboxylase and its regulatory component. *Biochem J* 339: 541–546, 1999.
149. Kozaki AK, Mayumi K, and Sasaki Y. Thiol-disulfide exchange between nuclear-encoded and chloroplast-encoded subunits of pea acetyl-CoA carboxylase. *J Biol Chem* 276: 39919–39925, 2001.
150. Kramer DM, Wise RR, Frederick JR, Alm DM, Hesketh JD, Ort DR, and Crofts AR. Regulation of coupling factor in field-grown sunflower: A redox model relating coupling factor activity to the activities of other thioredoxin-dependent chloroplast enzymes. *Photosynth Res* 26: 213–222, 1990.
151. Krimm I, Goyer A, Issakidis–Bourguet E, Miginiac–Maslow M, and Lancelin J–M. Direct NMR observation of the thioredoxin-mediated reduction of the chloroplast NADP-malate dehydrogenase provides a structural basis for the relief of autoinhibition. *J Biol Chem* 274: 34539–34542, 1999.
152. Laloi C, Rayapuram N, Chartier Y, Grienenberger JM, Bonnard G, and Meyer Y. Identification and characterization of a mitochondrial thioredoxin system in plants. *Proc Natl Acad Sci USA* 98: 14144–14149, 2001.
153. Lamkemeyer P, Laxa M, Collin V, Li W, Finkemeier I, Schottler MA, Holtkamp V, Tognetti VB, Issakidis–Bourguet E, Kandlbinder A, Weis E, Miginiac–Maslow M, and Dietz KJ. Peroxiredoxin Q of *Arabidopsis thaliana* is attached to the thylakoids and functions in context of photosynthesis. *Plant J* 45: 968–981, 2006.
154. Lamotte–Guéry Fd, Miginiac–Maslow M, Decottignies P, Stein M, Minard P, and Jacquot J–P. Mutation of a negatively charged amino acid in thioredoxin modifies its reactivity with chloroplastic enzymes. *Eur J Biochem* 196: 287–294, 1991.
155. Lancelin JM, Guilhaudis L, Krimm I, Blackledge MJ, Marion D, and Jacquot J–P. NMR structures of thioredoxin *m* from the green alga *Chlamydomonas reinhardtii*. *Proteins* 41: 334–349, 2000.
156. Laughner BJ, Sehnke PC, and Ferl RJ. A novel nuclear member of the thioredoxin superfamily. *Plant Physiol* 118: 987–996, 1998.
157. Laurent TC, Moore EC, and Reichard P. Enzymatic synthesis of deoxyribonucleotides. IV. Isolation and characterization of thioredoxin the hydrogen donor from *Escherichia coli* B. *J Biol Chem* 239: 3436–3444, 1964.
158. Leegood RC and Walker DA. Regulation of fructose-1,6-bisphosphatase activity in intact chloroplasts. Studies of the mechanism of inactivation. *Biochim Biophys Acta Bio-Energetics* 593: 362–370, 1980.
159. Lefebvre S, Lawson T, Zakhleniuk OV, Lloyd JC, Raines CA, and Fryer M. Increased sedoheptulose-1,7-bisphosphatase activity in transgenic tobacco plants stimulates photosynthesis and growth from an early stage in development. *Plant Physiol* 138: 451–460, 2005.

159a. Lehninger, Principles of Biochemistry, 4th Edition, by Nelson DL and Cox MM, W.H. Freeman Co., New York, 2004.

160. Lemaire SD, Collin V, Keryer E, Issakidis–Bourguet E, Lavergne D, and Miginiac–Maslow M. *Chlamydomonas reinhardtii*: a model organism for the study of the thioredoxin family. *Plant Physiol Biochem* 41: 513–521, 2003.
161. Lemaire SD, Collin V, Keryer E, Quesada A, and Miginiac–Maslow M. Characterization of thioredoxin *y*, a new type of thioredoxin identified in the genome of *Chlamydomonas reinhardtii*. *FEBS Lett* 543: 87–92, 2003.
162. Lemaire SD, Guillon B, Le Marechal P, Keryer E, Miginiac–Maslow M, and Decottignies P. New thioredoxin targets in the unicellular photosynthetic eukaryote *Chlamydomonas reinhardtii*. *Proc Natl Acad Sci USA* 101: 7475–7480, 2004.
163. Lemaire SD, Michelet L, Zaffagnini M, Massot V, and Issakidis–Bourguet E. Thioredoxins in chloroplasts. *Curr Genet* 51: 343–365, 2007.
164. Lemaire SD and Miginiac–Maslow M. The thioredoxin superfamily in *Chlamydomonas reinhardtii*. *Photosynth Res* 82: 203–220, 2004.
165. Lemaire SD, Quesada A, Merchan F, Corral JM, Igeno MI, Keryer E, Issakidis–Bourguet E, Hirasawa M, Knaff DB, and Miginiac–Maslow M. NADP-malate dehydrogenase from unicellular green alga *Chlamydomonas reinhardtii*. A first step toward redox regulation? *Plant Physiol* 137: 514–521, 2005.
166. Lennartz K, Plücken H, Seidler A, Westhoff P, Bechtold N, and Meierhoff K. *HCF164* encodes a thioredoxin-like protein involved in the biogenesis of the cytochrome b_6f complex in Arabidopsis. *Plant Cell* 13: 2539–2551, 2001.
167. Levings CS, III and Siedow JN. Regulation by redox poise in chloroplasts. *Science* 268: 695–696, 1995.
168. Lichter A and Häberlein I. A light-dependent redox signal participates in the regulation of ammonia fixation in chloroplasts of higher plants. Ferredoxin:glutamate synthase is a thioredoxin-dependent enzyme. *J Plant Physiol* 153: 83–90, 1998.
169. Lillig CH and Holmgren A. Thioredoxin and related molecules—from biology to health and disease. *Antioxid Redox Signal* 9: 25–47, 2007.
170. Lindahl M and Florencio FJ. Thioredoxin-linked processes in cyanobacteria are as numerous as in chloroplasts, but targets are different. *Proc Natl Acad Sci USA* 100: 16107–16112, 2003.
171. López–Jaramillo J, Chueca A, Jacquot J–P, Hermoso R, Lázaro JJ, Sahrawy M, and Gorgé JL. High-yield expression of pea thioredoxin *m* and assessment of its efficiency in chloroplast fructose-1,6-bisphosphatase activation. *Plant Physiol* 114: 1169–1175, 1997.
172. Maeda K, Hagglund P, Finnie C, Svensson B, and Henriksen A. Structural basis for target protein recognition by the protein disulfide reductase thioredoxin. *Structure* 14: 1701–1710, 2006.
173. Manieri W, Franchini L, Raeber L, Dai S, Stritt–Etter A–L, and Schürmann P. N-terminal truncation of the variable subunit stabilizes spinach ferredoxin:thioredoxin reductase . *FEBS Lett* 549: 167–170, 2003.
174. Marchand C, Le Marechal P, Meyer Y, Miginiac–Maslow M, Issakidis–Bourguet E, and Decottignies P. New targets of *Arabidopsis* thioredoxins revealed by proteomic analysis. *Proteomics* 4: 2696–2706, 2004.
175. Marcus F, Chamberlain SH, Chu C, Masiarz FR, Shin S, Yee BC, and Buchanan BB. Plant thioredoxin *h*: An animal-like thioredoxin occurring in multiple cell compartments. *Arch Biochem Biophys* 287: 195–198, 1991.
176. Maréchal E, Miège C, Block MA, Douce R, and Joyard J. The catalytic site of monogalactosyldiacylglycerol synthase from spinach chloroplast envelope membranes. *J Biol Chem* 270: 5714–5722, 1995.
177. Marri L, Trost P, Pupillo P, and Sparla F. Reconstitution and properties of the recombinant glyceraldehyde-3-phosphate dehydrogenase/CP12/phosphoribulokinase supramolecular complex of *Arabidopsis*. *Plant Physiol* 139: 1433–1443, 2005.
178. Martinsuo P, Pursiheimo S, Aro E–M, and Rintamäki E. Dithiol oxidant and disulfide reductant dynamically regulate the phosphorylation of light-harvesting complex II proteins in thylakoid membranes. *Plant Physiol* 133: 37–46, 2003.
179. McCarn DF, Whitaker RA, Alam J, Vrba J, and Curtis SE. Genes encoding the alpha, gamma, delta, and four F_0 subunits of ATP synthase constitute an operon in the cyanobacterium *Anabaena* sp. strain PCC 7120. *J Bacteriol* 170: 3448–3458, 1988.
179a. Mestres-Ortega D and Meyer Y. The *Arabidopsis thaliana* genome encodes at least four thioredoxins *m* and a new prokaryotic-like thioredoxin. *Gene* 240: 307–316, 1999.
180. Meyer Y, Miginiac–Maslow M, Schürmann P, and Jacquot J–P. Protein-protein interactions in the plant thioredoxin dependent systems. *Annu Plant Reviews* 7: 1–29, 2002.
181. Meyer Y, Reichheld JP, and Vignols F. Thioredoxins in *Arabidopsis* and other plants. *Photosynth Res* 86: 419–433, 2005.
181a. Meyer Y, Siala W, Bashandy T, Riondet C, Vignols F, and Reichheld JP. Glutaredoxins and thioredoxins in plants. *Biochim Biophys Acta* 2008 (in press).
182. Meyer Y, Vignols F, and Reichheld JP. Classification of plant thioredoxins by sequence similarity and intron position. *Methods Enzymol* 347: 394–402, 2002.
183. Michelet L, Zaffagnini M, Marchand C, Collin V, Decottignies P, Tsan P, Lancelin JM, Trost P, Miginiac–Maslow M, Noctor G, and Lemaire SD. Glutathionylation of chloroplast thioredoxin *f* is a redox signaling mechanism in plants. *Proc Natl Acad Sci USA* 102: 16478–16483, 2005.
184. Michelet L, Zaffagnini M, Massot V, Keryer E, Vanacker H, Miginiac–Maslow M, Issakidis–Bourguet E, and Lemaire SD. Thioredoxins, glutaredoxins and glutathionylation: new crosstalks to explore. *Photosynth Res* 89: 225–245, 2006.
185. Michels AK, Wedel N, and Kroth PG. Diatom plastids possess a phosphoribulokinase with an altered regulation and no oxidative pentose phosphate pathway. *Plant Physiol* 137: 911–920, 2005.
186. Miège C, Maréchal E, Shimojima M, Awai K, Block MA, Ohta H, Takamiya K, Douce R, and Joyard J. Biochemical and topological properties of type A MGDG synthase, a spinach chloroplast envelope enzyme catalyzing the synthesis of both prokaryotic and eukaryotic MGDG. *Eur J Biochem* 265: 990-1001, 1999.
187. Miginiac–Maslow M, Issakidis E, Lemaire M, Ruelland E, Jacquot J–P, and Decottignies P. Light-dependent activation of NADP-malate dehydrogenase: a complex process. *Aust J Plant Physiol* 24: 529–542, 1997.
188. Miginiac–Maslow M, Johansson K, Ruelland E, Issakidis–Bourguet E, Schepens I, Goyer A, Lemaire–Chamley M, Jacquot J–P, Le Maréchal P, and Decottignies P. Light-activation of NADP-malate dehydrogenase: A highly controlled process for an optimized function. *Physiol Plant* 110: 322–329, 2000.
189. Miginiac–Maslow M and Lancelin J–M. Intrasteric inhibition in redox signalling: Light activation of NADP-malate dehydrogenase. *Photosynth Res* 72: 1–12, 2002.
190. Miki J, Maeda M, Mukohata Y, and Futai M. The γ-subunit of ATP synthase from spinach chloroplasts. Primary structure deduced from the cloned cDNA sequence. *FEBS Lett* 232: 221–226, 1988.
191. Mikkelsen R, Mutenda KE, Mant A, Schürmann P, and Blennow A. α-Glucan, water dikinase (GWD): A plastidic enzyme with redox-regulated and coordinated catalytic activity and binding affinity. *Proc Natl Acad Sci USA* 102: 1785–1790, 2005.
192. Mills JD, Mitchell P, and Schürmann P. Modulation of coupling factor ATPase activity in intact chloroplasts. The role of the thioredoxin system. *FEBS Lett* 112: 173–177, 1980.
193. Mora–García S, Rodriguez–Suárez RJ, and Wolosiuk RA. Role of electrostatic interactions on the affinity of thioredoxin for target proteins. Recognition of chloroplast fructose-1,6-bisphosphatase by mutant *Escherichia coli* thioredoxins. *J Biol Chem* 273: 16273–16280, 1998.
194. Mora–Garcia S, Stolowicz FG, and Wolosiuk RA. Redox signal transduction in plant metabolism. *Annu Plant Rev* 22: 150–186, 2006.
195. Motohashi K and Hisabori T. HCF164 receives the reducing equivalents from stroma thioredoxin across thylakoid membrane and mediates reduction of target proteins in thylakoid lumen. *J Biol Chem* 281: 35039–35947, 2006.
196. Motohashi K, Kondoh A, Stumpp MT, and Hisabori T. Comprehensive survey of proteins targeted by chloroplast thioredoxin. *Proc Natl Acad Sci USA* 98: 11224–11229, 2001.
197. Motohashi K, Koyama F, Nakanishi Y, Ueoka–Nakanishi H, and Hisabori T. Chloroplast cyclophilin is a target protein of thioredoxin. Thiol modulation of the peptidyl-prolyl cis-trans isomerase activity. *J Biol Chem* 278: 31848–31852, 2003.

198. Navrot N, Collin V, Gualberto J, Gelhaye E, Hirasawa M, Rey P, Knaff DB, Issakidis E, Jacquot JP, and Rouhier N. Plant glutathione peroxidases are functional peroxiredoxins distributed in several subcellular compartments and regulated during biotic and abiotic stresses. *Plant Physiol* 142: 1364–1379, 2006.
199. Neira JL, González C, Toiron C, De Prat–Gay G, and Rico M. Three-dimensional solution structure and stability of thioredoxin *m* from spinach. *Biochemistry* 40: 15246–15256, 2001.
200. Nishizawa AN and Buchanan BB. Enzyme regulation in C4 photosynthesis. Purification and properties of thioredoxin-linked fructose bisphosphatase and sedoheptulose bisphosphatase from corn leaves. *J Biol Chem* 256: 6119–6126, 1981.
201. Nowak KF and McCarty RE. Regulatory role of the C-terminus of the epsilon subunit from the chloroplast ATP synthase. *Biochemistry* 43: 3273–3279, 2004.
202. Ocheretina O, Haferkamp I, Tellioglu H, and Scheibe R. Light-modulated NADP-malate dehydrogenases from mossfern and green algae: insights into evolution of the enzyme's regulation. *Gene* 258: 147–154, 2000.
203. Ocón E, Hermoso R, Chueca A, and Lázaro JJ. Cross-linking between chloroplast fructose-1,6-bisphosphatase and thioredoxin *f*. *Physiol Plant* 113: 452–460, 2001.
204. Oesterhelt C, Klocke S, Holtgrefe S, Linke V, Weber AP, and Scheibe R. Redox regulation of chloroplast enzymes in *Galdieria sulphuraria* in view of eukaryotic evolution. *Plant Cell Physiol* 48: 1359–1373, 2007.
205. Ohlrogge J and Browse J. Lipid biosynthesis. *The Plant Cell* 7: 957–970, 1995.
206. Ort DR and Oxborough K. In situ regulation of chloroplast coupling factor activity. *Annu Rev Plant Physiol Plant Mol Biol* 43: 269–291, 1992.
207. Pancic PG and Strotmann H. Structure of the nuclear encoded γ-subunit of CF_0CF_1 of the diatom *Odontella sinensis* including its presequence. *FEBS Lett* 320: 61–66, 1993.
208. Peltier JB, Emanuelsson O, Kalume DE, Ytterberg J, Friso G, Rudella A, Liberles DA, Söderberg L, Roepstorff P, Von Heijne G, and van Wijk KJ. Central functions of the lumenal and peripheral thylakoid proteome of *Arabidopsis* determined by experimentation and genome-wide prediction. *Plant Cell* 14: 211–236, 2002.
209. Perez–Ruiz JM, Spinola MC, Kirchsteiger K, Moreno J, Sahrawy M, and Cejudo FJ. Rice NTRC is a high-efficiency redox system for chloroplast protection against oxidative damage. *Plant Cell* 18: 2356–2368, 2006.
210. Petersson UA, Kieselbach T, Garcia–Cerdan JG, and Schroder WP. The Prx Q protein of *Arabidopsis thaliana* is a member of the luminal chloroplast proteome. *FEBS Lett* 580: 6055–6061, 2006.
211. Pinçon F, Chaillou S, and Issakidis–Bourguet E. Redox regulation of plastidic glucose-6-phosphate dehydrogenase from *Arabidopsis thaliana* by thioredoxins: a revisited relationship. *Conference on ROS in Plants*: September 12–14, 2007, Ghent, Belgium (Abstr.).
212. Porter MA. The aggregation states of spinach phosphoribulokinase. *Planta* 181: 349–357, 1990.
213. Porter MA and Hartman FC. Exploration of the function of a regulatory sulfhydryl of phosphoribulokinase from spinach. *Arch Biochem Biophys* 281: 330–334, 1990.
214. Porter MA, Potter MD, and Hartman FC. Affinity labeling of spinach phosphoribulokinase subsequent to *S*-methylation at Cys16. *J Protein Chem* 9: 445–452, 1990.
215. Porter MA, Stringer CD, and Hartman FC. Characterization of the regulatory thioredoxin site of phosphoribulokinase. *J Biol Chem* 263: 123–129, 1988.
216. Portis AR, Jr. and Salvucci ME. The discovery of Rubisco activase —yet another story of serendipity. *Photosynth Res* 73: 257–264, 2002.
217. Portis AR. Rubisco activase: Rubisco's catalytic chaperone. *Photosynth Res* 75: 11–27, 2003.
218. Preiss J. Regulation of the biosynthesis and degradation of starch. *Annu Rev Plant Physiol* 33: 431–454, 1982.
219. Qi J, Isupov MN, Littlechild JA, and Anderson LE. Chloroplast glyceraldehyde-3-phosphate dehydrogenase contains a single disulfide bond located in the C-terminal extension to the B subunit. *J Biol Chem* 276: 35247–35252, 2001.
220. Raines CA, Harrison EP, Ölçer H, and Lloyd JC. Investigating the role of the thiol-regulated enzyme sedoheptulose-1,7-bisphosphatase in the control of photosynthesis. *Physiol Plant* 110: 303–308, 2000.
221. Raines CA, Lloyd JC, and Dyer TA. New insights into the structure and function of sedoheptulose-1,7-bisphosphatase; an important but neglected Calvin cycle enzyme. *J Exp Bot* 50: 1–8, 1999.
222. Reichert A, Baalmann E, Vetter S, Backhausen JE, and Scheibe R. Activation properties of the redox-modulated chloroplast enzymes glyceraldehyde 3-phosphate dehydrogenase and fructose-1,6-bisphosphatase. *Physiol Plant* 110: 330–341, 2000.
223. Reichert A, Dennes A, Vetter S, and Scheibe R. Chloroplast fructose 1,6-bisphosphatase with changed redox modulation: comparison of the *Galdieria* enzyme with cysteine mutants from spinach. *Biochim Biophys Acta* 1645: 212–217, 2003.
224. Reith M and Munholland J. Complete nucleotide sequence of the *Porphyra purpurea* chloroplast genome. *Plant Mol Biol Reptr* 13: 333–335, 1997.
225. Rey P, Cuiné S, Eymery F, Garin J, Court M, Jacquot J-P, Rouhier N, and Broin M. Analysis of the proteins targeted by CDSP32, a plastidic thioredoxin participating in oxidative stress responses. *Plant J* 41: 31–42, 2005.
226. Reynolds AE, Chesnick JM, Woolford J, and Cattolico RA. Chloroplast encoded thioredoxin genes in the red algae *Porphyra yezoensis* and *Griffithsia pacifica*: Evolutionary implications. *Plant Mol Biol* 25: 13–21, 1994.
227. Riessland R and Jaenicke R. Determination of the regulatory disulfide bonds of NADP-dependent malate dehydrogenase from *Pisum sativum* by site-directed mutagenesis. *Biol Chem Hoppe Seyler* 378: 983–988, 1997.
228. Rintamäki E, Martinsuo P, Pursiheimo S, and Aro E–M. Cooperative regulation of light-harvesting complex II phosphorylation via the plastoquinol and ferredoxin-thioredoxin system in chloroplasts. *Proc Natl Acad Sci USA* 97: 11644–11649, 2000.
229. Rodriguez–Suárez RJ, Mora–García S, and Wolosiuk RA. Characterization of cysteine residues involved in the reductive activation and the structural stability of rapeseed (*Brassica napus*) chloroplast fructose-1,6-bisphosphatase. *Biochem Biophys Res Commun* 232: 388–393, 1997.
230. Ross SA, Zhang MX, and Selman BR. Role of the *Chlamydomonas reinhardtii* coupling factor 1 gamma-subunit cysteine bridge in the regulation of ATP synthase. *J Biol Chem* 270: 9813–9818, 1995.
231. Ross SA, Zhang MX, and Selman BR. A role for the disulfide bond spacer region of the *Chlamydomonas reinhardtii* coupling factor 1 γ-subunit in redox regulation of ATP synthase. *J Bioenerg Biomembr* 28: 49–57, 1996.
232. Rouhier N, Gelhaye E, Gualberto JM, Jordy MN, De Fay E, Hirasawa M, Duplessis S, Lemaire SD, Frey P, Martin F, Manieri W, Knaff DB, and Jacquot JP. Poplar peroxiredoxin Q. A thioredoxin-linked chloroplast antioxidant functional in pathogen defense. *Plant Physiol* 134: 1027–1038, 2004.
233. Rouhier N, Gelhaye E, and Jacquot JP. Redox control by dithiol-disulfide exchange in plants: II. The cytosolic and mitochondrial systems. *Ann NY Acad Sci* 973: 520–528, 2002.
234. Rouhier N and Jacquot JP. The plant multigenic family of thiol peroxidases. *Free Radic Biol Med* 38: 1413–1421, 2005.
235. Rouhier N, Lemaire SD, and Jacquot J–P. The role of glutathione in photosynthetic organisms: emerging functions for glutaredoxins and glutathionylation. *Annu Rev Plant Biol* 59: in press, 2008.
236. Ruelland E, Johansson K, Decottignies P, Djukic N, and Miginiac–Maslow M. The autoinhibition of sorghum NADP malate dehydrogenase is mediated by a C-terminal negative charge. *J Biol Chem* 273: 33482–33488, 1998.
237. Ruelland E, Lemaire–Chamley M, Le Maréchal P, Issakidis–Bourguet E, Djukic N, and Miginiac–Maslow M. An internal cysteine is involved in the thioredoxin-dependent activation of sorghum leaf NADP-malate dehydrogenase. *J Biol Chem* 272: 19851-19857, 1997.
238. Sahrawy M, Hecht V, López–Jaramillo J, Chueca A, Chartier Y, and Meyer Y. Intron position as an evolutionary marker of thioredoxins and thioredoxin domains. *J Mol Evol* 42: 422-431, 1996.

239. Salamon Z, Tollin G, Hirasawa M, Gardet–Salvi L, Stritt–Etter AL, Knaff DB, and Schürmann P. The oxidation-reduction properties of spinach thioredoxins *f* and *m* and of ferredoxin:thioredoxin reductase. *Biochim Biophys Acta* 1230: 114–118, 1995.
240. Sasaki Y, Konishi T, and Nagano Y. The compartmentation of acetyl-coenzyme A carboxylase in plants. *Plant Physiol* 108: 445–449, 1995.
241. Sasaki Y, Kozaki A, and Hatano M. Link between light and fatty acid synthesis: thioredoxin-linked reductive activation of plastidic acetyl-CoA carboxylase. *Proc Natl Acad Sci USA* 94: 11096–11101, 1997.
242. Sauer A and Heise K–P. On the light dependence of fatty acid synthesis in spinach chloroplasts. *Plant Physiol* 73: 11–15, 1983.
243. Scagliarini S, Trost P, and Pupillo P. The non-regulatory isoform of NAD(P)-glyceraldehyde-3-phosphate dehydrogenase from spinach chloroplasts. *J Exp Bot* 49: 1307–1315, 1998.
244. Scagliarini S, Trost P, Pupillo P, and Valenti V. Light activation and molecular-mass changes of NAD(P)-glyceraldehyde 3-phosphate dehydrogenase of spinach and maize leaves. *Planta* 190: 313–319, 1993.
245. Scheibe R. Redox-modulation of chloroplast enzymes. A common principle for individual control. *Plant Physiol* 96: 1–3, 1991.
246. Scheibe R and Anderson LE. Dark modulation of NADP-dependent malate dehydrogenase and glucose-6-phosphate dehydrogenase in the chloroplast. *Biochim Biophys Acta* 636: 58–64, 1981.
247. Scheibe R, Baalmann E, Backhausen JE, Rak C, and Vetter S. C-terminal truncation of spinach chloroplast NAD(P)-dependent glyceraldehyde-3-phosphate dehydrogenase prevents inactivation and reaggregation. *Biochim Biophys Acta Protein Struct Mol Enzymol* 1296: 228–234, 1996.
248. Scheibe R, Backhausen JE, Emmerlich V, and Holtgrefe S. Strategies to maintain redox homeostasis during photosynthesis under changing conditions. *J Exp Bot* 56: 1481–1489, 2005.
249. Scheibe R, Geissler A, and Fickenscher K. Chloroplast glucose-6-phosphate dehydrogenase: Km shift upon light modulation and reduction. *Arch Biochem Biophys* 274: 290–297, 1989.
250. Scheibe R, Wedel N, Vetter S, Emmerlich V, and Sauermann SM. Co-existence of two regulatory NADP-glyceraldehyde 3-P dehydrogenase complexes in higher plant chloroplasts. *Eur J Biochem* 269: 5617–5624, 2002.
251. Schepens I, Johansson K, Decottignies P, Gillibert M, Hirasawa M, Knaff DB, and Miginiac–Maslow M. Inhibition of the thioredoxin-dependent activation of the NADP-malate dehydrogenase and cofactor specificity. *J Biol Chem* 275: 20996–21001, 2000.
252. Schimkat D, Heineke D, and Heldt HW. Regulation of sedoheptulose-1,7-bisphosphatase by sedoheptulose-7-phosphate and glycerate, and of fructose-1,6-bisphosphatase by glycerate in spinach chloroplasts. *Planta* 181: 97–103, 1990.
253. Schürmann P. The light activation of chloroplast enzymes through the ferredoxin/thioredoxin system. In: *Photosynthesis and Plant Productivity*, edited by Metzner H. Stuttgart: Wissenschaftl. Verlagsgesellschaft mbH, 1983, pp. 255–258.
254. Schürmann P. Ferredoxin-dependent thioredoxin reductase: a unique Fe-S protein. *Methods in Enzymology* 347: 403–411, 2002.
255. Schürmann P. Redox signaling in the chloroplast—the ferredoxin/thioredoxin system. *Antioxid Redox Signal* 5: 69–78, 2003.
256. Schürmann P. The ferredoxin/thioredoxin system. A light-dependent redox regulatory system in oxygenic photosynthetic cells. In: *Cellular Implications of Redox Signalling*, edited by Gitler C, Danon A. London: Imperial College Press, 2003, pp. 73–98.
257. Schürmann P and Buchanan BB. The structure and function of the ferredoxin/thioredoxin system in photosynthesis. *Advances in Photosynthesis and Respiration* 11: 331–361, 2001.
258. Schürmann P and Jacquot J–P. Plant thioredoxin systems revisited. *Annu.Rev.Plant Physiol.Plant Mol.Biol.* 51: 371–400, 2000.
259. Schürmann P and Kobayashi Y. Regulation of chloroplast fructose 1,6-bisphosphatase activity by the ferredoxin/thioredoxin system. In: *Advances in Photosynthesis Research*, The Hague: Martinus Nijhoff/Dr.W.Junk Publishers, 1984, pp. 629–632.
260. Schwarz O, Schürmann P, and Strotmann H. Kinetics and thioredoxin specificity of thiol modulation of the chloroplast H^+-ATPase. *J Biol Chem* 272: 16924–16927, 1997.
261. Shen JB, Orozco EM, Jr., and Ogren WL. Expression of the two isoforms of spinach ribulose 1,5-bisphosphate carboxylase activase and essentiality of the conserved lysine in the consensus nucleotide-binding domain. *J Biol Chem* 266: 8963–8968, 1991.
262. Smith AM, Zeeman SC, and Smith SM. Starch degradation. *Annu.Rev.Plant Biol.* 56: 73–98, 2005.
263. Soll J and Roughan G. Acyl–acyl carrier protein and pool sizes during steady-state fatty acid synthesis by isolated spinach chloroplasts. *FEBS Lett* 146: 189–192, 1982.
264. Sparla F, Costa A, Lo Schiavo F., Pupillo P, and Trost P. Redox regulation of a novel plastid-targeted beta-amylase of *Arabidopsis*. *Plant Physiol* 141: 840–850, 2006.
265. Sparla F, Fermani S, Falini G, Zaffagnini M, Ripamonti A, Sabatino P, Pupillo P, and Trost P. Coenzyme site-directed mutants of photosynthetic A_4-GAPDH show selectively reduced NADPH-dependent catalysis, similar to regulatory AB-GAPDH inhibited by oxidized thioredoxin. *J Mol Biol* 340: 1025–1037, 2004.
266. Sparla F, Pupillo P, and Trost P. The C-terminal extension of glyceraldehyde-3-phosphate dehydrogenase subunit B acts as an autoinhibitory domain regulated by thioredoxins and nicotinamide adenine dinucleotide. *J Biol Chem* 277: 44946–44952, 2002.
267. Sparla F, Zaffagnini M, Wedel N, Scheibe R, Pupillo P, and Trost P. Regulation of photosynthetic GAPDH dissected by mutants. *Plant Physiol* 138: 2210–2219, 2005.
268. Staples CR, Ameyibor E, Fu W, Gardet–Salvi L, Stritt–Etter A–L, Schürmann P, Knaff DB, and Johnson MK. The function and properties of the iron–sulfur center in spinach ferredoxin:thioredoxin reductase: a new biological role for iron-sulfur clusters. *Biochemistry* 35: 11425–11434, 1996.
269. Staples CR, Gaymard E, Stritt–Etter AL, Telser J, Hoffman BM, Schürmann P, Knaff DB, and Johnson MK. Role of the $[Fe_4S_4]$ cluster in mediating disulfide reduction in spinach ferredoxin: thioredoxin reductase. *Biochemistry* 37: 4612–4620, 1998.
270. Stumpp MT, Motohashi K, and Hisabori T. Chloroplast thioredoxin mutants without active-site cysteines facilitate the reduction of the regulatory disulphide bridge on the gamma-subunit of chloroplast ATP synthase. *Biochem J* 341: 157–163, 1999.
271. Sundby C, Harndahl U, Gustavsson N, Ahrman E, and Murphy DJ. Conserved methionines in chloroplasts. *Biochim Biophys Acta* 1703: 191–202, 2005.
272. Tamoi M, Ishikawa T, Takeda T, and Shigeoka S. Molecular characterization and resistance to hydrogen peroxide of two fructose-1,6-bisphosphatases from *Synechococcus* PCC 7942. *Arch Biochem Biophys* 334: 27–36, 1996.
273. Tamoi M, Miyazaki T, Fukamizo T, and Shigeoka S. The Calvin cycle in cyanobacteria is regulated by CP12 via the NAD(H)/NADP(H) ratio under light/dark conditions. *Plant J* 42: 504–513, 2005.
274. Tiessen A, Hendriks JH, Stitt M, Branscheid A, Gibon Y, Farré EM, and Geigenberger P. Starch synthesis in potato tubers is regulated by post-translational redox modification of ADP-glucose pyrophosphorylase: a novel regulatory mechanism linking starch synthesis to the sucrose supply. *Plant Cell* 14: 2191–2213, 2002.
275. Trebitsh T and Danon A. Translation of chloroplast *psbA* mRNA is regulated by signals initiated by both photosystems II and I. *Proc Natl Acad Sci USA* 98: 12289–12294, 2001.
276. Trost P, Fermani S, Marri L, Zaffagnini M, Falini G, Scagliarini S, Pupillo P, and Sparla F. Thioredoxin-dependent regulation of photosynthetic glyceraldehyde-3-phosphate dehydrogenase: autonomous vs. CP12-dependent mechanisms. *Photosynth Res* 89: 263–275, 2006.
277. Trost P, Scagliarini S, Valenti V, and Pupillo P. Activation of spinach chloroplast glyceraldehyde 3-phosphate dehydrogenase: Effect of glycerate 1,3-bisphosphate. *Planta* 190: 320–326, 1993.
278. Tsugita A, Yano K, Gardet–Salvi L, and Schürmann P. Characterization of spinach ferredoxin-thioredoxin reductase. *Protein Seq Data Anal* 4: 9–13, 1991.
279. Ueoka–Nakanishi H, Nakanishi Y, Konno H, Motohashi K, Bald D, and Hisabori T. Inverse regulation of rotation of F_1-ATPase by the mutation at the regulatory region on the gamma subunit of chloroplast ATP synthase. *J Biol Chem* 279: 16272–16277, 2004.
280. Vieira Dos Santos C, Laugier E, Tarrago L, Massot V, Issakidis–Bourguet E, Rouhier N, and Rey P. Specificity of thioredoxins and glutaredoxins as electron donors to two distinct classes of *Arabidopsis* plastidial methionine sulfoxide reductases B. *FEBS Lett* 581: 4371–4376, 2007.

281. Villeret V, Huang S, Zhang Y, Xue Y, and Lipscomb WN. Crystal structure of spinach chloroplast fructose-1,6-bisphosphatase at 2.8 Å resolution. *Biochemistry* 34: 4299-4306, 1995.
282. Vlamis–Gardikas A and Holmgren A. Thioredoxin and glutaredoxin isoforms. *Methods Enzymol* 347: 286–296, 2002.
283. von Schaewen A, Langenkämper G, Graeve K, Wenderoth I, and Scheibe R. Molecular characterization of the plastidic glucose-6-phosphate dehydrogenase from potato in comparison to its cytosolic counterpart. *Plant Physiol* 109: 1327–1335, 1995.
284. Wakao S and Benning C. Genome-wide analysis of glucose-6-phosphate dehydrogenases in *Arabidopsis*. *Plant J* 41: 243–256, 2005.
285. Walters EM, Garcia–Serres R, Jameson GNL, Glauser DA, Bourquin F, Manieri W, Schürmann P, Johnson MK, and Huynh BH. Spectroscopic characterization of site-specific [Fe_4-S_4] cluster chemistry in ferredoxin:thioredoxin reductase : Implications for the catalytic mechanism. *J Am Chem Soc* 127: 9612–9624, 2005.
286. Walters EM and Johnson MK. Ferredoxin:thioredoxin reductase: disulfide reduction catalyzed via novel site-specific [4Fe-4S] cluster chemistry. *Photosynth Res* 79: 249–264, 2004.
287. Wang D and Portis AR, Jr. Increased sensitivity of oxidized large isoform of ribulose-1,5-bisphosphate carboxylase/oxygenase (rubisco) activase to ADP inhibition is due to an interaction between its carboxyl extension and nucleotide-binding pocket. *J Biol Chem* 281: 25241–25249, 2006.
288. Wangensteen OS, Chueca A, Hirasawa M, Sahrawy M, Knaff DB, and Lopez GJ. Binding features of chloroplast fructose-1,6-bisphosphatase-thioredoxin interaction. *Biochim Biophys Acta* 1547: 156–166, 2001.
289. Watanabe S, Matsumi R, Arai T, Atomi H, Imanaka T, and Miki K. Crystal structures of [NiFe] hydrogenase maturation proteins HypC, HypD, and HypE: insights into cyanation reaction by thiol redox signaling. *Mol Cell* 27: 29–40, 2007.
290. Wedel N and Soll J. Evolutionary conserved light regulation of Calvin cycle activity by NADPH-mediated reversible phosphoribulokinase/CP12/glyceraldehyde-3-phosphate dehydrogenase complex dissociation. *Proc Natl Acad Sci USA* 95: 9699–9704, 1998.
291. Wedel N, Soll J, and Paap BK. CP12 provides a new mode of light regulation of Calvin cycle activity in higher plants. *Proc Natl Acad Sci USA* 94: 10479–10484, 1997.
292. Weichsel A, Gasdaska JR, Powis G, and Montfort WR. Crystal structures of reduced, oxidized, and mutated human thioredoxins: evidence for a regulatory homodimer. *Structure* 4: 735–751, 1996.
293. Wenderoth I, Scheibe R, and von Schaewen A. Identification of the cysteine residues involved in redox modification of plant plastidic glucose-6-phosphate dehydrogenase. *J Biol Chem* 272: 26985–26990, 1997.
294. Wendt UK, Wenderoth I, Tegeler A, and von Schaewen A. Molecular characterization of a novel glucose-6-phosphate dehydrogenase from potato (*Solanum tuberosum* L.). *Plant J* 23: 723–733, 2000.
295. Werner S, Schumann J, and Strotmann H. The primary structure of the γ-subunit of the ATPase from *Synechocystis* 6803. *FEBS Lett* 261: 204–208, 1990.
296. Werner–Grüne S, Gunkel D, Schumann J, and Strotmann H. Insertion of a "chloroplast-like" regulatory segment responsible for thiol modulation into gamma-subunit of F_0F_1-ATPase of the cyanobacterium *Synechocystis* 6803 by mutagenesis of *atpC*. *Mol Gen Genet* 244: 144–150, 1994.
297. Wolosiuk RA and Buchanan BB. Thioredoxin and glutathione regulate photosynthesis in chloroplasts. *Nature* 266: 565–567, 1977.
298. Wolosiuk RA, Hertig CM, Nishizawa AN, and Buchanan BB. Enzyme regulation in C4 photosynthesis. Role of Ca^+ in thioredoxin-linked activation of sedoheptulose bisphosphatase from corn leaves. *FEBS Lett* 140: 31–35, 1982.
299. Wong JH, Cai N, Balmer Y, Tanaka CK, Vensel WH, Hurkman WJ, and Buchanan BB. Thioredoxin targets of developing wheat seeds identified by complementary proteomic approaches. *Phytochemistry* 65: 1629–1640, 2004.
300. Wood ZA, Schröder E, Robin Harris J, and Poole L. Structure, mechanism and regulation of peroxiredoxins. *Trends Biochem Sci* 28: 32–40, 2003.
300a. Wu G, Ortiz-Flores G, Ortiz-Lopez A, and Ort DR. A point mutation in atpC1 raises the redox potential of the *Arabidopsis* chloroplast ATP synthase γ-subunit regulatory disulfide above the range of thioredoxin modulation. *J Biol Chem* 282: 36782–36789, 2007.
301. Wu W, Watson JT, Stevens FJ, Yousefzai R, and Anderson LE. Mass spectrometric evidence for an alternate disulfide bond in chloroplast fructose bisphosphatase. *Photosynth Res* 79: 189–200, 2004.
302. Wünschiers R, Heide H, Follmann H, Senger H, and Schulz R. Redox control of hydrogenase activity in the green alga *Scenedesmus obliquus* by thioredoxin and other thiols. *FEBS Lett* 455: 162–164, 1999.
303. Xu X, Kim SK, Schürmann P, Knaff DB, and Ubbink M. *Synechocystis* ferredoxin/ferredoxin-thioredoxin reductase complex: Complete NMR mapping of the interaction site on ferredoxin by gallium substitution. *FEBS Lett* 580: 6714–6720, 2006.
304. Yamaryo Y, Kanai D, Awai K, Shimojima M, Masuda T, Shimada H, Takamiya K, and Ohta H. Light and cytokinin play a cooperative role in MGDG synthesis in greening cucumber cotyledons. *Plant Cell Physiol* 44: 844–855, 2003.
305. Yamaryo Y, Motohashi K, Takamiya K, Hisabori T, and Ohta H. *In vitro* reconstitution of monogalactosyldiacylglycerol (MGDG) synthase regulation by thioredoxin. *FEBS Lett* 580: 4086–4090, 2006.
306. Yamazaki D, Motohashi K, Kasama T, Hara Y, and Hisabori T. Target proteins of the cytosolic thioredoxins in *Arabidopsis thaliana*. *Plant Cell Physiol* 45: 18–27, 2004.
307. Yano H, Wong JH, Lee YM, Cho MJ, and Buchanan BB. A strategy for the identification of proteins targeted by thioredoxin. *Proc Natl Acad Sci USA* 98: 4794–4799, 2001.
308. Yu LM and Selman BR. cDNA sequence and predicted primary structure of the gamma subunit from the ATP synthase from *Chlamydomonas reinhardtii*. *J Biol Chem* 263: 19342–19345, 1988.
309. Zaffagnini M, Michelet L, Marchand C, Sparla F, Decottignies P, Le Marechal P, Miginiac–Maslow M, Noctor G, Trost P, and Lemaire SD. The thioredoxin-independent isoform of chloroplastic glyceraldehyde-3-phosphate dehydrogenase is selectively regulated by glutathionylation. *FEBS J* 274: 212–226, 2007.
310. Zer H, Vink M, Shochat S, Herrmann RG, Andersson B, and Ohad I. Light affects the accessibility of the thylakoid light harvesting complex II (LHCII) phosphorylation site to the membrane protein kinase(s). *Biochemistry* 42: 728–738, 2003.
311. Zhang N, Kallis RP, Ewy RG, and Portis AR, Jr. Light modulation of Rubisco in *Arabidopsis* requires a capacity for redox regulation of the larger Rubisco activase isoform. *Proc Natl Acad Sci USA* 99: 3330–3334, 2002.
312. Zhang N and Portis Jr AR. Mechanism of light regulation of Rubisco: A specific role for the larger Rubisco activase isoform involving reductive activation by thioredoxin-f. *Proc Natl Acad Sci USA* 96: 9438–9443, 1999.
313. Zhang N, Schürmann P, and Portis Jr AR. Characterization of the regulatory function of the 46-kDa isoform of Rubisco activase from Arabidopsis. *Photosynth Res* 68: 29–37, 2001.

Address reprint requests to:
Peter Schürmann
Laboratoire de biologie moléculaire et cellulaire
Université de Neuchâtel
Rue Emile-Argand 11, CP 158
CH-2009 Neuchâtel, Switzerland

E-mail: peter.schurmann@unine.ch